UNIVERSITY OF CALGARY

Effect of Salinity on the Interfacial Tension of Model and Crude Oil Systems

by

Bikky Kumar

A THESIS

SUBMITTED TO THE FACULTY OF GRADUATE STUDIES

IN PARTIAL FULFILMENT OF THE REQUIREMENTS FOR THE

DEGREE OF MASTER OF SCIENCE

DEPARTMENT OF CHEMICAL AND PETROLEUM ENGINEERING

CALGARY, ALBERTA

September, 2012

Abstract

It has been observed that the interfacial tension of a hydrocarbon versus water increases with the concentration of salt in the aqueous phase; but when a small amount of surfactant is present in the solution, the interfacial tension decreases with salinity. Crude oil consists of tens of thousands of unknown components, of which many are surface active. It is found in combination with reservoir water, which varies from place to place. The interfacial tension, or IFT, of crude oil is thus a complex function of salinity and surfactant concentration. The objective of this thesis is to study the effects of salinity on the interfacial tension of crude oil.

To complete this study, the following data has been measured using a drop shape analyzer at ambient conditions:

- IFT of pure hydrocarbons, mixtures of pure hydrocarbons, three crude oils of varying density, and a bitumen versus aqueous phases of different salinity. The pure hydrocarbons chosen are toluene, *n*-heptane, 50 vol. % mixture of *n*-heptane and toluene (heptol50), and cyclohexane. Salt solutions are sodium chloride, calcium chloride, and sodium sulphate. Salinities were varied between 0 and 15 wt% in water.
- IFT for the same above solutions(except crude oil) with the addition of different surface active materials including sodium dodecylsulphate, cetyltrimethylammonium bromide, a nonylphenol ethoxylate, Triton X-100, 5β-cholanic acid, and asphaltenes.

A model was developed to fit or predict the salinity, solvent, and surfactant concentration for the different mixtures involving pure hydrocarbons. It was observed that a simple model, similar to Gibbs-Langmuir isotherm, was found adequate to fit the data for

different surfactants. As expected, the behaviour of ionic surfactants was different from the non-ionic ones. The addition of salt in the solution containing surface active agents altered the distribution of surfactants at the interface due to electrostatic effects and consequently altered the interfacial tension. Such effects were absent in the case of non-ionic surfactants, and was verified experimentally for two non-ionic surfactants.

The results of naphthenic acids and asphaltenes, which are naturally occurring surface active materials found in crude oil, showed that that salinity has a weak effect on the interfacial tension of hydrocarbons versus brine containing these components. The trends of IFT observed for asphaltenes was also seen for crude oil/water system.

Acknowledgements

First of all, I would like to express my sincere gratitude to my supervisor, Dr. H.W. Yarranton for his constant support and encouragement throughout my master's degree program. This work would not have been possible without his guidance. It was an honour and a privilege to be a part of his research group.

Next, I wish to thank Ms. Elaine Baydak for all the support and help provided by her in completing this thesis. I would like to acknowledge her contribution in teaching me a lot of experimental work and basics about my research. She also assisted in collecting a lot of experimental data.

I am grateful to Chevron ETC for providing the financial support for this project. My special regards goes to Dr. Hussein Alboudwarej, Dr. Samuel Haines, and Dr. Donald A. Medwedeff, from Chevron, for providing valuable suggestions and inputs to this project. Their feedback was critical to the overall success of this work.

I am thankful to the Department of Chemical and Petroleum Engineering, at the University of Calgary, for providing wonderful facilities and a great educational ambience. The staffs were really supportive and friendly.

The contribution of the members of the Asphaltene and Emulsion Research group and fellow graduate students cannot be underestimated. Their support and encouragement was always there in difficult times.

Last, but not the least, my deepest gratitude to my family and friends for all the care and support provided by them. This work could not have culminated in flying colours without their patience and understanding.

Dedicated to

My Parents and my Sister

Table of Contents

List of Tables

List of Figures and Illustrations

List of Symbols, Abbreviations and Nomenclature

English Letters

P	Pressure
r	Pore throat radius
P_b	Buoyancy pressure
g	Acceleration due to gravity
T_h	Hydrocarbon column thickness
G	Gibbs free energy
A	Area
T	Temperature
P	Pressure
R	Universal gas constant
a	Activity
K_L	Langmuir adsorption constant
C	Concentration
E	Energy per mole of solute
C_{sp}	Salinity of solution in ppm
n	Constant depending on the system
K_F	Frumkin adsorption constant
K_D	Davies adsorption constant
z	Charge on an ion
F	Faraday's constant
K_c	Combined adsorption constant
c	Concentration of surfactant in the solution
c_s	Concentration of salt in the solution
D	Diffusion constant
t	Droplet formation time
C_s	Subsurface concentration of surfactant
a	Surfactant molecular dimension
K_B	Boltzmann constant
b	Strength of electrostatic interactions
$A(T)$	Temperature dependent coefficient
$B(T)$	Temperature dependent coefficient

n	Number of carbon atoms
$a_{i\ (i = 1,2,3,4)}$	Constants
C_o	Concentration of solute in the oleic phase
C_w	Concentration of solute in the aqueous phase
HA_0	Undissociated acid in oil phase
HA_w	Undissociated acid in water phase
A_w^-	Dissociated acid ion in the water phase
H^+	Hydroxyl ion
A_s	Amount of *n*-C7 asphaltenes
A_n	Acid number
B_n	Base number
HA	Acid component present in crude oil
A^-	Surface active ion
P	Point on the interface of a droplet
x_p	x coordinate of a point on the droplet
z_p	z coordinate of a point on the droplet
R_1	Radius of curvature in the x-z plane
R_2	Radius of curvature in the y-z plane
R_{apex}	Radius of curvature at the apex of a droplet
x	Mole fraction
K	Adsorption constant
x_{salt}	Mole fraction of the salt in the aqueous phase
K_e	Partitioning coefficient
C	Equilibrium concentration
$Ai\ (i = 1,2,3)$	Constant unique to the given surfactant and solvent
v	Specific volume
w	Mass fraction

Greek Letters

γ	Interfacial tension
$d\gamma$	Differential change in interfacial tension
θ	Contact angle between hydrocarbon and water
ρ	Density
Γ	Surface excess concentration
θ	Fractional surface coverage

$\Delta\gamma$	Change in interfacial tension
Φ	Surface potential
ε_0	Permittivity of the free space
ε_r	Solution dielectric constant
Ω	Integral capacitance of Helmholtz layer
λ	Dummy variable
τ	Time constant
Ψ_0	Surfactant volume fraction at the interface
Ψ_1	Local volume fraction of surfactant in the sub-surface layer
Ψ_b	Surfactant volume fraction in the bulk solution
α	Langmuir adsorption parameter
β	Frumkin lateral interaction parameter
μ	Viscosity of oil
ΔP	Pressure difference across the interface between two phases
$\Delta\rho$	Density difference between two fluids

Subscripts

c_m	Capillary entry
w	Water
h	Hydrocarbons
b	Buoyancy
i	i^{th} component in the solution
2	Solute component in a solution
m	Monolayer coverage
correction	Change in IFT due to salinity
o	Pure or initial
d	d plane in the stern layer
oβ	Between o and β planes
od	Between o and d planes
e	Equilibrium
c	Critical
oR	Degree Rankine
hw	Water-hydrocarbon

exterior	External phase of a droplet
interior	Internal phase of a droplet
salt	Brine systems
s	Surfactants
H	Heavy Crude
C10	*n*-decane
counterion	Mole fraction of counterions in the solution

Superscripts

o	Pure solvent
s	Excluding the effect of surfactant
org	Organic phase
aq	Aqueous phase

Abbreviations

IFT	Interfacial tension
Heptol50	50:50 volume mixture of heptane and toluene
SDS	Sodium dodecylsulphate
CTAB	Cetyltrimethylammonium bromide
NEO10	Nonylphenol ethoxylate with 10 ethoxy groups in the molecule
CA	5β-cholanic acid
WC_B1	Western Canadian bitumen
DSA	Drop shape analyser
CMC	Critical micelle concentration
SARA	Saturates aromatics resins and asphaltenes
TAN	Total acid number
API	American petroleum institute
ASTM	American society of testing materials
PPM	Parts per million
TDS	Total dissolved solids
ACS	American chemical society

RO	Reverse osmosis
TX-100	Triton X-100
CCD	Charge-coupled device
HC	Hydrocarbon
AARD	Average absolute relative deviation
TDS	Total dissolved solids

Chapter One: Introduction

Oil and gas exploration involves the discovery of hydrocarbon accumulations and is a critical component of the oil industry. For a hydrocarbon accumulation to exist in nature, three components must be present (e.g., Arps, 1964; Talal *et al.*, 2009): 1) a source rock where hydrocarbons are generated from organic matter; 2) porous and permeable reservoir rocks where hydrocarbons are accumulated; 3) a non-permeable seal to trap the hydrocarbons and prevent their upward migration. A seal is defined as a sediment, rock, or immobile fluid with high capillary entry pressure that acts to stop the flow of hydrocarbons (Vavra *et al.*, 1992). Some of the common seal lithologies include salts, anhydrites and shales. Shales are important in petroleum exploration and production systems because they act as both source and seal rocks.

For any seal with non-zero permeability, also known as membrane seals (Watts, 1987) the height of the trapped hydrocarbon column is related to the capillary properties of the cap-rock. The minimum entry pressure of the hydrocarbon into the cap-rock is equal to the pressure required for hydrocarbons to enter the largest interconnected pore throat of the seal. In other words, a membrane seal will trap a hydrocarbon column until the net buoyancy pressure of the hydrocarbons exceeds the minimum capillary displacement pressure of the seal rock.

Capillary pressure is the difference in pressure across the interface separating two immiscible fluids. One fluid is the wetting phase, which adsorbs preferentially onto the reservoir rock, and the other is the non-wetting phase. In a seal rock, water is almost always the wetting phase while oil and/or gas is the non-wetting phase. The entry pressure of a non-wetting phase into a rock containing the wetting phase is given by (Purcell, 1949):

$$P_{c_m} = \frac{2\gamma \cos\theta}{r} \qquad \textbf{Equation 1.1}$$

where γ is the interfacial tension between water and hydrocarbons, P_{c_m} is the entry pressure, θ is the wettability measured in terms of hydrocarbon/water contact angle and r is the pore throat radius. The pressure required to enter the largest interconnected pore throat is defined as the minimum capillary entry pressure of the rock.

The entry pressure of a membrane cap-rock is capable of supporting a given buoyancy pressure at the cap-rock/reservoir interface before leaking. The buoyancy pressure of a hydrocarbon column (P_b) is related to the density difference between water (ρ_w) and the hydrocarbon (ρ_h) :

$$P_b = (\rho_w - \rho_h) g\, T_h \qquad \textbf{Equation 1.2}$$

where P_b is the buoyancy pressure at a seal boundary below which a hydrocarbon column of thickness T_h is trapped (Smith, 1966), ρ_w and ρ_h are the density of the water and the hydrocarbon, respectively, and g is the acceleration due to gravity. Equation 1.1 and 1.2 are equated to give the maximum height of hydrocarbon column that can be supported by a given membrane seal:

$$T_h = \frac{2\gamma cos\theta}{rg(\rho_w - \rho_h)} \qquad \textbf{Equation 1.3}$$

This equation shows that the maximum height of hydrocarbon column trapped in subsurface depends on the interfacial tension between oil and reservoir water, subsurface fluid densities, pore throat radii, and contact angle. One of the largest uncertainties in determining this height lies in the determination of hydrocarbon/water interfacial tension (Smith, 1966; Berg, 1975; Schowalter, 1979). In particular, reservoir water contains salts and there is considerable uncertainly in the effect of salt on the interfacial tension (IFT) of petroleum versus brine (O'Connor, 2000). If this IFT can be predicted, it will aid in predicting the height of trapped oil columns and therefore in developing exploration and production strategies for new oil fields.

Crude oil is a complex mixture of various components including pure hydrocarbons, heteroatomic species, and surface active substances such as asphaltenes and naphthenic

acids. It has been observed that the IFT of a pure hydrocarbon versus brine system increases with salt concentration; however, when a small amount of surfactant is present, the IFT can decrease with salinity (Heimenz *et al*., 1997; Cai *et al.* 1996). The IFT also varies with the type of hydrocarbons. Hence, the interfacial tension of crude oil versus reservoir brine depends on type and concentration of hydrocarbons, salts, and surfactants present in the system. The interfacial tension also depends on temperature and pressure. While there is considerable data in the literature on the IFT of systems of pure hydrocarbons, surfactants, and water, there are few data on the effect of salt concentration on IFT.

1.1 Objectives

The primary objective of this study is to investigate the effect of salinity on the interfacial tension of hydrocarbons with and without added surfactants and then to apply the results to crude oil/brine systems. The specific objectives of this study are:

1. Measurement and modeling of IFT of pure hydrocarbons and mixtures of pure hydrocarbons versus aqueous phases containing different salts.
2. Measurement and modeling of IFT of hydrocarbons/sodium chloride/surfactant system in varying concentrations of salts and surfactants.
3. Measurement of IFT of toluene/sodium sulphate and calcium chloride/SDS and CTAB system at one surfactant concentration and varying concentrations of salt.
4. Measurement of IFT of crude oils and bitumen versus sodium chloride solutions of varying concentrations. The IFT of heavy crude oil and bitumen is measured by dilution with different concentrations of *n*-decane.

The model hydrocarbon phases used in this work are toluene, *n*-heptane, cyclohexane, and a 50:50 volume mixture of *n*-heptane and toluene (heptol50). These hydrocarbons are representative of aromatic, aliphatic, and cyclic compounds and are the classes of compounds that may be found in a crude oil. The model aqueous phases are aqueous solutions of sodium chloride, calcium chloride, and sodium sulphate in concentrations ranging from 0 to 15 wt%. This concentration range covers a wide variety of reservoir

brine conditions. The surfactants (or surface active components) studied are sodium dodecylsulphate (SDS), cetyltrimethylammonium bromide (CTAB), Triton X-100 (TX-100), a nonylphenol ethoxylate (NEO10), 5β-cholanic acid (CA), and asphaltenes. The first three are examples of an anionic, cationic, and non-ionic surfactants, respectively, 5β-cholanic acid is a surfactant that represents a class of surface active components present in crude oil, and asphaltenes are another class of surface active component in crude oils. Three crude oils of varying density (light, medium, and heavy) and a Western Canadian bitumen (WC_B1) are also studied. All measurements are performed at ambient temperature and pressure.

1.2 Thesis Structure

This thesis is presented in five chapters. Chapter 2 is a literature review and is divided into three sections. The first section discusses the fundamentals of interfacial tension, including basic definitions, the relationship of IFT to composition including hydrocarbon, salt, and surfactant contributions, and the effect of temperature, pressure, and time on IFT. The second section discusses the chemistry of surfactants, crude oils, and reservoir brine. The third section presents a literature review on crude oil/brine IFT.

Chapter 3 describes materials, instrumentation, and experimental methods used in this thesis including:

- the materials and chemicals used in the experiments
- the instrument used for the IFT measurements (drop shape analyser, DSA)
- the principles of drop shape analysis
- the preparation of the solutions and the apparatus for taking measurements

Chapter 4 discusses the model development and present the experimental and modeling results for the various systems studied in this thesis. The effect of salinity on the IFT of various hydrocarbon/salt/surfactant systems is presented and analysed. The IFT of crude oils and bitumen versus brine are also presented and compared with the model systems.

Chapter 5 is the concluding chapter which summarizes the findings of this study. Recommendations for future research work related to this topic are also provided.

Chapter Two: Literature Review

In this chapter, the fundamentals of interfacial tension and the factors on which it depends are reviewed. A brief review of surfactants and crude oil chemistry is also included. The literature on the interfacial tension of crude oil and brines is discussed.

2.1 Fundamentals of Interfacial Tension

2.1.1 Definition of Interfacial Tension

Figure 2.1 is a schematic of molecules in the bulk phase and at an interface. Molecules in the bulk phases are surrounded by similar molecules and therefore have net force of zero acting on them. On the other hand, the molecules at the interface are forced into proximity to molecules of the other bulk phase and therefore are subjected to a net force. Thus, interfacial tension is the amount of work that should be supplied to bring the molecules from the bulk phases to the contact boundary to create a new interface of unit area. Since energy is minimized, the surface tends to contract so surface energy can also be expressed as a tension force per length. Conventionally, the tension between the liquid and air/vapour is called surface tension while the tension between two liquids is called interfacial tension, or IFT.

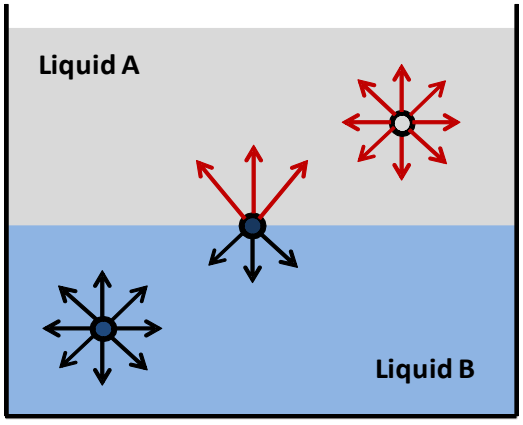

Figure 2.1 Schematic diagram of the forces involved in interfacial tension.

The amount of energy required to create a surface per unit area is called the surface free energy and can be related to Gibbs free energy as follows:

$$dG = \gamma dA \ (T, P \ constant) \qquad \textbf{Equation 2.1}$$

where γ is the surface free energy per unit area (J/m^2) or force per unit length (N/m). The interfacial tension can be related to the composition of the system through the Gibbs adsorption isotherm.

2.1.2 Gibbs Adsorption Isotherm

Gibbs derived the following equation to relate the change in interfacial solution of a solution to the change in chemical activity of the components in the solution (Hiemenz *et al.*, 1997):

$$d\gamma = -RT \sum \Gamma_i \, dlna_i \qquad \textbf{Equation 2.2}$$

where $d\gamma$ is the change in interfacial tension of the solution, R is the gas constant, T is the absolute temperature, and Γ_i and a_i are the surface excess concentration and the activity of the i^{th} component in the solution, respectively. The summation is taken over all the species in the solution.

The surface excess concentration is the concentration of a species in the interfacial region which is in excess of the concentration of that species in the bulk. It is expressed in units of moles per unit area. Figure 2.2 shows the concentration profile of a surfactant (or surface active component) which tends to concentrate at the interface in a water/oil system. The Gibbs interface, also shown, defines the boundary between the two bulk phases and is formally defined as the location where the excess concentration of the solvent is zero. The excess concentration of surfactant (the solute) is determined from the difference between its actual concentration and its solubility in the bulk phases (shaded area).

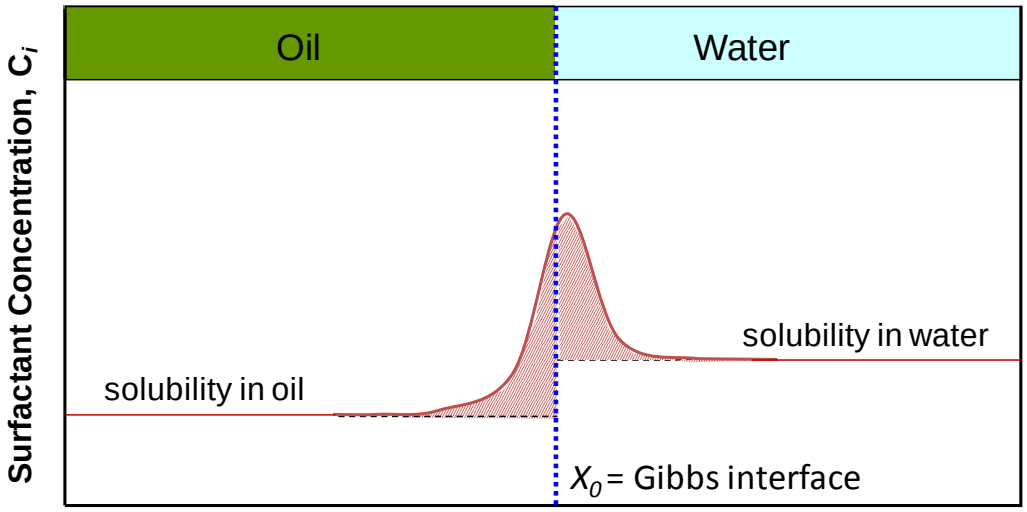

Figure 2.2 Schematic diagram to demonstrate the concept of surface excess concentration. The solid line is the concentration profile of a surfactant near an oil-water interface. The shaded region is the excess surface concentration.

For a binary system, the surface excess of one of the components (the solute) is zero and the Gibbs adsorption equation can be written as:

$$d\gamma = -RT\Gamma_2 \, d \, lna_2 \qquad \textbf{Equation 2.3}$$

where Γ_2 and a_2 are the surface excess concentration and activity of the solute, respectively. Since the surface excess concentration of a surfactant is positive, Equation 2.3 shows that the addition of surfactant decreases the interfacial tension of a solution.

A typical plot of surface or interfacial tension versus log concentration of solute is shown schematically in Figure 2.3. At low surfactant concentrations, the interface is only partially covered with surfactant. As more surfactant is added, the interface becomes saturated with the surfactant and the surface excess concentration becomes nearly

constant. The interfacial tension then becomes linearly related to log of the activity of the surfactant. For an ideal system and when the surfactant mole fraction is much lower than the solute mole fraction, the activity is proportional to the surfactant concentration. Therefore, the interfacial tension becomes linearly related to the log of concentration. At low surfactant concentrations, the change in surface excess concentration with changing surfactant concentration must also be accounted for; for example, using the Gibbs–Langmuir isotherm (Yarranton and Masliyah, 1996) which models surfactant adsorption with a Langmuir isotherm.

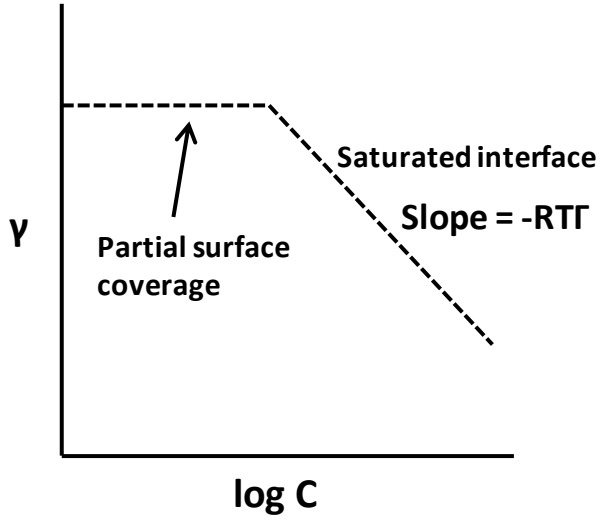

Figure 2.3 Schematic of a typical plot of interfacial tension (γ) versus bulk concentration (C) of a surface active substance in a solution.

2.1.3 Gibbs-Langmuir Isotherm

The surface excess concentration of a component can be expressed as follows:

$$\Gamma_i = \theta_i \Gamma_{\mathrm{mi}} \qquad \textbf{Equation 2.4}$$

where θ_i and Γ_{mi} are the fractional surface coverage and monolayer surface excess concentration of component i, respectively. The fractional surface coverage can be related to the bulk phase concentration using the Langmuir adsorption isotherm given by:

$$\theta_i = \frac{\Gamma_i}{\Gamma_{mi}} = \frac{K_{Li}C_i}{1 + K_{Li}C_i} \qquad \textbf{Equation 2.5}$$

where K_{Li} and C_i are the Langmuir adsorption constant and concentration of component i, respectively. Equation 2.5 is substituted into the Gibbs adsorption isotherm, Equation 2.2, to obtain the following:

$$d\gamma = -RT\Gamma_m \ln(1 + K_L C) \qquad \textbf{Equation 2.6}$$

The adsorption constant and monolayer surface excess concentration can be found by fitting Equation 2.6 to experimental data.

For a liquid-liquid interface, the Langmuir constant K_L is directly proportional to $exp\{-E/RT\}$, where E is the energy per mole of the solute (Hiemenz *et al*., 1997). This relationship allows the modeling of temperature dependence of interfacial tension at low concentrations of solute.

2.1.4 Effect of Salinity on Water/Hydrocarbon Interfacial Tension

When inorganic salts are present in the aqueous phase, the water molecules form a cage-like hydrogen bonded structure around the salt ions, Figure 2.4. At the interface, water molecules are in contact with another phase and the hydrogen bonding is disrupted creating a higher energy environment for the ions. Hence, the salts are depleted near the interface and the surface excess concentration of salts is negative. As dictated by the Gibbs adsorption isotherm, interfacial tension increases when inorganic salts are added to the aqueous phase.

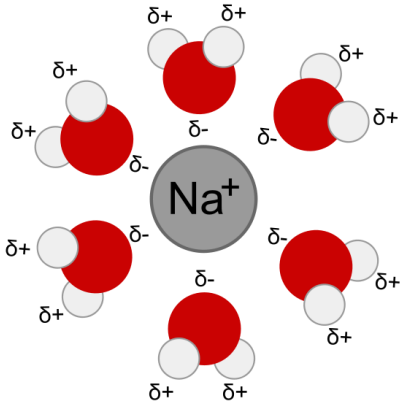

Figure 2.4 Schematic diagram showing hydrogen bonding in water and the formation of a cage-like structure surrounding an inorganic ion such as Na+.

Data for the effect of salt on interfacial tension are sparse and present contrasting trends. An increase in interfacial tension with salt addition has been reported by several authors (Aveyard and Saleem, 1976; Ikeda *et al.*, 1992; Cai *et al.*, 1996; Badakshan and Bakes, 1990). The opposite trend has been observed by a few authors (Aveyard and Saleem, 1976 for KI in a dodecane-water system; Alotaibi *et al.*, 2009; Serrano-Saldana *et al.*, 2004). Table 2.1 summarises the conditions at which these literature data were collected.

Sutton (2009) observed the inconsistencies in the data reported by various authors for the IFT of hydrocarbon system against saline water. He developed a correlation to predict IFT of hydrocarbon/salt systems by regression analysis of the literature data. The correction in hydrocarbon IFT due to salinity was reported as $\gamma_{correction} = 3.44 \times 10^{-5} C_{sp}$, where C_{sp} is the salinity of the solution in ppm. Note, the negative trend was ruled out and the correction is positive.

Cai *et al.* (1996) investigated the effect of carbon number on the IFT of hydrocarbon/brine systems. They measured the IFT of 5 normal alkanes versus water/brine as well as some hydrocarbon mixture versus water/brine using pendant drop tensiometry. The salts were sodium chloride, calcium chloride and magnesium chloride.

The presence of salt in the aqueous phase increased the interfacial tension and although IFT was dependent on the salt concentration, it was independent of the salt species. IFT also increased with the molecular weight of the normal alkane but no explanation was provided for this behaviour.

Table 2.1 Literature data of IFT for hydrocarbon/brine systems.

Reference	Compounds	Conditions	Salinity 10^3 ppm
Alotaibi and El-Din, 2009	*n*-C12	25 to 90 ^{o}C 1.0 to 10.3 MPa	20-100
Serrano-Saldana *et al.*, 2004	*n*-C12	25 ^{o}C Atmospheric	0 – 75
Cai et al, 1996	*n*-C6, *n*-C10, *n*-C12 *n*-C14, *n*-C16, *n*-C6+*n*-C10 *n*-C6+*n*-C10+*n*-C16	25 to 80 ^{o}C 0.1 to 30 MPa	50
Cai *et al.*, 1996	*n*-C8	25 ^{o}C 3.9 to 29MPa	5 - 100
Badakshan and Bakes, 1990	*n*-C6, cyclohexane, toluene	22 to 200 ^{o}C 0.1 to 300 MPa	150
Aveyard and Saleem, 1976	*n*-C10 and *n*-C12	20 ^{o}C Atmospheric	6 – 56
Aveyard and Haydon, 1965	*n*-C7	20 to 30 ^{o}C Atmospheric	6
Aveyard and Haydon, 1965	*n*-C14	20 to 30 ^{o}C Atmospheric	6 - 150
Ikeda *et al.*, 1992	*n*-C6	10 to 40 ^{o}C 0.1 to 99 MPa	6 – 55

When an ionic surfactant is present in solution, increasing the salinity decreases the interfacial tension (Bonfillion *et al.*, 1994; Hamouda and Karoussi, 2008). Several mechanisms have been proposed for this effect. An increase in ionic strength may increase the activity coefficient of the surfactant in the aqueous phase which decreases the interfacial tension (Gurkov *et al.*, 2005; Yarranton and Masliyah, 1996). The presence of salt can also alter the distribution of surfactant between oil and aqueous phase (Al-Sahhaf *et al.*, 2005). The increase in salt concentration can also enhance the adsorption of surfactant at the interface, decreasing the interfacial tension (Prosser *et al.*, 2001). Various models have been developed to relate the surface tensions of salts and surfactants system with their concentrations in the bulk and they are reviewed below.

2.1.5 Other Models for Equilibrium IFT

A number of models have been developed to study the adsorption and tension behaviour of ionic surfactants at the air/water or oil/water interface in the presence of a supporting electrolyte. Most of these models were developed for ideal, premicellar surfactant solutions, in the presence of an indifferent electrolyte with the same counterion as the surfactant. Examples of current models are given in Table 2.2.

The adsorption models in Table 2.2 describe the fractional surface coverage of the surfactant at the interface as if the interface was a planar surface. The Langmuir isotherm was described previously. The Frumkin isotherm is a non-ionic, three-parameter model relating the adsorbed surface density to the bulk concentration. In this isotherm, the lateral interactions among adsorbed molecules are taken into account using the parameter β. The interactions are assumed to occur in a pair wise fashion between the neighbouring adsorbed molecules. The Davies ionic model is a two parameter model relating the adsorbed surface excess concentration with the bulk concentration and the surface potential, ϕ_0. The bulk solution is considered to be ideal and the ions at the interface non-interacting. When the surface potential is zero, the Davies isotherm reduces to the Langmuir isotherm. In the Frumkin-Davies model, the Davies model was extended to

account for surfactant interactions between both chains and head group. The basic framework of Davies model was kept intact.

Table 2.2 A selection of models used to describe adsorption and interfacial tension of surfactants in the presence of inorganic salts.

Model	Equation	Model Type
Langmuir	$\theta = \frac{\Gamma}{\Gamma_m} = \frac{K_L C}{1 + K_L C}$	Adsorption
Frumkin [2]	$\theta = \frac{\Gamma}{\Gamma_m} = \frac{K_F \exp(-\beta\theta)\, C}{1 + K_F \exp(-\beta\theta)\, C}$	Adsorption
Davies [3]	$\theta = \frac{\Gamma}{\Gamma_m} = \frac{K_D \exp\left(\frac{-zF\phi_O}{RT}\right) C}{1 + K_D \exp\left(\frac{-zF\phi_O}{RT}\right) C}$	Adsorption
Frumkin-Davies [4]	$\theta = \frac{\Gamma}{\Gamma_m} = \frac{K_c \exp(-\beta\theta) \exp\left(\frac{-zF\phi_O}{RT}\right) c}{1 + K_c \exp(-\beta\theta) \exp\left(\frac{-zF\phi_O}{RT}\right) c}$	Adsorption
Gibbs-Langmuir or Szyszkowski [1]	$\gamma - \gamma_o = -RT\Gamma_m \ln(1 + K_L C)$	Non-Ionic
Borwankar and Wasan [5](BW)	$\frac{\gamma - \gamma_o}{RT\Gamma_m} \ln(1-\theta) - \frac{\beta}{2}\theta^2 - \frac{4\sqrt{2\varepsilon_O \varepsilon_r RT(c + c_s)}}{F\Gamma_m}\left[\cosh\left(\frac{F\phi_O}{2RT}\right) - 1\right]$	Ionic
Kalinin and Radke[6]	$\gamma_{ionbinding} = -4RT\varepsilon_O\varepsilon_r(c + c_s)\left(\Omega_{o\beta}^{-1}\alpha^2 + \Omega_{od}^{-1}\right) sinh^2\left(\frac{F\phi_d}{2RT}\right)$	Counterion Binding

References: 1. Szyszkowski, 1908, 2. Frumkin, 1925, 3. Davies, 1958, 4. Prosser *et al.*, 2001, 5. Borwankar and Wasan, 1988, 6. Kalinin and Radke, 1996

Three interfacial tension models are shown in Table 2.2: the general Gibbs-Langmuir model described previously, an ionic model, and a counterion binding model. Ionic models compensate for effects of salt concentration in the bulk solution, the dissociation of electrolytes, and the adsorbed surface density of surfactant ions. The charge creates a potential, which is modeled by Gouy-Chapman theory. For their model, Borwankar and Wasan (1988) assumed that surfactant ions adsorb at the interface and the point-like counterions diffuse outward from this layer into the aqueous phase. The surface excess concentration was taken as the combination of actual adsorbed surface concentration of the surfactant and the contribution from the diffuse layer. The surface adsorption is modeled using the combined Frumkin-Davis model and the double layer contribution by the Gouy-Chapman theory.

The counterion binding models take the complexity of the dependence on salinity one step further and account for the interaction between the adsorbed surfactant molecule at the interface and the counterions arranged in the diffuse layer. Kalinin and Radke (1996) proposed a triple layer interfacial structure: a plane of adsorbed surfactant ions, plane of partially dehydrated counterions, and a plane of hydrated counterions at which the diffuse layer begins. A new term, $\gamma_{ionbinding}$ was added to the equation to account for counterion binding effect.

2.1.6 Effect of Time on Interfacial Tension

The variation of interfacial tension with time is known as dynamic interfacial tension. When a surfactant solution, such as one that is aqueous-based, is placed in contact with an opposing phase, such as a hydrocarbon or oil phase, a finite time is required for the surfactants to diffuse, adsorb at the interface, and reach equilibrium. In interfacial processes where equilibrium conditions are not attained, such as high speed wetting or foaming, dynamic processes play an important role. Dynamic interfacial tension must also be considered when measuring interfacial tension; for example, to ensure that equilibrium values are obtained.

2.1.6.1 Dynamic Adsorption Models

Dynamic adsorption is controlled by two processes (Defay, 1971): 1) the transfer of molecules between the surface layer and the subsurface layer, which lies immediately below the surface at a thickness of a few molecular diameters; 2) the exchange of molecules between the subsurface and the bulk solution. The first step is an adsorption process and the second step is mainly diffusion, with occasional convection. There are two schools of thought to describe the adsorption of surfactants at the liquid interface (Dukhin *et al.* 1995; Diamant *et al.* 1996; He *et al.* 2002). The diffusion-controlled model assumes the diffusive transport of molecules from the bulk to the subsurface to be the rate-determining process, while the kinetic-controlled model is based on attachment of molecules at the interface due to high adsorption activation energy barriers.

2.1.6.2 Diffusion-Controlled Adsorption Models

In diffusion-controlled adsorption models, it is assumed that there is no activation energy barrier to the transfer of solute molecules between the subsurface and the surface. In short, the time required for the solute to transfer from the bulk to the subsurface is much larger than the time required for the transfer between subsurface and surface. The first theoretical attempt to describe the mechanism mathematically was made by Ward and Tordai (1946). They, however, did not account for the convective term in the diffusion equation for the transfer of surface active materials from the bulk to the surface. This point was corrected by Miller (1980) and the following equation was derived:

$$\Gamma = 2C\left(\frac{3Dt}{7\pi}\right)^{1/2} - 2\left(\frac{D}{\pi}\right)^{1/2} \times t^{-2/3}\int_0^{\sqrt{\tau}} C_s\,(\tau-\lambda)d\sqrt{\lambda} \qquad \textbf{Equation 2.7}$$

where D is the diffusion constant, C_s is the subsurface concentration, τ is equal to $\frac{3}{7}t^{7/3}$, t is the bubble formation time, and λ is a dummy variable. This equation was simplified by

considering a short time approximation such that the second term became negligible (Dukhin *et al.*, 1995; Joos *et al.*, 1992; Miller and Kretzschmar, 1991):

$$\Gamma = 2C\left(\frac{3Dt}{7\pi}\right)^{1/2} \qquad \textbf{Equation 2.8}$$

Equation 2.8 can be expressed in terms of interfacial tension through the introduction of an appropriate adsorption isotherm (Campanelli *et al.*, 1998).

$$\gamma(t) = \gamma(0) - 2RTC\left(\frac{3Dt}{7\pi}\right) \qquad \textbf{Equation 2.9}$$

It was assumed that the relationship between $\Gamma(t)$ and $\gamma(t)$ is the same as that at equilibrium. Equation 2.9 provides an adequate description of the beginning of the adsorption process for many surfactants. A long time approximation of the general diffusion equation becomes valid when the adsorption process is near equilibrium (Rosen *et al.*, 1995, Joos *et al.*, 1992) and is given by:

$$\gamma(t) = \gamma_e + \frac{RT\Gamma^2}{C}\left(\frac{7\pi}{12Dt}\right)^{1/2} \qquad \textbf{Equation 2.10}$$

where γ_e is the equilibrium interfacial tension. Equation 2.10 shows that after a long time a linear relation is expected between γ and $t^{-1/2}$. The surface adsorption can be estimated from the slope of this line if the diffusivity is known.

Diamant *et al.* (1996) summarised that although diffusion theories have been successful in describing the experimentally observed adsorption of non-ionic surfactants, they suffer from the following drawbacks:

1) The relation between the surface density and subsurface concentration, which expresses the kinetics taking place at the surface, is introduced as an external boundary condition and does not uniquely arise from the model itself.
2) The calculated dynamic surface tension relies on an equilibrium equation of state and assumes that it also holds out of equilibrium.

3) Similar theories cannot be easily extended to describe more complicated systems, such as ionic surfactant solutions (Bonfillion *et al.,* 1994).

They also developed models to present an alternative approach for the kinetics of non-ionic and ionic surfactant adsorption at fluid/fluid interfaces. The advantage of their model is that the diffusion inside the aqueous solution and the kinetics of adsorption at the interface are not introduced as two separate independent processes, but both arise from the same model. They found that adsorption was limited by bulk diffusion in cases of non-ionic surfactants and ionic surfactants with added salt, and by kinetics at the interface in the case of salt-free ionic surfactant solutions. Their findings were in agreement with experimental observations. Their model equations are provided below.

Non-ionic Surfactant:

$$\psi_0\ (t) = \frac{1}{a}\sqrt{\frac{D}{\pi}}\left[2\psi_b\sqrt{t} - \int_0^t \frac{\psi_1(\tau)}{\sqrt{t-\tau}}d\tau\right] + 2\psi_b - \psi_1 \qquad \textbf{Equation 2.11}$$

$$\frac{\partial\psi_0}{\partial t} = \frac{D}{a^2}\psi_1\left[\ln\frac{\psi_1(1-\psi_0)}{\psi_0} + \frac{\alpha}{T} + \frac{\beta\psi_0}{T}\right] \qquad \textbf{Equation 2.12}$$

This relation is similar to the Ward and Tordai (Eq 2.7), except for the term $(2\psi_b - \psi_1)$ which arises due to the consideration of fine details near the interface and the initial condition. ψ_0 and ψ_b are the surfactant volume fraction at the interface and in the bulk solution respectively, ψ_1 is the local volume fraction in the sub-surface layer, *a* denotes the surfactant molecular dimension, α is the Langmuir adsorption parameter, and β is the Frumkin lateral interaction parameter. Equations with appropriate initial conditions completely determine the adsorption kinetics and equilibrium state. Full solution can only be obtained numerically.

Ionic Surfactant:

$$\psi_{0,e} = \frac{\psi_b}{\psi_b + \left[b\psi_{0,e} + \sqrt{\left(b\psi_{0,e}\right)^2 + 1}\right]^2 e^{-\alpha-\beta\psi_{0,e}}} \qquad \textbf{Equation 2.13}$$

$$\Delta\gamma_e = \frac{K_B T}{a^2}\left[\ln\left(1-\psi_{0,e}\right) + \frac{\beta}{2}{\psi_{0,e}}^2 - \frac{2}{b}\left(\sqrt{\left(b\psi_{0,e}\right)^2 + 1} - 1\right)\right] \qquad \textbf{Equation 2.14}$$

where $\psi_{0,e}$ is the surface volume fraction of the surfactant at equilibrium, *a* is the average size of a surfactant molecule, and *b* is a parameter characterizing the strength of electrostatic interactions. The equations become kinetically limited in the case of salt-free ionic surfactant solutions. Addition of salt to the ionic solutions leads to screening of the electrostatic interactions and the adsorption becomes similar to non-ionic ones, *i.e.*, diffusion-controlled.

2.1.6.3 Kinetic Controlled Models

The qualitative and quantitative models of adsorption kinetics for various surfactants and polymers were described by Dukhin (1995). General agreement in the literature is that adsorption of non-ionic surfactant is diffusion-controlled (Diamant *et al.*, 1996, 2001). For ionic surfactants, the surface potential acts as an adsorption barrier for additional surfactant molecules as they try to accumulate at the interface. Addition of salt to the system reverses the behaviour back to diffusion-controlled (Bonfillion *et al.*, 1994) due to electrostatic screening of the surface potential in the presence of added electrolyte.

2.1.6.4 Exponential Decay Model

Although the diffusion-controlled model was found to generally describe the behaviour of surfactant solutions, it failed in certain instances. In such cases a rearrangement of surfactant molecules at the surface also occurred (Lucassen *et al,*. 1987; Germansheva *et al.*, 1981; Serrien *et al.*, 1990; Hunsel *et al.*, 1988), which affected the dynamics of surfactant adsorption. According to Hunsel *et al.* (1988), the process is controlled by a free-energy barrier situated at the interface. This was verified by them for an *i*-heptane/water interface of several cholesterol solutions in *i*-heptane. This relation was presented as:

$$\gamma = \gamma_e + (\gamma_0 - \gamma_e)e^{\frac{-t}{\tau}} \qquad \textbf{Equation 2.15}$$

where γ_0 is the interfacial tension at time zero, γ_e is the equilibrium interfacial tension and τ is a parameter with the same unit as time which signifies the relaxation time. The model has been applied to find equilibrium IFT for asphaltenes (Jeribi *et al.*, 2002) and crude oil systems (Buckley *et al.*, 2007; Kelesoglu *et al.*, 2011). This model was found to be adequate to obtain the equilibrium IFT values in this thesis.

2.1.7 Effect of Pressure and Temperature on the IFT of Hydrocarbons

The literature survey of the effects of pressure and temperature on the IFT indicated several contrasting trends. The behaviour depends on the type of the system studied and the pressure and temperature range used. In general, the IFT between oil/water decreases with increasing temperature, reaching a value of zero at a "critical" temperature. This may be due to the increase in the solubility of oil in water. The increased solubility decreases the interfacial energy, which subsequently leads to a lower value of IFT. It may also be due to an increase in surface mobility; which increases the total entropy of the surface and thereby reduces its free energy (Gibbs, 1957; Hirasaki, 1999; Myers, 1999). Although the effect of pressure is highly dependent on the type of system, IFT generally increases with an increase in pressure.

For hydrocarbon/aqueous systems, several authors have reported an increasing trend in IFT with increasing pressure, Figure 2.5, and a decreasing trend of IFT with increasing temperature, Figure 2.6 (Hough *et al.*, 1951; Jennings, 1967; Aveyard and Haydon, 1965; McCaffery, 1972; Wiegand *et al.*, 1994; Al-Sahhaf *et al.*, 2005; Cai *et al.*, 1996; Zeppieri *et al.*, 2001; Ikeda *et al.*, 1992; Badakshan and Bakes, 1990). In most cases the effect of pressure was found to be much less than the effect of temperature (Jennings, 1967; Cai *et al.*, 1996). Some authors have reported a decreasing trend in IFT with increasing pressure (Hassan *et al.*, 1953) and an increasing trend in IFT with increasing temperature (Jennings, 1971), which is opposite to the expected behaviour. Table 2.3 summarises the sources of literature data available on the effect of pressure and temperature on IFT.

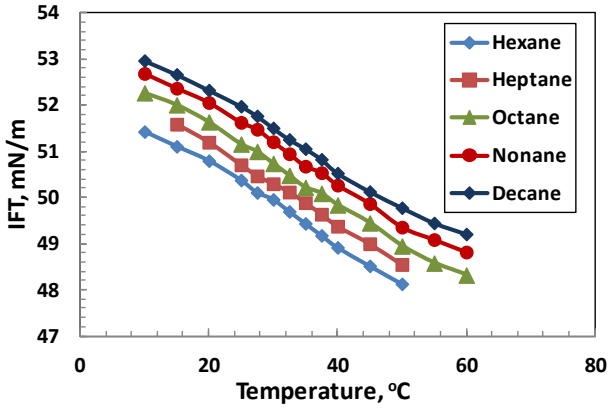

Figure 2.5 Effect of temperature on the IFT of pure hydrocarbons versus water at atmospheric pressure (data taken from Zeppieri *et al.*, 2001).

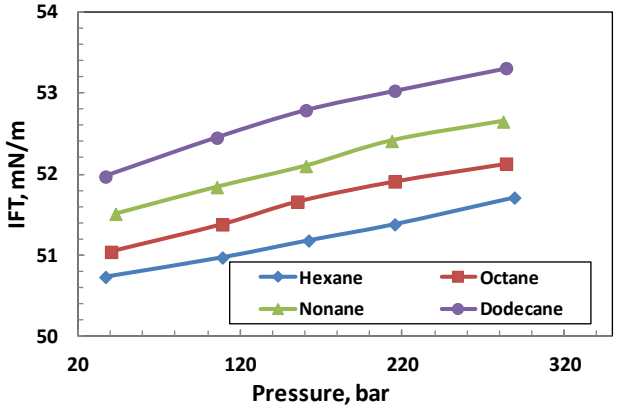

Figure 2.6 Effect of pressure on the IFT of pure hydrocarbons versus water at 25°C (data taken from Cai *et al*. 1996).

Table 2.3 Sources of literature data on the effect of pressure and temperature on IFT of hydrocarbon-water systems.

Reference	Hydrocarbon / Aqueous system	Pressure (MPa)	Temperature (^{o}C)
Zeppieri *et al.*, 2001	hexane, heptane, heptane, octane, nonane, undecane , dodecane / water	0.1	10 to 60
Cai *et al.*, 1996	*n*-alkane/water or brine, hydrocarbon mixtures/water or brine	0.1 to 30	25 to 80
Sahhaf *et al.*, 1995	*n*-octane/water or brine	0.7 to 31	25 to 65
Wiegand and Franck, 1994	*n*-hexane, *n*-decane, toluene / water	0.1 to 300	25 to 200
Ikeda *et al.*, 1992	hexane/water	0.1 to 99	10 to 40
Badakshan and Bakes, 1990	*n*-hexane, cyclohexane, toluene / water	0.1	15 to 80
McCaffery, 1972	*n*-dodecane, *n*-octane/water	0.1 to 41	25 to 148.9
Jennings, 1971	*n*-decane + methane /water	0.1 to 83	23.4 to 176.7
Jennings, 1967	benzene, *n*-decane/water	0.1 to 83	25 to 176
Aveyard and Haydon, 1965	*n*-alkane/water	0.1	20 to 37.5

In almost all cases, the decreasing IFT was related linearly to the increasing temperature and pressure. Zepierri *et al.* (2001) related IFT of *n*-alkanes to temperature using an empirical equation of the type:

$$\gamma = A(T)n^{B(T)} \qquad \textbf{Equation 2.16}$$

where n is the number of carbon atoms, and A and B are temperature dependent coefficients. Sutton (2009) assembled a database of 1902 data points for water/hydrocarbon interfacial tension. Hydrocarbons ranging from methane through

hexadecane as well as benzene and toluene were included in the main database. In addition, natural gas, natural gas-carbon dioxide and natural gas-nitrogen mixtures were also tested with the new correlation. Pressure data covered the range from 14.7 to 43,526 psia while temperature ranged from 0.5-260^{o}C. Sutton (2009) also developed a correlation for estimating water/hydrocarbon interfacial tension, given as:

$$f(\gamma_{hw}) = \frac{\gamma_{hw}^{a_1}}{\rho_w - \rho_h}\left(\frac{T_{oR}}{T_c}\right)^{\left(a_2 + a_3 T_{oR} + a_4 T_{oR}^2\right)} \qquad \textbf{Equation 2.17}$$

where γ_{hw} is the pure water-hydrocarbon IFT, ρ_w and ρ_h are the density of water and hydrocarbon phases respectively, T_{oR} is the temperature in degree Rankine, T_c is the critical temperature of the hydrocarbon, and a's are the constants

2.2 Surfactants

2.2.1 Definition

Surfactants or surface active agents are organic compounds with at least one lyophilic (hydrocarbon solvent, or oil, loving) and a lyophobic (hydrocarbon solvent, or oil, hating) group. Alternatively, they possess both hydrophilic (water-loving) and hydrophobic (water-hating) components. They are also known as amphiphilic compounds. The hydrophilic group can be ionic or polar in nature, imparting some water solubility to the surfactant molecule. They adsorb strongly at the oil/water and air/water interface and significantly reduce the surface energy even at low concentrations (Hiemenz *et al.*, 1997). The definition of surfactants is often constrained to surface active components that can self-assemble at higher concentrations (Laughlin, 1996).

When surfactants are dissolved in a solvent, the lyophobic group increases the local interaction energy. However, the surfactant can orient at the interface so that the lyophilic group resides adjacent to the oil phase while the hydrophilic group resides adjacent to the water phase. This reduces the energy of the interface relative to the hydrocarbon-water interactions. Therefore, surfactants tend to adsorb strongly at the interface and significantly decrease interfacial tension.

Surfactants are generally classified on the basis of the charge of hydrophilic group as follows.

- Anionic: hydrophilic group carries a negative charge. Examples include carboxyl ($RCOO^-M^+$), sulfonate ($RSO_3^-M^+$) or sulfate ($ROSO_3^-M^+$)
- Cationic: hydrophilic group carries a positive charge as in quaternary ammonium halides ($R_4N^+Cl^-$)
- Amphoteric (or zwitterionic): in which molecules can potentially contain both a positive and negative charge, such as in sulfobetaines $RN^+(CH_3)CH_2CH_2SO_3^-$
- Non-ionic: hydrophile has no charge but may contain highly polar groups. For example, polyoxyethylene ($-OCH_2CH_2O-$) or polyol ($-RX\ (C_3H_5OH)_nOH-$) groups.

2.2.2 Surfactants Properties

Some of the properties of the surfactants which are important for this thesis are discussed below.

2.2.2.1 Partitioning of Surfactants in Oil and Water

When a polar organic compound dissolved in an organic solvent is in contact with an immiscible aqueous solvent, the compound distributes between the two phases depending on pH, salinity and the ionic strength in the water phase.

Surfactants dissolved in either the water or oil phase have a tendency to partition to some degree into the other phase, depending on its relative solubility between the phases. The relative solubility depends on the structure of the surfactant. For example, a highly polar hydrophilic group or a large number of polar groups will make the surfactant more water soluble and less oil soluble. Surfactant partitioning (and solubility) is also dependent on the salt concentration in the solution. The concentration of surfactant increases in the

oleic phase with an increase in salt concentration (Chan and Shah, 1980). A partitioning coefficient of unity corresponds to minima in the IFT of the system.

The partitioning can be characterized by partitioning coefficient, K_e, which is defined as:

$$K_e = \frac{C_S^{org}}{C_s^{aq}} \qquad \textbf{Equation 2.18}$$

where C_S^{org} is the concentration of the solute in the oleic phase and C_S^{aq} is its concentration in the aqueous phase. The partition coefficient depends on the ionic strength, pH, oil type, co-solvents (Pollard *et al.,* 2006), temperature, and surfactant composition at the interface (BenGhoulam *et al.,* 2004). For non-ionic surfactants the partitioning coefficient between water and oil, K_e, was greater than unity for surfactants with more than 10 ethylene oxide units, which also gives high water solubility (BenGhoulam *et al.,* 2004). For naphthenic acids, the partition coefficient was correlated to the number of cyclic rings in the compound (Havre *et al.,* 2003).

2.2.2.2 Micelles and Critical Micelle Concentration

When surfactant molecules reach a certain "critical" concentration in an aqueous phase, they form aggregates, or micelles, such that the hydrocarbon tails cluster together inside the aggregate while the head groups are oriented toward the aqueous solution forming a polar shell (Carale *et al.,* 1994), Figure 2.7. In this way, the hydrophilic head groups reside in an aqueous environment while the hydrophobic tail groups reside in an organic environment. This configuration minimizes the free energy of the solution.

The concentration at which micelles begin to form is the critical micelle concentration (CMC). At the CMC there is an equilibrium between monomers of surfactant (and counterions in the case of ionic surfactants) and micelles. A similar phenomenon, but in oleic phase with oil-soluble surfactants, is known as reverse micellization. The interfacial tension of a solution becomes constant above the CMC because the additional surfactant

forms additional micelles and the concentration of free surfactant in the bulk phase and adsorbed surfactant at the interface change little.

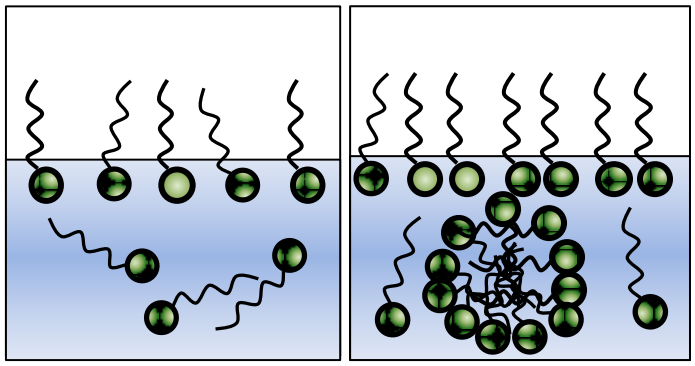

Figure 2.7 Micelle formations of surfactants in an aqueous solution at the critical micelle concentration.

2.3 Chemistry of Crude Oils and Reservoir Brines

2.3.1 Petroleum Chemistry

Crude oils are classified as light, medium, or heavy based on the specific gravity and viscosity of the oil. All crude oils are complex mixtures of hydrocarbons and polar organic compounds of oxygen, sulphur and nitrogen, as well as metal-containing compounds (particularly vanadium, nickel, iron, and copper). Approximately 11000 compositionally distinct components have been detected in one crude oil (Hughey *et al.* 2002). This too is a very conservative lower limit. The composition of reservoir oil may vary with geographic location and geological age of a field. Crude oil can be classified in several different ways; for example, by its physical properties (e.g., density, viscosity), elemental composition (e.g., amount of carbon, hydrogen, sulphur, nitrogen), carbon distribution, distillation curve, or solubility class (SARA fractionation into saturates, aromatics, resins and asphaltenes). Typically, the heavier the oil, the greater is the asphaltene content.

Saturates are the nonpolar materials in the crude oil including linear, branched and cyclic saturated hydrocarbons. Aromatics are those compounds that contain one or more aromatic rings. Resins and asphaltenes are similar to aromatics but are, larger, contain more fused aromatic rings, and contain more heteroatoms (Fan *et al.* 2002). Asphaltenes and resins are considered to be interfacially active components and contribute to the lowering of IFT of crude oil (Havre *et al.* 2003). Other classes of surface active components present in crude oil are: carboxylic acids, waxes, porphyrins, and phenols.

Total Acid Number:

One of the parameter which correlates with the concentration of surface active components present in the crude oil is total acid number (TAN). The total acid number of a crude oil, as defined by American Society of Testing Materials (ASTM), is the quantity of base, expressed as milligrams of KOH required to neutralize the acidic components in one gram of oil. In general, the TAN decreases with increasing API gravity of crude oils (Fan and Buckley, 2007). A similar parameter is the base number, which is defined as the amount of perchloric acid necessary for titration of one gram sample of crude oil to a well defined inflection point. A high acid number usually corresponds to a high base number (Skauge *et al.* 1999).

2.3.2 Natural Surface Active Components Present in Crude Oil

The important naturally occurring surface active components asphaltenes and naphthenic acids are discussed in this section.

2.3.2.1 Asphaltenes:

Asphaltenes are large, polar, polynuclear molecules consisting of condensed aromatic rings, aliphatic side chains, and various heteroatom groups (Payzant *et al.* 1991). The heteroatoms present in the molecule are N, S, O, V, and Ni. Asphaltenes are soluble in aromatic solvents such as toluene, but precipitate in excess amounts of aliphatic solvents like *n*-pentane and *n*-heptane. Hence, asphaltenes are not a pure component, but rather a

solubility class of materials. They are a mixture of tens of thousands or perhaps millions of different species. Their elemental compositions vary from source to source and molecular structures have not been determined precisely. They are largely responsible for very high viscosities of heavy oil (Henaut *et al.* 2001).

Asphaltene Structure

The structure of asphaltenes is largely unknown but two types of structure have been postulated: (1) "continent" structure and (2) "archipelago" structure. The continent structure consists of a large aromatic structure and alkyl branches. This structure is based on x-ray diffraction measurements on solid asphaltenes (Dickie and Yen, 1967). It is shown schematically in Figure 2.8.

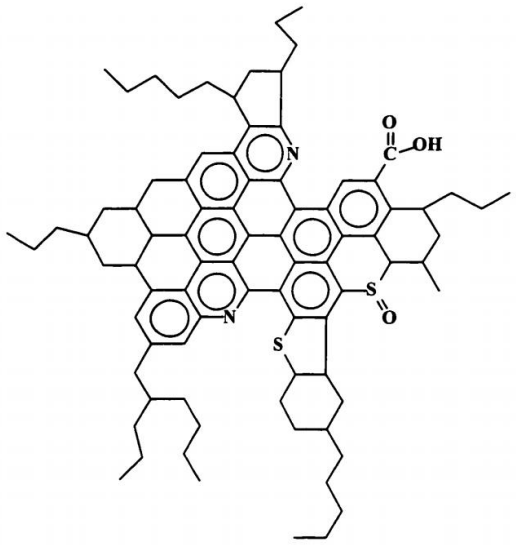

Figure 2.8 Continental structure of asphaltene molecule.

Strausz *et al.* (1992) proposed a so-called "archipelago" structure that consists of small aromatic islands connected by alkyl bridges. This structure is based on chemical and thermal degradation studies. Figure 2.9 shows a slight modification of the first model proposed also by Strausz in 1992. It is still debated which of the proposed structures is most representative. However, the archipelago structure is the most consistent with the

observed reaction products from upgraded residues which are rich in asphaltenes (Gray, 1994).

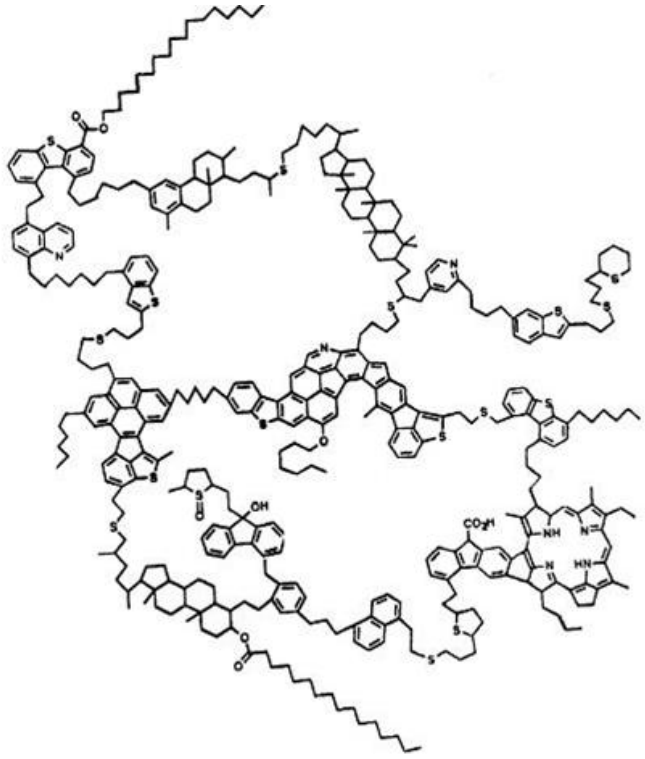

Figure 2.9 Archipelago structure for asphaltene molecule (Murgich *et al.*, 1999).

Surface activity of asphaltenes:

Although asphaltenes have a large hydrocarbon skeleton, they contain a wide variety of polar heteroatom groups such as oxygen, sulphur, or nitrogen. The hydrocarbon skeleton is hydrophobic while the polar groups are hydrophilic. The presence of both groups on a single molecule makes asphaltenes surface active; that is, they tend to adsorb at the water-oil interface with the hydrophobic groups aligned in the organic phase and the hydrophilic group in the aqueous phase. Of various heteroatoms present, N- and O-bearing moieties are the most likely candidates to contribute to interfacial activity

(Varadaraj and Brons, 2007). Interfacial tension measurements have confirmed that asphaltenes adsorb at the water-oil interface lowering the interfacial tension in the same manner as surfactants (Mohamed *et al.,* 1999; Schildberg *et al.,* 1995; Yarranton *et al.,* 2000).

2.3.2.2 Naphthenic Acids:

Naphthenic acids are a class of organic monoacids with the general formula of RCOOH, where R is a cycloaliphatic moiety. In general, in crude oils, the term "naphthenic acid" is used to account for all carboxylic acids including acyclic and aromatic acids (Brient *et al.,* 1995). In crude oils, naphthenic acids are in the group of resin molecules and it is generally believed that these acids interact with basic components in the asphaltenes molecules (Havre *et al.,* 2003). They are found in large concentrations in acidic crude oils.

Naphthenic acids are complicated mixtures, and many different methods and analytical techniques have been used to analyze them (Brient *et al.,* 1995; Acevedo *et al.,* 1999; Hsu *et al.,* 2000; Headley *et al.,* 2002). In general, naphthenic acids are C_{10}–C_{50} compounds with 0–6 fused saturated rings, and the carboxylic acid group is apparently attached to a ring with a short side chain (Robbins *et al.,* 1998). The carbon number and ring content distribution depends on the crude oil source. The total acid number (TAN) due to naphthenic acids and their average molecular weight can also have different profiles for each crude oil (Brient, 1998).

The smaller molecular weight acids are readily dissolved in the aqueous phase at a pH of 5, while the larger molecules are preferably soluble in oleic phase. Most of these can be made soluble in aqueous phase at higher pH (Rudin *et al.,* 1992; Sjoblom *et al.,* 2000). Several equilibria will be involved in a system consisting of naphthenic acids with a combination of water phase and an oil phase (Havre *et al.,* 2003). At low pH, the partitioning of undissociated acid between the phases and the dissociation of carboxylic

acid in the water are dominant processes. At high pH, formation of micelles in both phases is an important mechanism (Figure 2.10) Havre *et al.* (2003) measured the partitioning coefficient of various naphthenic acids and arrived at the conclusion that the logarithm of the partitioning coefficients varies linearly versus the number of methyl groups in the acid molecules. Increasing the concentration of monovalent salt in the water phase increases the concentration of the component in the oil phase (Jafvert *et al.,* 1990) due to the salting-out of organic compounds in the aqueous phase.

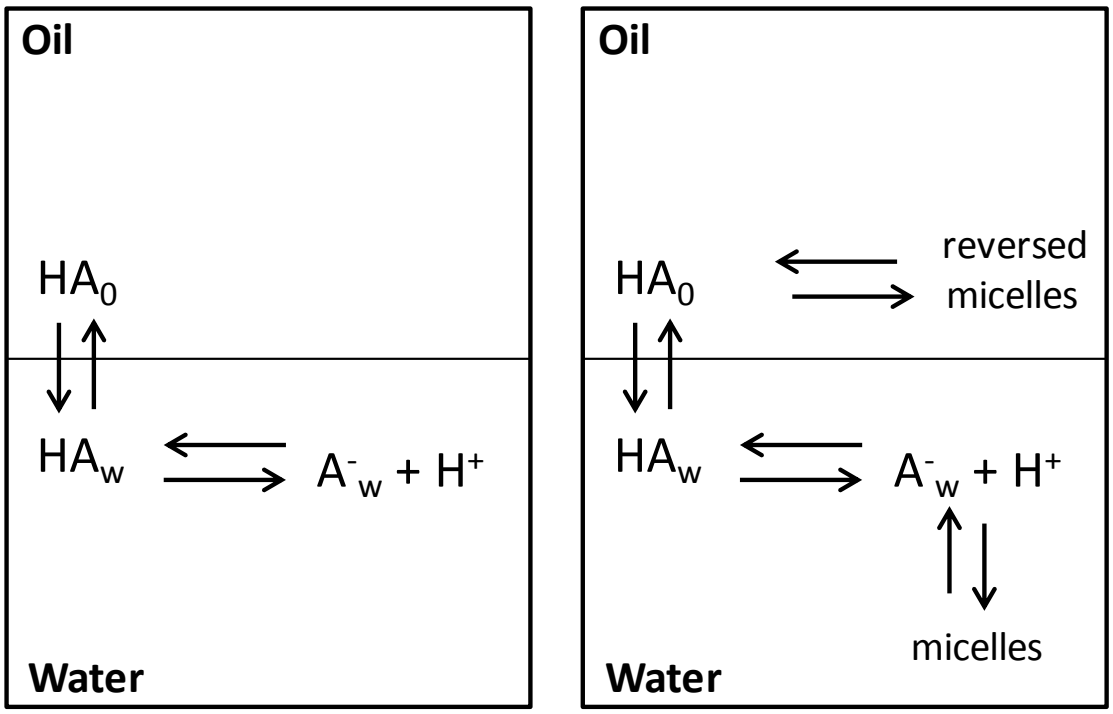

Figure 2.10 Various equilibria involved in an oil/water system containing naphthenic acids. HA_0 and HA_w, represents undissociated acid in the oil and water phase respectively. A_w^- is the dissociated acid ion in the water phase. H^+ is the hydroxyl ion (adapted from Havre *et al.,* 2003).

Naphthenic acids decrease the interfacial tension between aqueous and oleic phases. A marked decrease in IFT is observed as the pH of the solution is increased. This behaviour was found to be the same for different hydrocarbon phases and for both synthetic acids and acids derived from crude oil (Havre *et al.,* 2003). At high pH values the acid

molecules dissociates and the IFT approaches a value of 0 for full dissociation. It is interesting, however, to note that the IFT does not change much in the pH range 2 to 8. Since the pH of the reservoir is expected to be in the range of 5-7 (Reinsel *et al.*, 1994), the pH is not expected to significantly affect the IFT of crude oils due to naphthenic acids at reservoir conditions.

Varadaraj and Brons (2007) studied the interfacial properties at the hydrocarbon-water interface for 5β-cholanic acid and other naphthenic acids separated from crude oil. They concluded that these properties are influenced by the composition and chemical structure of the crude oil naphthenic acids. Crude oil naphthenic acids are more effective than crude oil asphaltenes in reducing the interfacial tension, but the crude oil asphaltenes exhibit a higher propensity to aggregate at the hydrocarbon-water interface and in the bulk. Crude oil naphthenic acids are relatively more interfacially active in a native crude oil medium than in a mixture of aliphatic-aromatic solvents.

The effectiveness of crude oil surface active components in lowering the IFT is more if they act together, as opposed to working individually. In other words, the surface active components in crude oil show synergistic effects (Varadaraj and Brons, 2007).

2.3.3 Reservoir Brine Chemistry

The water found in reservoirs contains dissolved solids. The main dissolved solids are sodium chloride, calcium chloride, magnesium chloride, strontium chloride, sodium sulfate, and sodium bicarbonate (Dandekar, 2006). Sodium chloride is found in greater concentration than the other salts. Dissolved salt concentration is usually expressed in milligrams of each solid per liter or parts per million on a mass basis (ppm). The composition of brine is expressed as the concentration of individual ions or total dissolved solids (TDS).

The brine composition varies from field to field. Badakshan and Bakes (1990) reported the total dissolved solids percentage for a number of North American reservoirs. The

majority of the reservoirs were found to have total dissolved solids (TDS) content from 0 to 25 wt%. Table 2.4 shows the ranges of sodium and chloride ions and the total dissolved solids for a number of major oil producing regions, as reported by Collins (1992). The composition of reservoir brine varies over a very wide range.

Table 2.4 Oil field water compositions for some major oil producing regions.

Field	Na^+ (mg/L)	Cl^- (mg/L)	TDS (mg/L)
Appalachian	50 - 98,300	70 – 216,300	475 - 344,110
California	40 - 15,015	10 - 27,100	80 - 47,995
Gulf Coast	30 - 61,000	20 – 105,000	353 - 171,300
Mid-continent(Texas)	210 - 122,500	460 – 212,000	1710 - 356,600
Rocky Mountain	5 - 20,000	3 - 27,900	98 - 57,340
Canadian	660 - 104,600	200 – 173,500	1205 - 290,070
Venezuelan	1260 - 12,360	90 - 19,800	4424 - 36,500

2.4 Crude Oil/Brine IFT

Earlier sections have discussed the factors affecting the IFT of hydrocarbon/brine systems. This section examines how those factors affect the IFT of crude oils.

2.4.1 IFT of Crude Oils

The interfacial properties of crude oil can be complex and are not well understood. The IFT of crude oil in a reservoir is a complex function of a wide variety of unknown factors, including temperature, pressure, salinity, amount and type of hetero-atoms present, acid number, base number, pH of the aqueous phase, viscosity, amount of asphaltenes, amount of dissolved gases (Buckley and Fan 2007), and presence of fine solids (Sztukowski and Yarranton, 2004). Other properties of crude oil which may affect

the IFT are density, solubilising power, composition (such as SARA fractions), and iso-electric points (Buckley and Fan 2007).

After the importance of interfacial tension in predicting the height of hydrocarbon column was established, the first attempt to throw some light on IFT values was made by Schowalter (1979). After an extensive literature review of the IFT data, he concluded that increasing temperature lowers the IFT of oil/water systems and increasing pressure has a little impact above 1500 psi. Schowalter used the experimental results of Livingston (1938) who had presented data for IFT of 34 Texas crude oils. The mean value of data presented by Livingston was 21 mN/m at 70^{o}F. Livingston reported that no particular correlation existed between IFT and geologic formation. In general, IFT was found to be higher for denser, viscous, and more paraffinic crudes.

Firoozabadi and Ramey (1988) proposed a correlation involving IFT and density differences between phases as shown in Equation 2.19. For a density difference typically found in reservoirs, the IFT was calculated to be in the range of 25-35 mN/m.

$$f(\gamma_{hw}) = \frac{\gamma_{hw}^{0.25}}{\rho_w - \rho_h}\left(\frac{T_{oR}}{T_c}\right)^{0.3125} \qquad \textbf{Equation 2.19}$$

Buckley and Fan (2007) measured the IFT of various well characterized stock tank samples of crude oil. They tested all the available chemical and physical properties of crude oil individually for correlation with both the initial and equilibrium IFT values. The absence of any significant correlation demonstrates that it is difficult to predict IFT of crude oils using a single parameter. A multivariate linear statistical analysis of the equilibrium IFT data produced the following correlation:

$$\gamma_{eq} = 21.7 - 1.14pH + 0.745A_s - 1.21A_n + 1.15B_n + 0.0073\mu$$

where A_s is the amount of *n*-C_7 asphaltenes, A_n is the acid number, B_n is the base number, and μ is the viscosity of oil. An increased concentration of asphaltenes, higher

base number, and higher viscosity all increased the IFT of crude oil versus brine at a particular pH. An increasing acid number decreased the IFT. Note, contrary to studies on model systems, the asphaltenes did not appear to behave as surfactants.

Bai *et al.* (2010) measured the IFT of crude oil and its components versus aqueous phase. The IFT values were found to increase in the order: heavy oil, asphaltenes and resins. According to the authors, the interfacial activity of crude oil components is decided by their content of hetero-atoms and acid number.

2.4.2 Effect of Salinity on Crude Oil IFT

Salts can have a pronounced effect on the IFT of crude oil/water system. The effect of salts on the IFT of crude oil depends on the type and amount of surface active material present in it. The presence of salt can alter the distribution of surface active component present in oil phase to aqueous phase. This is due to a salting-out effect. Salts can also accelerate the diffusion of surface active components from bulk solution to the interface (Bai *et al.*, 2010).

The increase in the concentration of the components in the oil phase on increasing the concentration of monovalent salts in the water phase has been reported by several authors (Bennett and Larter, 1997; Standal *et al.*, 1999). The aqueous solubility of petroleum hydrocarbon species decreases with increasing salinity due to salting-out effects (Price, 1976).

The IFT of Athabasca bitumen versus an aqueous phase was measured by Isaacs and Smolek (1983). The tension data in the absence of salt was 18 mN/m. An increase in salinity of the aqueous phase was accompanied by a decrease in IFT.

Vijapurapu and Rao (2004) reported the effect of brine dilution on the IFT of dead Yates crude oil. The IFT of oil/water systems decreased initially on decreasing the volume

percent of brine in the reservoir brine-deionised water mixture, but increased on further dilution of formation brine. Similar results were obtained using synthetic brine, which had a composition similar to the reservoir brine. A critical brine concentration was found to exist that lowered the IFT to a minimum value.

Xu (2005) studied the effect of the brine composition on IFT by changing the salinity and salt composition of the aqueous phase. Five systems were examined in live crude oil: deionised water, NaCl, $CaCl_2$, formation brine, and 50% formation brine in deionised water. The dilution of formation brine did not influence the IFT behaviour, but it increased the IFT as compared to the original brine. The live oil system in $CaCl_2$ solution had the highest equilibrium IFT values compared to the others.

Okasha and Al-Shiwaish (2009) studied the effect of formation brine salinity level on the crude oil/water IFT measurements. Both dead and live oil samples were examined. Synthetic brine solutions were prepared at three different salinities: 52,346, 107,906, and 214,943 ppm. IFTs for low, medium and high salinity solutions varied between 17.7 and 34.4 mN/m. The IFT between live oil and brine decreased on decreasing the volume percent of brine in the mixture.

Bai *et al.* (2010), after studying the effects of salt concentration on the IFT of a heavy crude oil and its polar components (asphaltenes and resins), concluded that NaCl concentration had no significant effect on the interfacial tension. The authors reasoned that most of the interfacial active substance might be oil-soluble and hence the effect of salt was minimal.

The effect of salt concentration on crude oil IFT is not well documented in the literature. Also, a consistent trend could not be found and the effect seems to vary depending on the composition and type of crude oil under consideration.

2.4.3 Effect of Temperature and Pressure on Crude Oil IFT

The effect of temperature and pressure on crude oil interfacial tension is not well understood. Although the expected and typical trend was to increase IFT with increasing pressure and to decrease with increasing temperature, contrasting trends were reported by many authors as listed below.

- Akstinat (1981) observed that temperature dependence of IFT was strongly influenced by oil composition. Crude oils with a high naphthenic content showed a decrease in IFT with increasing temperature. In contrast, aromatic and paraffinic crudes were virtually unaffected.

- The IFT of Athabasca bitumen versus an aqueous phases decreased (0.07 mN/m/^{o}C) with increasing temperature in the range 50-150^{o}C (Isaacs and Smolek, 1983). A decrease in IFT of bitumen with temperature was also reported by Drelich *et al.* (1994).

- Hjelmeland and Larrondo (1986) showed that the IFT between stock tank crude oil and brine increased with an increase in temperature under anaerobic conditions, whereas at aerobic conditions, IFT decreased with an increase of temperature.

- Firoozabadi and Ramey (1988) measured the IFT between artificial brine and three live reservoir oils. In one of the systems, IFT increased on increasing the temperature from 185 to 195^{o}F. For one system, the IFT increased with pressure. However, the other systems were not much affected by pressure and temperature changes.

- Wang and Gupta (1995) measured IFT for distilled mineral-oil and two crude oils versus brine. One crude oil was taken from a carbonate and the other from a sandstone reservoir. The composition of the brine was the same as found in the source reservoirs. The pressure ranged from 200 to 3000 psig, while the temperature varied from room temperature to 94^{o}C. The IFT for the three systems studied was found to increase with pressure. However, IFT values, either increased or decreased with temperature depending on system composition.

- Pressure and temperature effects were investigated on live oil/formation brine systems by Xu (2005). IFT results were reported at 58^{o}C and pressures up to 3000 psi. The measurements were performed before and after reaching equilibrium at 4.5 hours. IFT increased linearly as pressure increased. At 3000 psi, IFT decreased on increasing the temperature from 23 to 58^{o}C.
- Okasha and Al-Shiwaish (2009) reported a decreasing trend in IFT for an oil/water system in the temperature range from 25 to 90^{o}C. Increasing the pressure from 500 up to 2500 psig increased the IFT by 2 mN/m.

The literature survey on the effect of pressure and temperature on crude oil IFT does not show a clear trend. While temperature and pressure do have an impact on IFT, the effect seems to be less than that of composition of the systems studied. Thus, the effects of pressure and temperature have been excluded in the present study.

2.4.4 Effect of pH on the IFT of Crude Oil

The pH of the aqueous phase can have a pronounced effect on the interfacial tension of crude oil versus brine. The pH of the aqueous phase affects the dissociation of acidic and basic components present in a crude oil. It may also change the partitioning of the surface active components between the two phases. The dissociation of acidic components present in crude oil can be represented as:

$$HA \rightleftharpoons H^{+} + A^{-}$$

where *HA* represents acid components present in crude oil, A^{-} is the surface active ion, and H^{+} is the hydroxyl ion. When the pH of the aqueous phase is high, the concentration of hydroxyl ion is low and according to Le Chatelier's principle, the above reaction proceeds in the forward direction. This favours an increase in the surface active ions and a consequent decrease in interfacial tension of the system. Similarly, the basic components present in crude oil causes the IFT to drop at lower pH values.

A reduction in IFT values between oil solutions of water-insoluble fatty acids and aqueous solutions was observed with increasing pH due to dissociation (Cratin, 1993; Danielli, 1937; Hartridge and Peters, 1922; Peters, 1931). Similarly, the dissociation of water-insoluble bases results in lower IFT values at low pH (Peters, 1931). At the crude oil/brine interface, both acids and bases are active, thus the IFT is highest near neutral pH and decreases as pH is either increased or decreased (Buckley 1996; Reisberg and Doscher, 1956; Bai *et al.,* 2010). When only crude oil acids are present, the decrease in IFT is observed only at high pH (Hoeiland, 2001).

Kelesoglu *et al.* (2011) observed that the initial interfacial tension, equilibrium interfacial tension, reduction of the interfacial tension and the reorganization of the indigenous surfactants at the water/oil interface, all depend on the aqueous phase pH. The reorganization of the interfacial film at the crude oil/water interface is fast when the pH is less than 5 because of less partitioning of indigenous surfactants into the aqueous phase and less dissociation at the interface.

The effect of pH on IFT of solutions containing asphaltenes was studied by Poteau (2005). Asphaltenes are amphoteric materials, so the charge acquired at low pH (cationic) and high pH (anionic) increases their hydrophilic behaviour and makes them more surface-active. They accumulate more easily at the interface when they are charged. The behaviour is similar to crude oils with the IFT being highest near neutral pH and decreases both at low and high pH values.

The pH of the reservoir is expected to be in the range of 5-7 (Reisnel *et al.,* 1994). Therefore, the role of pH at reservoir conditions is unlikely to be significant. It can become important when acid is injected into the reservoir.

2.5 Chapter Summary

Interfacial tension of a solution depends on the amount and type of components present in it. Gibbs adsorption isotherm can be used to relate the change in interfacial tension of a solution to the concentration of various solutes present in it. The surface excess concentration of a solute can be calculated using the slope of the Gibbs adsorption isotherm. In general, the effect of salinity is to increase the interfacial tension of pure hydrocarbons versus aqueous phase. Several ionic and non-ionic models have been developed in the past to correlate the interfacial tension of a solution containing surfactants, in the presence of inorganic salts. Interfacial tension of pure hydrocarbons as well as that of crude oil generally increases with an increase in pressure and decreases with increasing temperature.

Naphthenic acids and asphaltenes are two of the most important surfactants found naturally in crude oil. Their behaviour is similar to other common classes of surfactants. However, it is not possibly to find their exact structure and quantity as present in crude oils. The water found in reservoirs in combination with crude oils contains dissolved inorganic salts in proportions which vary widely from one location to another.

The interfacial tension of crude oils is not well understood. An attempt by several authors to relate it to some measurable quantity did not yield significant results. One of the factors on which the IFT of crude oil depends is the salinity of water. The literature survey of the effect of salinity on crude oil IFT showed contrasting trends.

Chapter Three: Experimental Methods

This chapter describes the experimental methods and instrumentation used in this research project. The interfacial tension measurements were made using a drop shape analyser at ambient conditions of temperature and pressure. The instrument was set to record interfacial tension over time.

3.1 Materials

Interfacial tension measurements require organic phase and an aqueous phase. The solvent used for the model system organic phases were: toluene (OmniSolv of 99.9% purity), *n*-heptane (OmniSolv of purity of 99.5%), and cyclohexane (ACS grade of 99.5% purity). All were supplied by EMD and were purchased through VWR. A 50:50 mixture by volume of *n*-heptane and toluene, denoted as heptol50, was also used as a model hydrocarbon phase.

Aqueous phases were prepared from water, salts, and surfactants. Reverse osmosis (RO) water was supplied by the University of Calgary water plant. The salts included: sodium chloride, calcium chloride dihydrate, and sodium sulphate anhydrous, all ACS grade from EMD and purchased through VWR. The surfactants included: sodium dodecylsulphate >99% pure (SDS) purchased from Fisher Scientific, cetyltrimethylammonium bromide >99% pure (CTAB) from Aldrich Chemical Company, nonylphenol ethoxylate (with 10 moles of ethylene oxide, NEO10) >99% pure from Champion Technologies Ltd., Triton X-100 from ROHM and HASS Company and 5β-cholanic acid >99% pure (CA) from Sigma-Aldrich Chemical Company.

2-Propanol, toluene and *n*-heptane (all reagent grades) were used to clean the cuvette, syringe and needle used in the experiment. *n*-Decane (99.7%) was used to dilute heavy oils and was purchased from Sigma-Aldrich Chemical Company. All chemicals were used as received without further purification.

Three crude oils, described as light, medium and heavy, were provided by Chevron Corp. No information was provided about their source or composition. WC_B1 bitumen was obtained from a SAGD operation and was provided by Shell.

3.1.1 Surfactants Used in this Thesis

Table 3.1 summarises the properties of the surfactants used in this study. A detailed description of each surfactant is provided below.

Table 3.1 Properties of surfactants used in this thesis.

Surfactant	Type	Molecular Weight	CMC (mM)	CMC(g/L)
NEO10	Non-ionic	644	0.075	0.048
TX-100	Non-ionic	625	0.22	0.137
SDS	Anionic	288	8.2	2.362
CTAB	Cationic	364.5	0.98	0.357
5β-Cholanic acid	Naphthenic acid	360	1	0.36

3.1.1.1 Nonylphenol Ethoxylate:

Nonylphenol ethoxylates, NEOs, are non-ionic surfactants, the properties of which changes with varying number of ethoxylate groups. NEOs up to about the 12-mole ethoxylate are liquid at room temperature. As more ethylene oxide is added to the NEO structure, some physical properties change. For example, the cloud point increases thereby changing the solubility of different components in NEO surfactants. The flash point also rises with the addition of ethylene oxide. The solidification point decreases until around 50% ethylene oxide in the NEO molecule, and higher content of ethylene oxide increases the solidification point. NEO surfactants containing greater than 75% ethylene oxide are solids at room temperature. NEO surfactants become water soluble when they contain about 50 per cent of ethylene oxide, the larger the amount of ethylene

oxide the better the water solubility (Porter, 1991). The molecular structure of NEO is represented in Figure 3.1. In this study NEO with 10 moles of ethylene oxide is used.

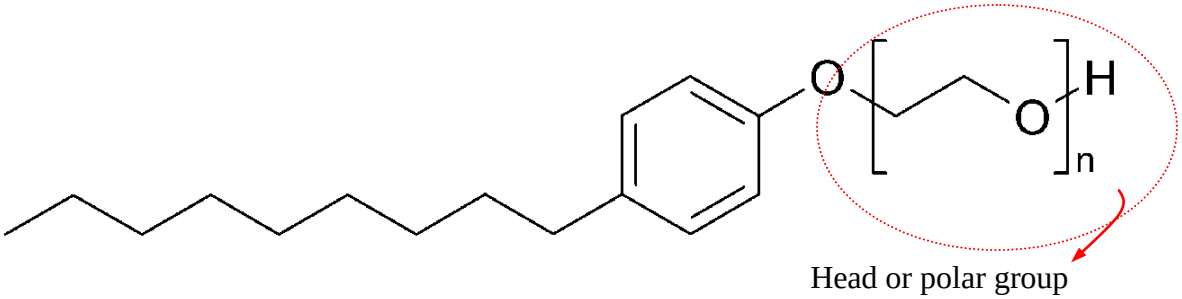

Figure 3.1 Molecular structure of nonylphenol ethoxylate with *n* ethoxy groups (*n* = number of ethylene oxide groups in the molecule).

3.1.1.2 Sodium Dodecylsulphate:

Sodium dodecylsulphate (SDS) is an anionic surfactant which is common in many household cleaning detergents. It contains 12 carbon atoms and has a chemical formula $CH_3(CH_2)_{11}OSO_3Na$. It is readily soluble in water and the partition coefficient in toluene is zero at a pH of 7 (Pollard *et al.,* 2006). The molecular structure is represented in Figure 3.2.

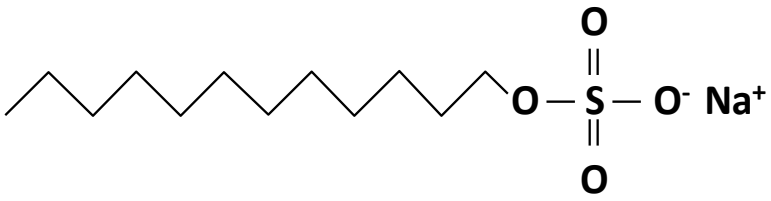

Figure 3.2 Molecular structure of sodium dodecylsulphate.

3.1.1.3 Triton X-100:

Triton X-100 (TX-100) is a non-ionic surfactant with a chemical formula $C_{14}H_{22}O(C_2H_4O)_{n,}$ with an average of *n*=9.5 ethylene oxide groups. It is a colourless or light yellow liquid at room temperature. Triton X-100 is soluble at 25°C in water, benzene, toluene, xylene, trichloroethylene, ethylene glycol, ethyl ether, ethanol, 2-propanol, and

ethylene dichloride. It has a partition coefficient of 0.62 in toluene at a pH of 7 (Pollard *et al.*, 2006). The molecular structure is shown in Figure 3.3.

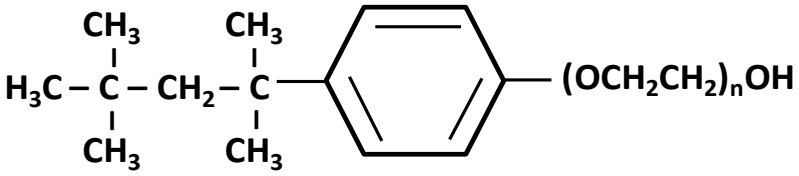

Figure 3.3 Molecular structure of Triton X-100.

3.1.1.4 Cetyltrimethylammonium Bromide

Cetyltrimethylammonium bromide (CTAB) is a cationic surfactant with a molecular formula $(C_{16}H_{33})$ N $(CH_3)_3Br$. It is soluble in water and has a partition coefficient of zero in toluene at pH of 7 (Pollard *et al.*, 2006). The molecular structure is shown in Figure 3.4.

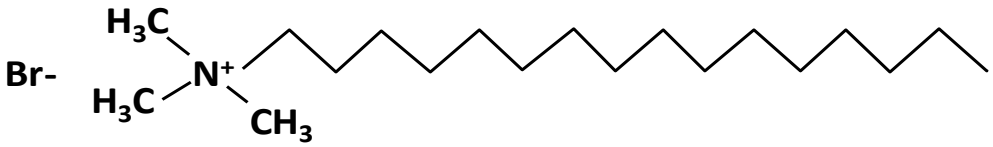

Figure 3.4 Molecular structure of CTAB.

3.1.1.5 5β-Cholanic acid:

5β-cholanic acid is a type of ionic surfactant which has been used by researchers to model the effect of naphthenic acids. It is also known as 17β-(1-methyl-3-carboxypropyl)etiocholane. In this acid, the COOH group is attached to a primary carbon. Therefore, it is less sterically hindered from aggregating at the oil-water interface and in the bulk and hence its propensity to aggregate at the oil-water interface and in the bulk is high (Varadaraj and Brons, 2007). This acid is oil soluble and has a water solubility of only 0.003352 mg/L at 25°C. The structure is shown in Figure 3.5.

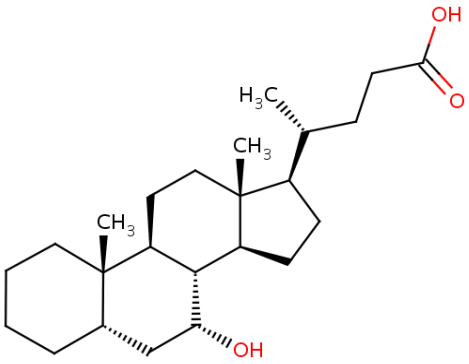

Figure 3.5 Molecular structure of 5β-cholanic acid.

3.2 Preparation of Asphaltene Samples

Asphaltenes were extracted from WC_B1 bitumen using *n*-heptane. The method is described in detail elsewhere (Alboudwarej *et al.*, 2003) and is summarised here. First, *n*-heptane is added to the crude oil at a 40:1 weight/volume ratio. After sonicating for 45 minutes at room temperature, the mixture is left to equilibrate for a contact time of 24 hours. The supernatant is filtered to obtain asphaltenes on a filter paper. The asphaltenes are then purified with toluene and centrifugation to remove solids.

3.3 Interfacial Tension Measurements

3.3.1 Principle of Drop Shape Analysis

The method used to measure the interfacial tension was drop shape analysis. To illustrate the method, consider the profile of an axisymmetric pendant droplet formed at the tip of a capillary (Figure 3.6). *P* is a point on the interface of the droplet with coordinates x_p and z_p, R_1 is the radius of curvature in the x-z plane, R_2 is the radius of curvature in the y-z plane and θ is the angle between R_2 and the z-axis.

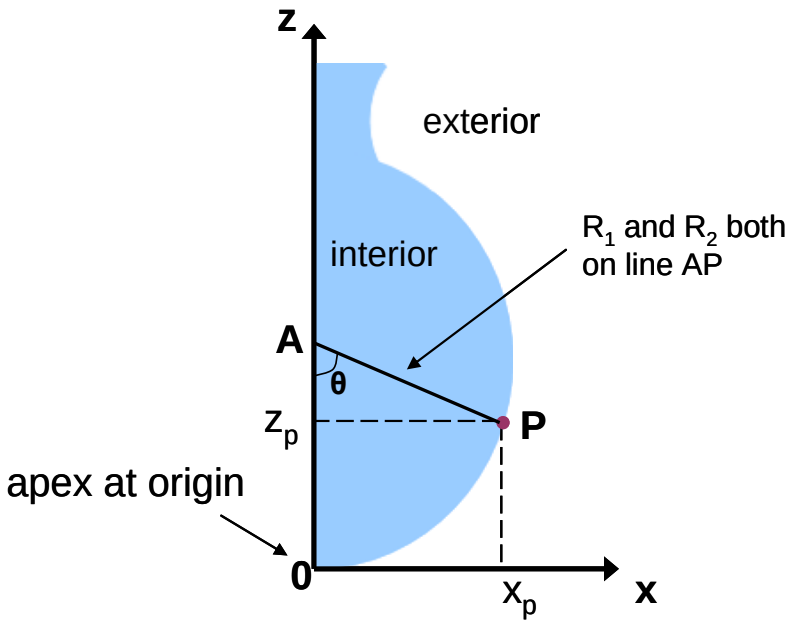

Figure 3.6 Schematic of an axisymmetric pendant droplet and its coordinates for drop shape analysis (adapted from Ortiz, 2009).

The shape of the droplet is governed by the balance between interfacial and gravity forces. The interfacial tension tends to give a spherical shape to the droplet whereas gravity elongates or broadens a droplet depending on the density difference between the phases and droplet configuration (pendant or sessile). The interfacial tension is determined from a force balance applied to any point on the interface.

According to the Laplace equation, when the radii of curvature are sufficiently large compared to the thickness of a non-homogenous film separating two bulk phases, the pressure difference across any point on a curved fluid interface is given by

$$\Delta P = \gamma \left(\frac{1}{R_1} + \frac{1}{R_2} \right) \qquad \textbf{Equation 3.1}$$

where R_1 and R_2 are the principal radii of curvature for the droplet, ΔP is the pressure difference across the fluid interface, and γ is the interfacial tension. The pressure

difference across the interface at any point is also related to the hydrostatic (gravity) forces as follows:

$$\Delta P = P_{exterior} - P_{interior} = \Delta P_{Apex} + \Delta \rho g z \qquad \textbf{Equation 3.2}$$

where, $\Delta\rho$ is the density difference between the two fluids given by:

$$\Delta \rho = \rho_{exterior} - \rho_{interior} \qquad \textbf{Equation 3.3}$$

where subscripts interior and exterior refer to the internal phase of the droplet and the surrounding fluid, respectively.

The two expressions for the pressure differences are equated at the apex of the droplet where $R_1 = R_2 = R_{apex}$ due to symmetry to obtain:

$$\Delta P_{Apex} = \left(\frac{2\gamma}{R_{apex}}\right) \qquad \textbf{Equation 3.4}$$

Equation 3.4 is substituted into Equation 3.2 to obtain the following expression which applies at any point on the interface:

$$\Delta P = \left(\frac{2\gamma}{R_{apex}}\right) + \Delta \rho g z = \gamma\left(\frac{1}{R_1} + \frac{1}{R_2}\right) \qquad \textbf{Equation 3.5}$$

To complete the analysis, the radius of curvature must be determined at any given point on the interface. Since point P varies with z, the two radii of curvature, R_1 and R_2, also vary with z. The following expressions for R_1 and R_2 are obtained from analytical geometry:

$$\frac{1}{R_1} = \frac{{}^{d^2z}/_{dx^2}}{\left[1 + \left({}^{dz}/_{dx}\right)^2\right]^{3/2}} \qquad \textbf{Equation 3.6}$$

$$R_2 = \frac{x}{\sin\theta} \qquad \textbf{Equation 3.7}$$

The radii of curvature, R_1 and R_2, are determined from the measured drop profile (a set of x and y coordinates) using Equations 3.6 and 3.7 respectively. The densities of the fluids

are known and R_{apex} is measured; therefore, the interfacial tension can be computed from Equation 3.5 The drop shape analyser used in this work uses the same principle, but in curvilinear coordinates instead of Cartesian coordinates. The interfacial tension is the value that minimises the error between the calculated and measured drop profiles.

3.3.2 Drop Shape Analyser

All interfacial tension measurements were performed on IT Concept (now known as Teclis) drop shape analyser (DSA) using Tracker software. The instrument is composed of five main parts, as shown in Figure 3.7: 1) syringe piston actuator, 2) sample cell, 3) light source, 4) lens and CCD camera and 5) instrument control with a personal computer and a manual motor control.

For the measurements of interfacial tension, a micro-syringe was fitted with a U-shaped needle and loaded with the less dense fluid, which in the present case was a hydrocarbon or crude oil. The syringe was placed in a motor driven piston (Part 1 in Figure 3.7) and the tip of the U-shaped needle was positioned in an optically clear quartz cuvette and immersed in the aqueous phase (Part 2). The hydrocarbon droplet is formed at the tip of the needle. The light source, Part 3, uniformly illuminated the droplet and the CCD camera, Part 4, captured the drop profile. The image was then analysed using drop shape analysis software to determine the interfacial tension, drop surface area, and the drop volume. The apparatus was placed on an anti-vibration bench to avoid disturbances during measurements. The configuration of a droplet can be either pendant (extending from the capillary in the buoyant direction, elongated) or sessile (resting on the capillary counter to the buoyant direction, oblate) depending on the relative densities of the two fluids. The configuration used in this work was a rising pendant droplet.

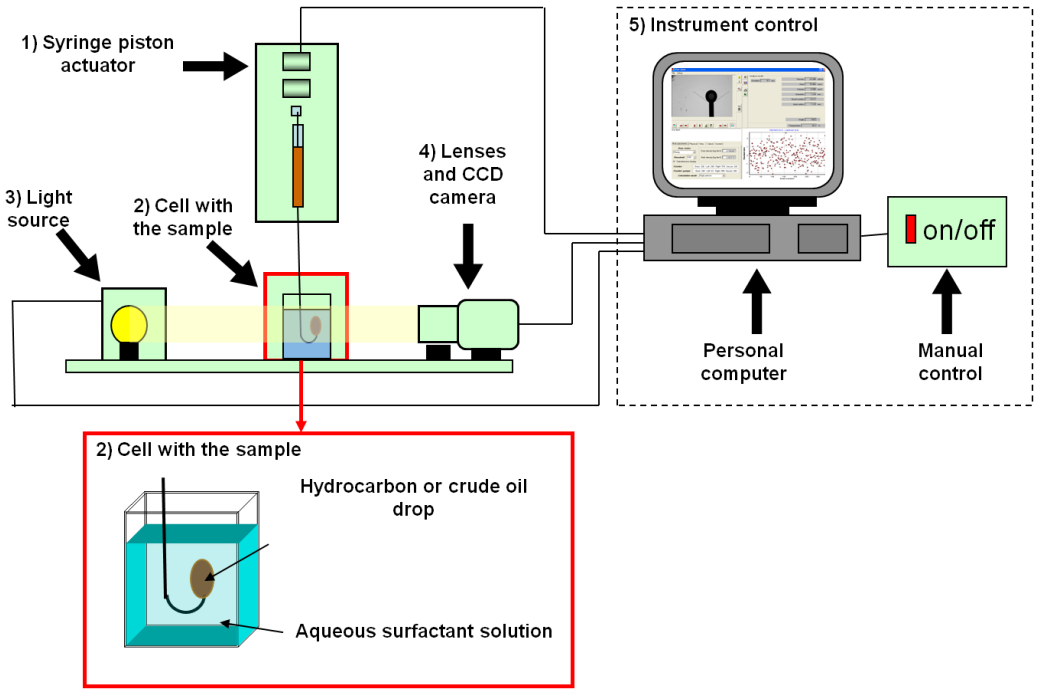

Figure 3.7 Diagram of the drop shape analyser.

The drop shape analyser apparatus runs on three different modes of calculation: high precise, precise and normal. These calculation modes account for the precision in which the Laplace equation is solved and the number of iterations done per second to converge the solution, thus determining the speed and accuracy of the measurement. High-precise and precise mode allows a very high precision and performs up to 20 and 15 iterations per second, respectively. Normal mode allows a slightly less precise measurement and performs up to 10 iterations per second. In the present work, the high precise mode was used for measuring the interfacial tension.

3.3.3 Interfacial Tension Measurement Procedure

The preparation of the solutions and the apparatus and the procedure for the measurement of interfacial tension is described in this section.

Preparation of Solutions

The heptol50 solution was prepared by mixing equal volumes of *n*-heptane and toluene together in a glass vial. The heptol50 solution was used within a day or two to avoid changes in concentration due to different volatility of the components.

To prepare the salt solutions, the salts were exactly weighed and dissolved in an appropriate mass of water and shaken until completely dissolved. The range of concentration of salt solutions was between 0.1 and 15% by weight. The surfactant solution was prepared in a similar manner, but was dissolved in the brine of interest (for water soluble surfactants). The lower concentrations were prepared by serial dilution by diluting the stock solutions. The surfactant concentrations ranged from 10^{-6} to 1% by weight (*i.e.*, from 0.01 to 10,000 ppm). Oil-soluble surfactant solutions were prepared similarly, but in the hydrocarbon phase. All the concentrations used were below the critical micelle concentration.

To compensate for diffusion effects, before performing the experiments the two phases were presaturated with the other phase. This involved adding two drops of each phase into the other phase and letting the solution sit for at least an hour to equilibrate before the measurement was made.

Preparation of the Drop Shape Analyser

In order to obtain accurate and reproducible measurements, the accessories of the instrument were rigorously cleaned. The syringe, needle and cuvette were carefully washed sequentially and repeatedly with hot water, 2-propanol and toluene. The accessories were also flushed with reverse osmosis water. The parts were then dried by vacuum. The cuvette was soaked in 6M nitric acid overnight periodically for enhanced cleaning. The cleanliness of the instrument was verified by measuring the interfacial tension of a pure solvent (usually toluene) versus water and comparing it to the literature value. For instance, the interfacial tension for toluene versus water was measured with

the drop shape analyser and the average value was found to be 35.1 mN/m at 25 ^{o}C, which was close to the literature value of 35.8 mN/m (Li and Fu, 1992).

Interfacial Tension Measurements

The hydrocarbon phase was loaded into a syringe with a U-shaped needle and was immersed in aqueous solution (containing salt and/or surfactants) in a cuvette. A droplet was then formed at the tip of the needle using the motor control. The volume of the droplet was selected to be small enough to remain on the tip of the needle throughout the experiment, but large enough to provide a large profile and an accurate value of interfacial tension. The droplets were typically 8-10 μL for the model hydrocarbon/brine systems.

Figure 3.8 shows a typical drop profile.

The interfacial tension was recorded long enough to obtain an equilibrium value, usually 2 hours. In some of the experiments, equilibrium was not reached within two hours. Therefore, in all cases, an exponential decay model (described in literature review chapter) was fitted to the data collected after the first ten minutes to obtain the equilibrium interfacial tension value. The data fitting is discussed in Chapter 4. Some of the experiments were done more than once to check the repeatability. The statistical analysis is presented in Appendix B.

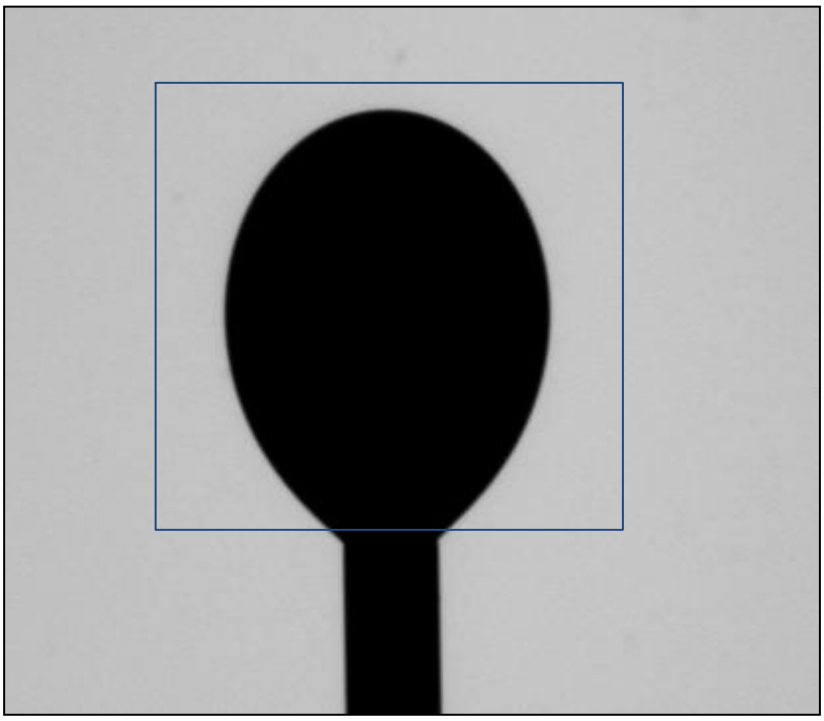

Figure 3.8 Typical drop profile obtained using the drop shape analyser. The box defines the portion of the drop profile to be analysed.

3.4 Other Measurements

Density of brine and surfactant solutions as well as decane diluted crude oils was measured using an Anton Paar DMA46 density meter at ambient conditions. The total acid numbers (TAN) of the crude oil samples were measured using ASTM D664 by Metrotech Systems Ltd., Calgary.

Chapter Four: Results and Discussion

This chapter introduces a Gibbs-Langmuir type model for the effect of salts and surfactants on the interfacial tension (IFT) of hydrocarbons versus brine. Data on the interfacial tension (IFT) of hydrocarbon/brine systems and hydrocarbon/brine/surfactant systems are presented and modeled. Then, IFT data are presented for crude oil/brine systems which are interpreted based on the observations from the hydrocarbon/brine/surfactant dataset.

4.1 Model Development

Yarranton and Masliyah (1996) showed that for an organic phase with a surface active component, the IFT is related to the concentration of the surface active component as follows:

$$\gamma = \gamma^o - RT\Gamma_{m,S} \ln (1 + K_S^{org} x_S^{org}) \qquad \textbf{Equation 4.1}$$

where γ^o is the IFT between pure solvent and water, R is the universal gas constant, T is the absolute temperature, and $\Gamma_{m,S}$, K_S^{org}, and x_S^{org} are the monolayer surface excess concentration, adsorption constant, and mole fraction in the organic phase, respectively, of the surface active component.

Brine: The same logic is applied to the aqueous phase to relate IFT between a hydrocarbon (HC) and brine to the brine concentration:

$$\gamma_{salt}^o = \gamma^o - RT\Gamma_{m,salt} \ln (1 + K_{salt} x_{salt}) \qquad \textbf{Equation 4.2}$$

where γ_{salt}^o is the IFT of the HC/brine system, K_{salt} is the adsorption constant of the salt, x_{salt} is the mole fraction of the salt in the aqueous phase, and $\Gamma_{m,salt}$ is the monolayer surface excess concentration of the salt.

Non-Ionic Surfactants: For hydrocarbon/brine with a non-ionic surfactant, it is assumed that the brine and the surfactant do not interact and that the IFT can be modeled as follows:

$$\gamma = \gamma^{o}_{salt} - RT\Gamma_{m,S} \ln (1 + K_S^{org} x_S^{org}) \qquad \textbf{Equation 4.3}$$

Note, the surfactant will partition between the bulk phases and the equilibrium condition is given by:

$$K_e = \frac{x_S^{org}}{x_S^{aq}} \qquad \textbf{Equation 4.4}$$

where K_e is the partitioning coefficient and x_S^{aq} is the mole fraction of surfactant in the aqueous phase. Hence, Equation 4.3 can also be expressed as:

$$\begin{aligned} \gamma = \gamma^{o}_{salt} - RT\Gamma_{m,S} \ln(1 + K_S^{org} K_e x_S^{aq}) \\ = \gamma^{o}_{salt} - RT\Gamma_{\mathrm{m,S}} \ln (1 + K_S^{aq} x_S^{aq}) \end{aligned} \qquad \textbf{Equation 4.5}$$

where $K_S^{aq} = K_S^{org} K_e$. Therefore, the IFT can be related to the equilibrium concentration of the surfactant in either of the bulk phases.

Ionic Surfactants: For a hydrocarbon/brine system with an ionic surfactant, the ionic surfactants form a charged monolayer at the interface which is expected to mitigate the salt depletion effect at the interface. Recall that salt is depleted near the interface because the hydrogen bonding network in the water is disrupted. A charged interface tends to restore this network. It is assumed that the salt depletion effect is proportional to the area left unoccupied by the surfactant and Equation 4.2 is modified as follows:

$$\gamma^{s}_{salt} = \gamma^{o} - RT(1 - \theta_s)\Gamma_{m,salt} \ln (1 + K_{salt} x_{salt}) \qquad \textbf{Equation 4.6}$$

where γ^{s}_{salt} is the IFT of the HC/brine system (excluding the effect of any surfactant) when the interface is partially covered with an ionic surfactant, and θ_s is the fractional surface coverage of the ionic surfactant. When the ionic surfactant is the only strongly

surface active component, the fractional surface coverage of the surfactant is approximated by:

$$\theta_s = \frac{K_s x_s}{1 + K_s x_s} \qquad \textbf{Equation 4.7}$$

Equation 4.6 is substituted into Equation 4.3 or 4.5 to obtain the following expressions for the IFT of the solution:

$$\gamma = \left(\gamma^o - RT(1-\theta_s)\Gamma_{m,salt} \ln(1 + K_{salt} x_{salt}) \right) - RT\Gamma_{m,S} \ln\left(1 + K_S^{org} x_S^{org}\right) \qquad \textbf{Equation 4.8}$$

$$\gamma = (\gamma^o - RT(1-\theta_s)\Gamma_{m,salt}\, ln\, (1 + K_{salt} x_{salt})) - RT\Gamma_{\mathrm{m,S}} \ln\,(1 + K_S^{aq} x_S^{aq}) \qquad \textbf{Equation 4.9}$$

4.2 Hydrocarbon/Brine Systems

The IFT of four model hydrocarbons was measured against pure water and brine. Three sets of brines were prepared at 0.1, 5, 10 and 15 wt% salt content, one with sodium chloride, one with calcium chloride, and one with sodium sulphate. The densities of the brines and hydrocarbons were required to calculate the IFT from the drop profile. The densities of the aqueous solutions were measured and are given in Table 4.1. The densities of pure hydrocarbons were taken from the literature (CRC Handbook of Chemistry and Physics) and are reported in Table 4.2.

Table 4.1 Density (g/cm^3) of salt solutions as measured using a density meter

Concentration	Sodium Chloride	Calcium Chloride	Sodium Sulphate
0	0.9978	0.9978	0.9978
0.1	0.9988	0.9992	0.9993
1	1.0054	1.0059	1.0072
5	1.0360	1.0382	1.0439
10	1.0683	1.0795	1.0901
15	1.1068	1.1243	1.1346

Table 4.2 Density ($g/cm^{3)}$ of hydrocarbons used in this study at room temperature.

Hydrocarbon	Density
Toluene	0.867
Heptane	0.684
Cyclohexane	0.779
Decane	0.726
50:50 Heptol	0.775

The IFT with hydrocarbon brine systems reached a stable value in less than 50 seconds and this value was taken to be the equilibrium IFT. The effect of salt concentration (NaCl, $CaCl_2$, and Na_2SO_4) on the equilibrium IFT of pure hydrocarbons versus water at 23°C and atmospheric pressure is shown in Figures 4.1 to 4.4 for toluene, *n*-heptane, cyclohexane, and heptol50 respectively. The error bars represent an 85% confidence interval (1.5 times the standard deviation) based on several sets of data with at least three repeats. The data are also provided in Appendix A.

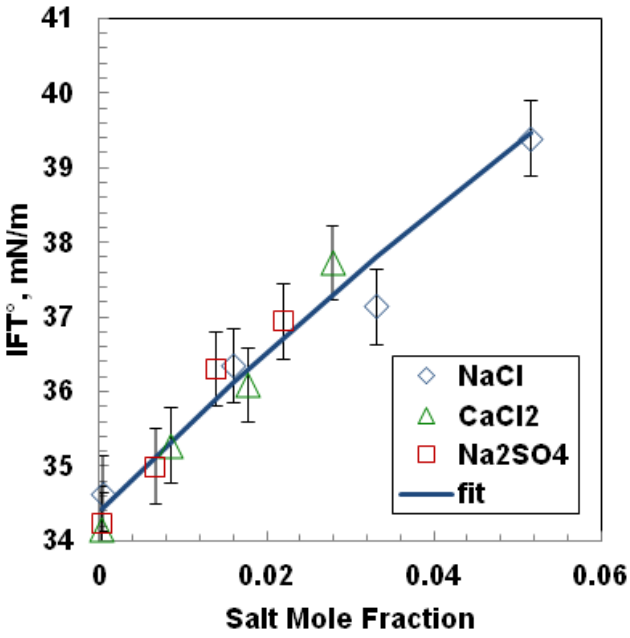

Figure 4.1 Measured (symbols) and modeled (line) effect of salt concentration on interfacial tension of toluene versus brine.

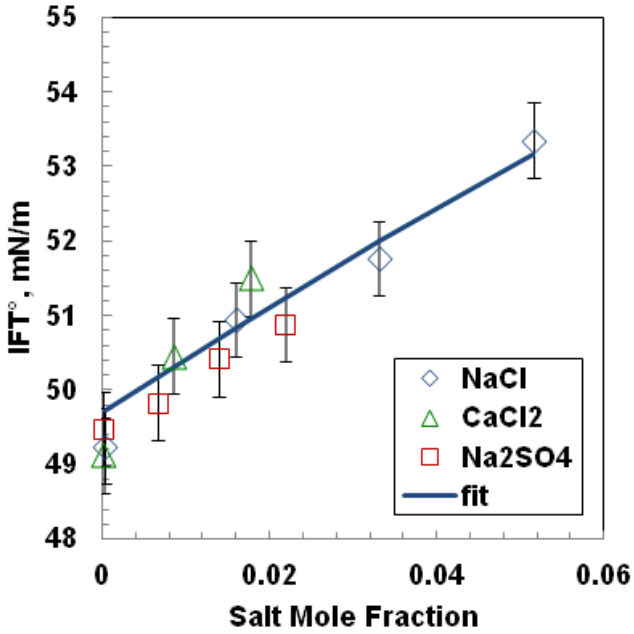

Figure 4.2 Measured (symbols) and modeled (line) effect of salt concentration on interfacial tension of *n*-heptane versus brine.

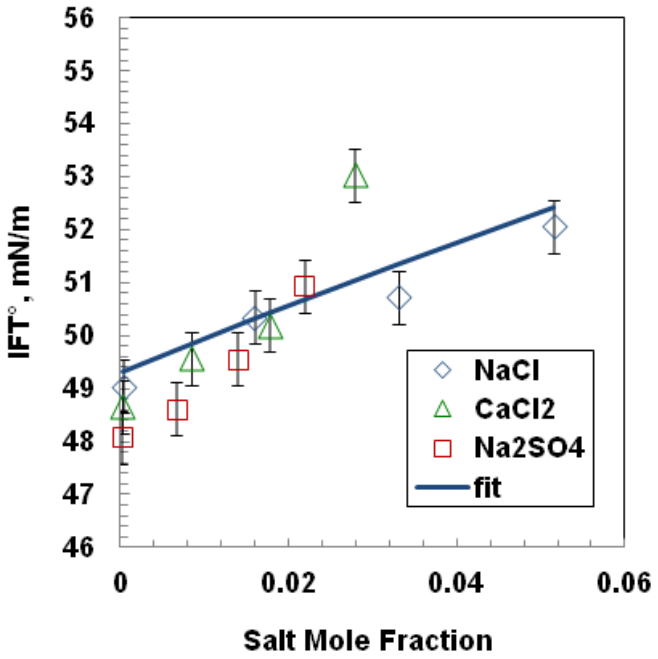

Figure 4.3 Measured (symbols) and modeled (line) effect of salt concentration on interfacial tension of cyclohexane versus brine.

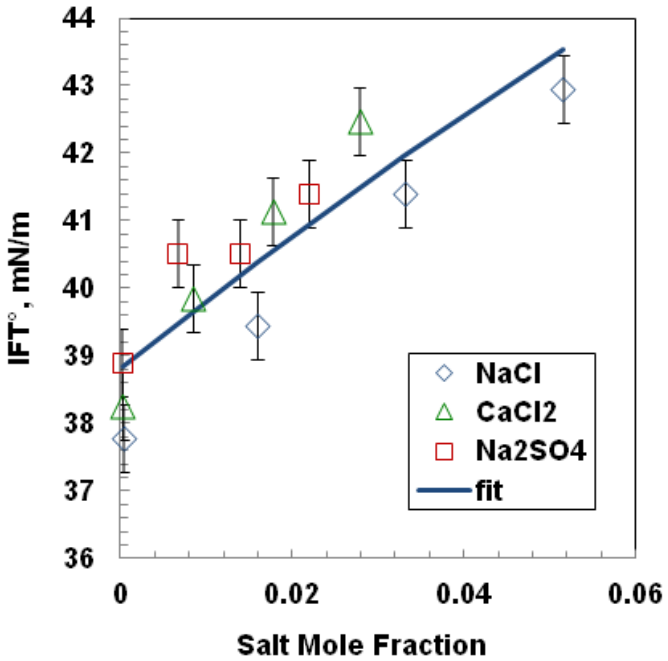

Figure 4.4 Measured (symbols) and modeled (line) effect of salt concentration on interfacial tension of heptol50 versus brine.

In all cases, the IFT increases almost linearly with increasing salt mole fraction in the solution. The IFT data were fitted with Equation 4.2 using a $\Gamma_{m,salt}$ of -4.0·10^{-6} mol/m² in all cases and different values of K_{salt} for each solvent. The value of $\Gamma_{m,salt}$ is approximately double that of a typical surfactant (equivalent to a molecular cross-section half the size) which is reasonable for an ion. A uniform value of $\Gamma_{m,salt}$ was found to be adequate to fit the data for all three salts. Note, some theories (Hiemenz and Rajagopalan, 1997) predict a slope of -$RT\Gamma_{m,salt}$ for monovalent ions and -$2RT\Gamma_{m,salt}$ for divalent ions but a slope of -$RT\Gamma_{m,salt}$ was found to fit the data in all cases examined in this thesis.

The fitted values of K_{salt} are provided in Table 4.3. The maximum absolute relative deviation was less than 4%. The average value of K_{salt} was 4.43 and if the data are modeled with this value, the average and maximum deviation are 1.3% and 3.2%, respectively. Note, while the average deviation increased, the maximum deviation decreased. Hence, the effect of salt concentration on the IFT of pure hydrocarbons versus brine can be modeled with acceptable accuracy with the following expression:

$$\gamma^{o}_{salt} = \gamma^{o} - 0.0334T \ln(1 + 4.43x_{salt}) \qquad \textbf{Equation 4.10}$$

where γ has units of mN/m and T is in K.

Table 4.3 Salt adsorption constant (K_{salt}) and average absolute relative deviation (AARD) for various hydrocarbons considered in this study.

Hydrocarbon	γ^{o}(mN/m)	K_{salt}	AARD (%)
Toluene	34.4	5.60	0.70
Heptane	49.7	3.67	0.63
Cyclohexane	49.3	3.27	1.27
Heptol50	38.8	5.19	1.53
Average		**4.43**	

4.3 Hydrocarbon/Surfactant/Brine Systems

Since the salt effect was similar for all three salts considered, the effect of surfactants was investigated with only one salt, NaCl. Typical plots of interfacial tension versus time for surfactant solutions are shown in Figure 4.5. Although IFT measurements were recorded over 1 hour, data are shown to 1000 seconds here because the most significant changes occur at early times. The IFT trends over time were fitted with Equation 2.15 to determine the equilibrium IFT value, as shown in Figure 4.6. Only equilibrium values are reported hereafter.

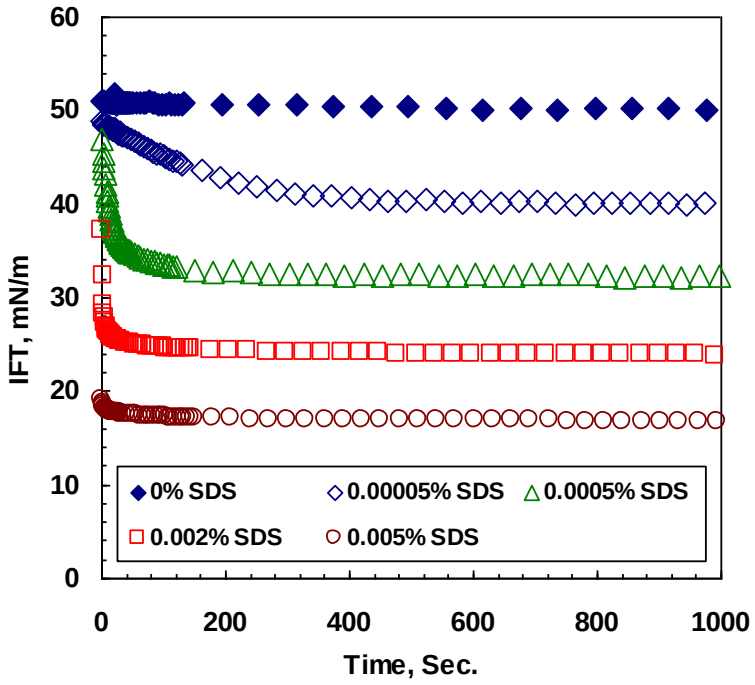

Figure 4.5 The change in interfacial tension over time of n-heptane versus 1 wt% NaCl in water with SDS concentrations from 0 to 0.005 wt%.

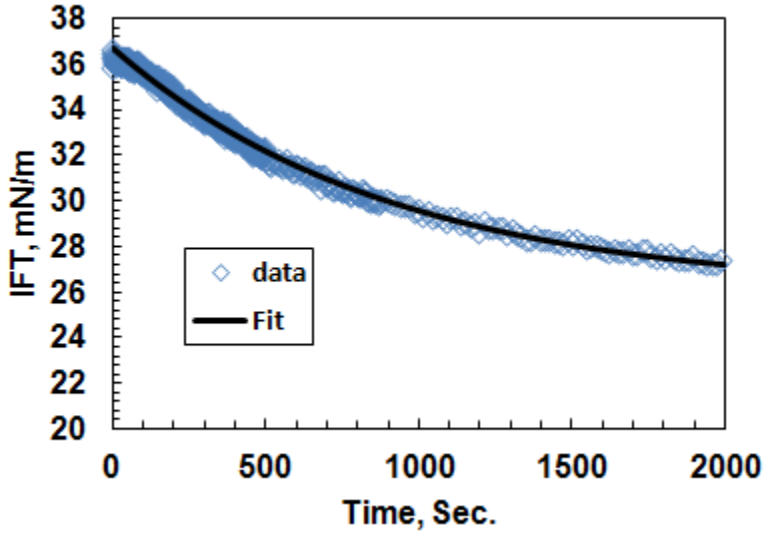

Figure 4.6 The dynamic interfacial tension of toluene versus water. The data are fit with the exponential model, Equation 2.15.

The IFT data were modeled using Equations 4.3, 4.5, 4.8, or 4.9 as appropriate. All of these equations include a monolayer surface excess concentration and an adsorption constant for the surfactant. Surfactants adsorb strongly at the interface and therefore the product of the adsorption constant and the surfactant mole fraction, $K_S x_S$, is much greater than unity even at relatively low surfactant concentrations. In this case, the derivative of Equation 4.1 simplifies to:

$$\Gamma_{m,S} = -\frac{1}{RT}\left(\frac{d\gamma}{dlnx_S^{org}}\right) = -\frac{1}{RT}\left(\frac{d\gamma}{dlnx_S^{aq}}\right) \qquad \textbf{Equation 4.11}$$

Note, at dilute conditions, the mole fraction is proportional to concentration and Equation 4.11 can be expressed in terms of concentration as follows:

$$\Gamma_{m,S} = -\frac{1}{RT}\left(\frac{d\gamma}{dlnC_S^{org}}\right) = -\frac{1}{RT}\left(\frac{d\gamma}{dlnC_S^{aq}}\right) \qquad \textbf{Equation 4.12}$$

where C_S is the equilibrium surfactant concentration in the solution. Equation 4.12 is the well known Gibbs adsorption isotherm. In this thesis and in all cases, the value of $\Gamma_{m,S}$

for a given surfactant was determined from the slope of the linear region in a plot of IFT versus surfactant mole fraction or concentration for a water/hydrocarbon system, such as Figure 4.7. The value of the adsorption constant was determined from fitting the whole trend of IFT versus mole fraction.

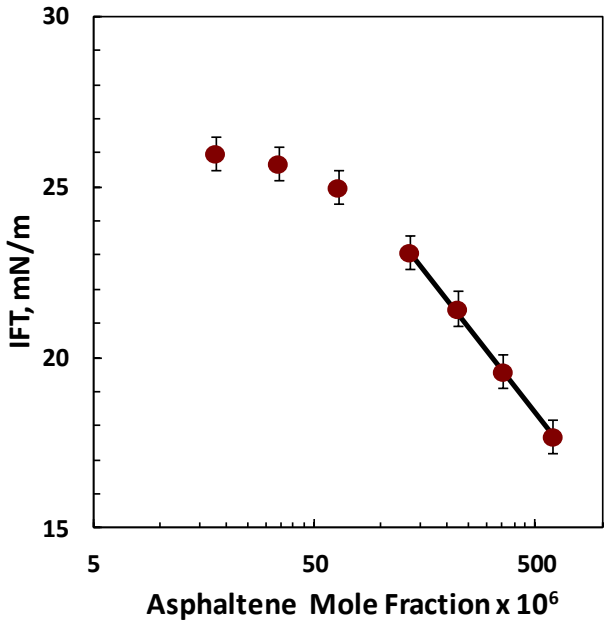

Figure 4.7 Interfacial tension of toluene versus water and varying amounts of asphaltenes. The value of surface excess can be determined from the slope of the linear region.

4.4 Interfacial Tension of Hydrocarbon versus Brine with Non-Ionic Surfactants

Nonylphenol ethoxylate (NEO10) was selected to study the effect of a non-ionic surfactant on the IFT of toluene versus brine systems, Figure 4.8. NEO10 is water soluble and the IFT was modeled based on its concentration in the aqueous phase. As expected with a surfactant, the IFT decreased dramatically at low concentrations of added surfactant. The monolayer surface excess concentration was $6 \cdot 10^{-7}$ mol/m². This value is in close agreement to the value of $7.3 \cdot 10^{-7}$ calculated using data reported for water solutions of nonylphenol ethoxylates versus air, by Calvo *et al*. (2009).

Figure 4.8 shows that the IFT increased as salt was added at any given surfactant concentration and the IFT decreased as surfactant was added at any given salt concentration. In other words, there was no interaction between the salt and the non-ionic surfactant, and the data could be modeled with Equation 4.5. Consistent with the observed lack of interaction between salt and the non-ionic surfactant, the adsorption constant K_S^{aq}, was found to be independent of salt concentration. The value of K_S^{aq} was $4.15 \cdot 10^9$ and the average absolute relative deviation (AARD) of the fitted model was 2.2%.

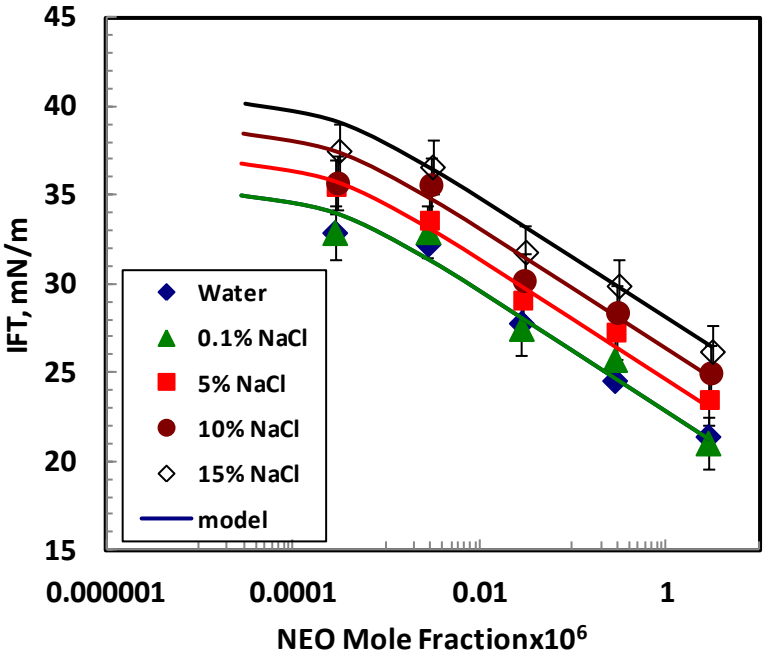

Figure 4.8 Measured (symbols) and modeled (lines) effect of NEO10 concentration on the interfacial tension of toluene versus NaCl brine.

To verify the findings for non-ionic surfactants, the IFT of another non-ionic surfactant, Triton X-100, in NaCl brines versus toluene were measured (Figure 4.9). The results were similar to those for NEO10. The value of K_S^{aq} for this surfactant was found to be $2.5 \cdot 10^9$ and the AARD of the fitted model was 2.6%. Table 4.4 summarises the model parameters and AARD for the non-ionic surfactants.

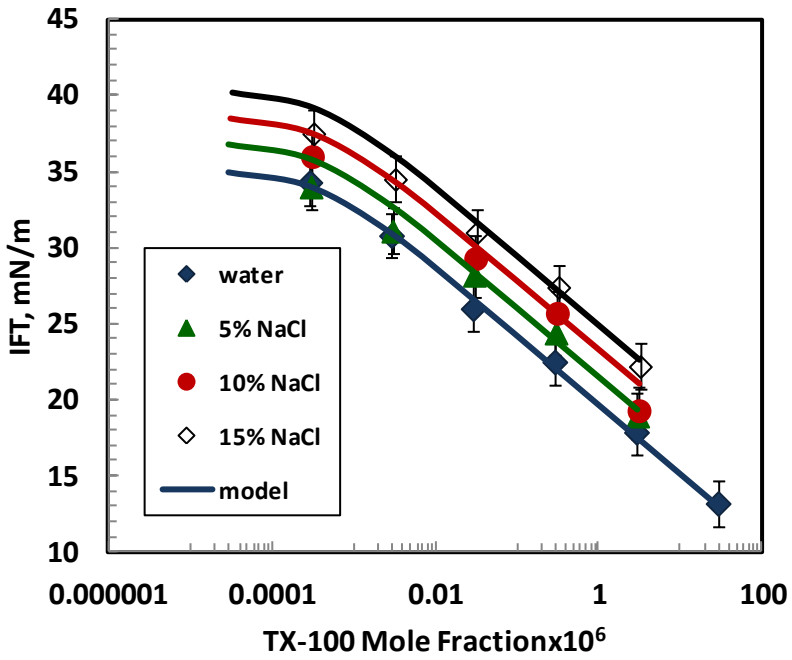

Figure 4.9 Measured (symbols) and modeled (lines) effect of Triton X-100 concentration on the interfacial tension of toluene versus brine.

Table 4.4 Model parameters and AARD for IFT of non-ionic surfactants in NaCl brines versus toluene.

Surfactant	$\Gamma_{m,S}$ (mol/m^2)	K_s	AARD (%)
NEO 10	$6 \cdot 10^{-7}$	$4.2 \cdot 10^{9}$	2.2
Triton X-100	$8 \cdot 10^{-7}$	$2.5 \cdot 10^{9}$	2.6

4.5 Interfacial Tension of Hydrocarbon versus Brine with an Ionic Surfactant

Strong Anionic Surfactant – Sodium Dodecylsulphate (SDS)

Sodium dodecylsulphate was chosen to study the effects of anionic surfactant on the IFT of toluene versus NaCl brine systems (Figure 4.10). Like NEO10, SDS is water soluble and the IFT was modeled based on its concentration in the aqueous phase. The monolayer

surface excess concentration was $2.5 \cdot 10^{-6}$ mol/m². The same value was reported by Bonfillion *et al*. (1994) for a system of dodecane and SDS.

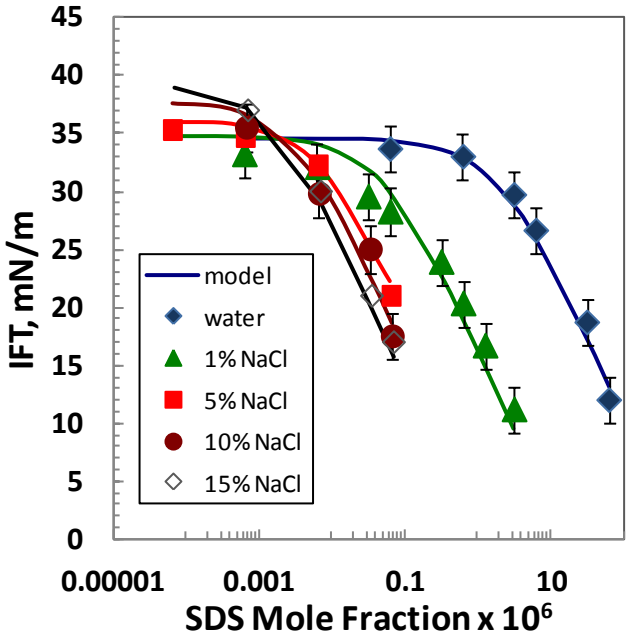

Figure 4.10 Measured (symbols) and modeled (lines) effect of SDS concentration on the equilibrium interfacial tension of toluene versus brine.

At low surfactant concentrations, the IFT increased as the salt concentration increased, just as observed with brine or with a non-ionic surfactant. However, at higher surfactant concentrations, the IFT decreased with increased salt concentration. Hence, the IFT curves at different salt concentrations cross-over each other. There appear to be two factors contributing to this behaviour. First, adsorption of an ionic surfactant at the interface eliminates the salt effect. Second, the surfactant adsorbs more strongly at higher salt concentrations because it is less ionized. When a water soluble surfactant is less ionized, it becomes less water soluble and will adsorb more strongly at the interface. The adsorption constant, K_S^{aq}, was found to vary linearly with the mole fraction of counter ion in the solution as follows:

$$K_S^{aq} = A_1 + A_2 x_{counterion} \qquad \textbf{Equation 4.13}$$

where A_1 and A_2 are constants unique to the given surfactant and solvent. The dependence of adsorption constant on the counter ion mole fraction is discussed in more detail later. Equation 4.13 was fitted to the experimental values of K_S^{aq} (Figure 4.11), which are provided in Table 4.5. A linear relationship of the adsorption constant to salt content was also observed by Prosser *et al*. (2001) for the surface tensions of SDS/NaCl/water versus air. The fitted K_S^{aq} values were then used to model the IFT data using Equation 4.9 as shown in Figures 4.10.

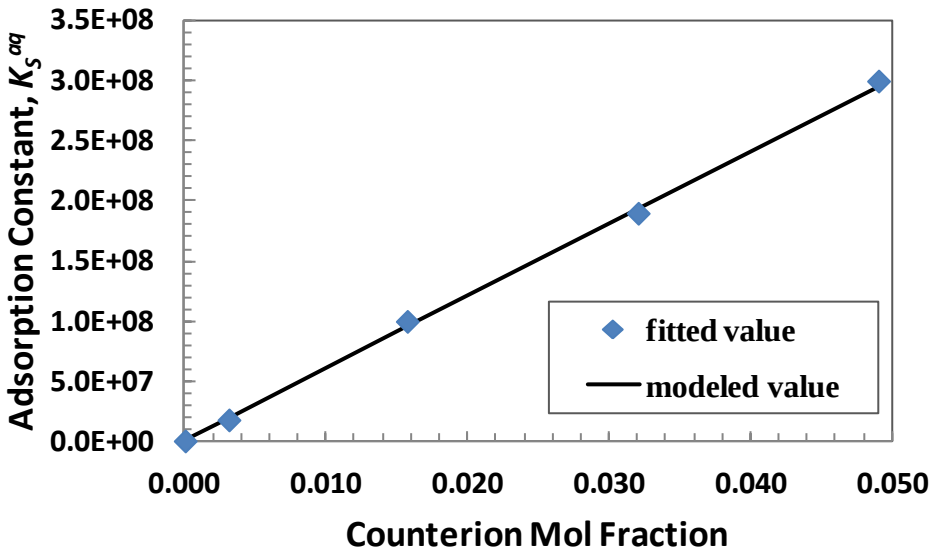

Figure 4.11 The effect of salt counterion concentration (Na^+) on K_S^{aq} for toluene versus NaCl brine with SDS. The data points are values fitted to IFT data and the line is Equation 4.13 fitted to the K_S^{aq} values.

Table 4.5 Model parameters and AARD for IFT of SDS in NaCl brines versus four hydrocarbon solvents.

Hydrocarbon	$A1$	$A2$	AARD (%)
Toluene	$5.0 \cdot 10^{5}$	$6.0 \cdot 10^{9}$	5.2
Heptane	$2.5 \cdot 10^{6}$	$3.0 \cdot 10^{10}$	4.7
Cyclohexane	$3.0 \cdot 10^{6}$	$4.0 \cdot 10^{10}$	5.6
Heptol	$1.0 \cdot 10^{6}$	$1.1 \cdot 10^{10}$	5.2

As a further test, the IFT were measured for other hydrocarbon versus NaCl brines, Figures 4.12 to 4.14. The trends in the IFT data were the same as observed in toluene. The monolayer coverage was also the same for all solvents. The data were again modeled with Equation 4.9 and the values of the coefficients of the adsorption constant correlation, Equation 4.13, were adjusted to fit the data, Table 4.5. Overall, this simple model fit the data with a maximum deviation of 20%.

It is interesting that all of the data could be fitted with a constant value of the surfactant monolayer surface excess concentration. This observation suggests that the surfactant layer at the interface does not compress or expand significantly when salt is added to the system. If this conclusion holds, relatively simple models are likely to be sufficient for most applications of crude oils and brines.

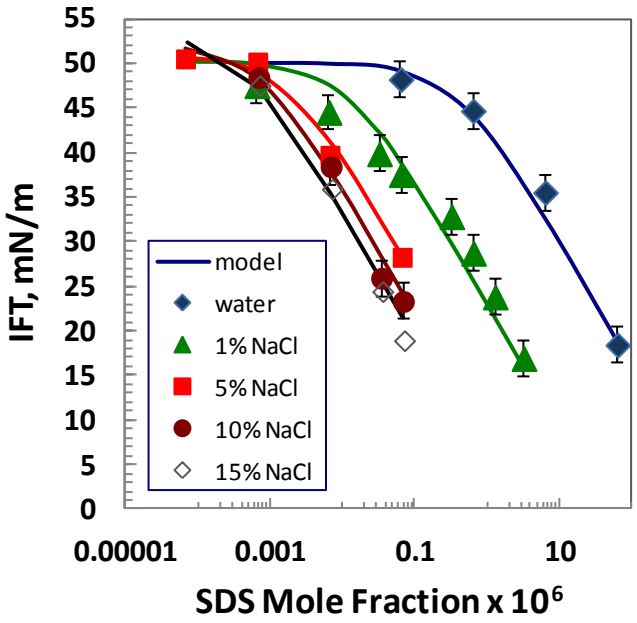

Figure 4.12 Measured (symbols) and modeled (lines) effect of SDS concentration on the equilibrium interfacial tension of heptane versus NaCl brine.

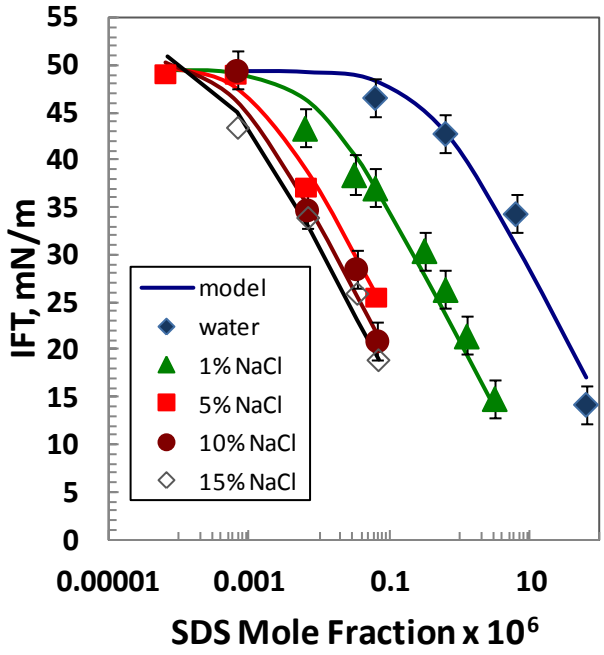

Figure 4.13 Measured (symbols) and modeled (lines) effect of SDS concentration on the equilibrium interfacial tension of cyclohexane versus NaCl brine.

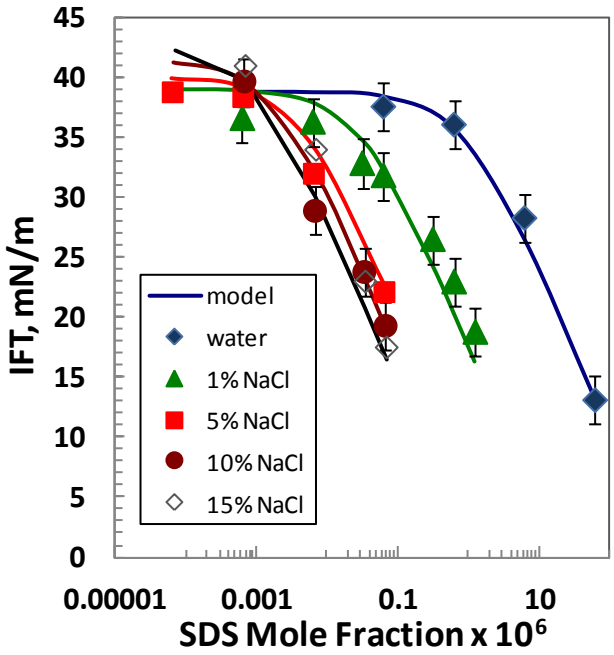

Figure 4.14 Measured (symbols) and modeled (lines) effect of SDS concentration on the equilibrium interfacial tension of heptol50 versus NaCl brine.

Strong Cationic: Cetyltrimethylammonium Bromide (CTAB)

The behaviour of CTAB was found to be similar to SDS, but the effect of salt concentration was much more pronounced, Figure 4.15. Note, the IFT could not be measured at salt concentrations above 5 wt% because the interfacial tension became too low to form a stable drop. The monolayer surface excess concentration was found to be the same as SDS ($2.5 \cdot 10^{-6}$ mol/m²). This value is slightly lower than the value of $3.1 \cdot 10^{-6}$ mol/m² reported for air/water surface by Szymczyk *et al*. (2007). This difference is in accordance with the findings of Van Voorst Vander (1960) that the saturation adsorption increases with increase in surface tension between two phases. Air/water surface tensions are larger than hydrocarbon/water tensions and therefore greater surfactant monolayer coverage is to be expected.

The data were again modeled using Equation 4.9. The fitted K_S^{aq} values were higher than those found for SDS indicating that CTAB is a stronger surfactant; that is; it reduces IFT

more than SDS at the same concentration. The adsorption constant was correlated to the mole fraction of counterion in the solution with the following exponential function:

$$K_S^{aq} = A_1 + A_2(1 - \exp(-A_3 x_{counterion})) \qquad \textbf{Equation 4.14}$$

where A_1, A_2, and A_3 are constants unique to the given surfactant and solvent. The IFT data were then remodelled with the correlated adsorption constants, K_S^{aq}, Figure 4.15. Figure 4.16 shows the fitted K_S^{aq} value and the fitting parameters are summarised in Table 4.6. The model fits the IFT data with an average deviation of 5.7%.

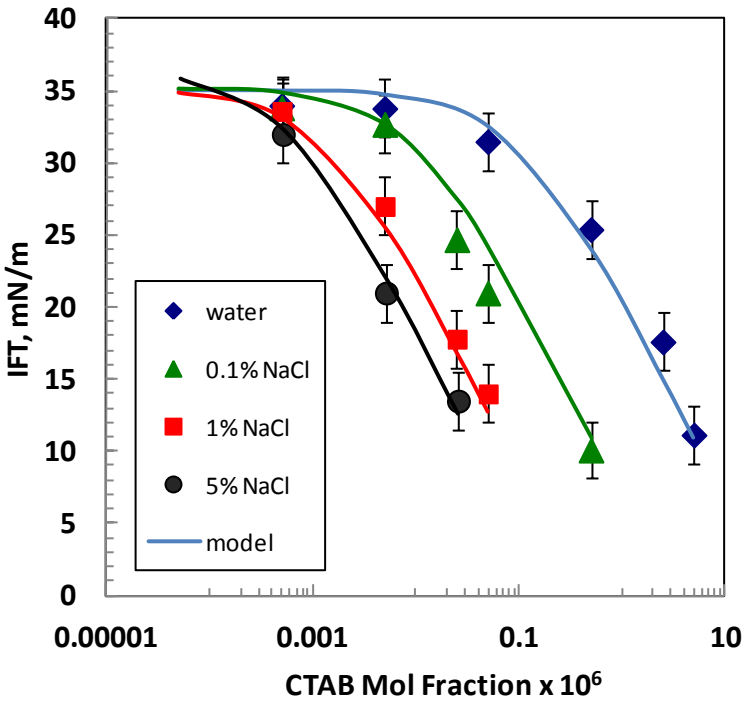

Figure 4.15 Measured (symbols) and modeled (lines) effect of CTAB concentration on the interfacial tension of toluene versus NaCl brine.

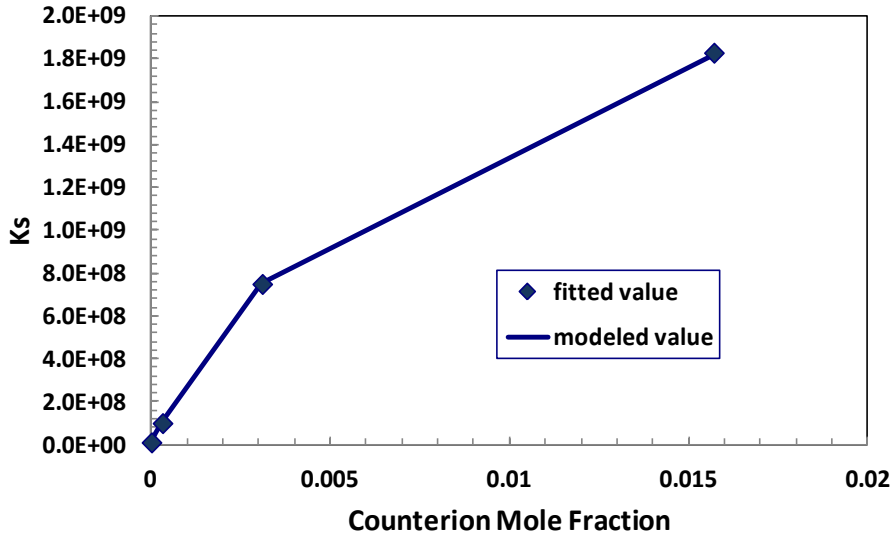

Figure 4.16 The effect of salt counterion concentration (Cl^-) on K_S^{aq} for toluene versus NaCl brine with CTAB. The data points are values fitted to IFT data and the line is Equation 4.14 fitted to the K_S^{aq} values.

Table 4.6 Model parameters and AARD for IFT of CTAB in NaCl brines versus toluene.

Hydrocarbon	A_1	A_2	A_3	**AARD (%)**
Toluene	$1.0 \cdot 10^7$	$2.0 \cdot 10^9$	$1.5 \cdot 10^2$	5.7

Effect of Counterions on IFT

The adsorption constant of an ionic surfactant was observed to depend on the salt concentration. With NaCl, it is not obvious if the constant depends on the total salt concentration or the counter ion concentration. Given that the surfactant forms a charged layer at the interface, it is expected that the adsorption constant (and therefore the IFT at constant surfactant concentration) should depend on the counter ion concentration. To test this hypothesis, the IFT of toluene with 0.0001 wt% SDS or CTAB was measured at varying concentrations of NaCl, Na_2SO_4, and $CaCl_2$. Note, since the valences of the ions are not all equal, the counter ion concentrations are different than the salt concentrations.

It was found that the IFT depended on the counter ions mole fraction and the dependence was the same for all the salts for a given surfactant, Figure 4.17. In other words, the adsorption constant followed the same relationship to the counter ion concentration. Note, SDS was not soluble in solutions of $CaCl_2$ and therefore the IFT could not be measured for that system.

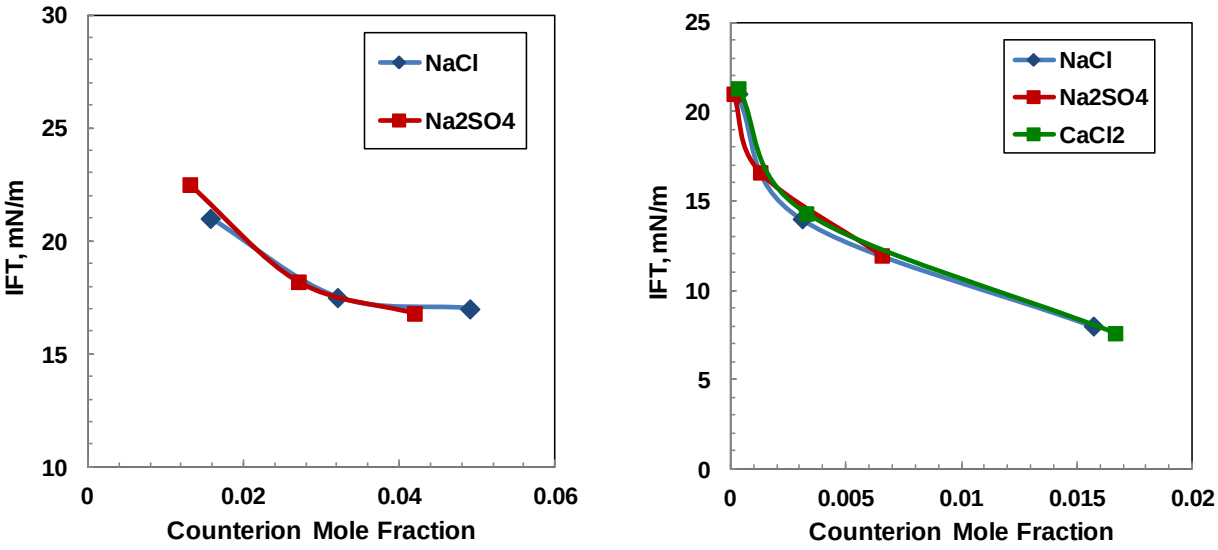

Figure 4.17 (a) IFT of toluene versus an aqueous phase containing 0.0001 wt% SDS against mole fraction of counterions (Na^+) in the solution. **(b)** IFT of toluene versus an aqueous phase containing 0.0001 wt% CTAB against mol fraction of counterions (Cl^- and SO_4^-) in the solution.

Naphthenic Acid

Naphthenic acids are a class of surfactants found in crude oils. 5β-cholanic acid is a model naphthenic acid and its effect on the IFT of toluene versus NaCl brine was studied. 5β-cholanic acid is oil soluble and was modeled based on its concentration in the organic phase. The monolayer surface excess concentration was $5.5 \cdot 10^{-7}$ mol/m². This value is similar to the value of $7 \cdot 10^{-7}$ mol/m², reported by Varadaraj and Brons (2007), for a hexadecane-toluene mixture.

5β-cholanic acid is a weak surface active component and the effect of salt concentration on IFT is more apparent than with the strong ionic surfactants, Figure 4.18. At low surfactant concentrations, the salt effect dominates, but at higher surfactant concentrations the surfactant dominates and the salt effect disappears. The magnitude of K_S^{org} is much less than the values obtained for SDS and CTAB, consistent with a weaker surfactant. The adsorption constant, K_S^{org}, was fitted with Eq. 4.13 for each salt concentration and was found to decrease linearly with salt counterion mole fraction, Figure 4.19. The constants *A*1 and *A2* were found to be 10,000 and -100,000 respectively and the model fit the IFT data with an average deviation of 1%. The negative slope indicates that, unlike SDS and CTAB, less 5β-cholanic acid adsorbs on the interface at higher salt concentrations. Unlike SDS and CTAB, 5β-cholanic acid is an oil soluble surfactant. When an oil soluble surfactant is less ionized (*e.g.* it higher salt concentrations), it will become more oil soluble and adsorb less at the interface.

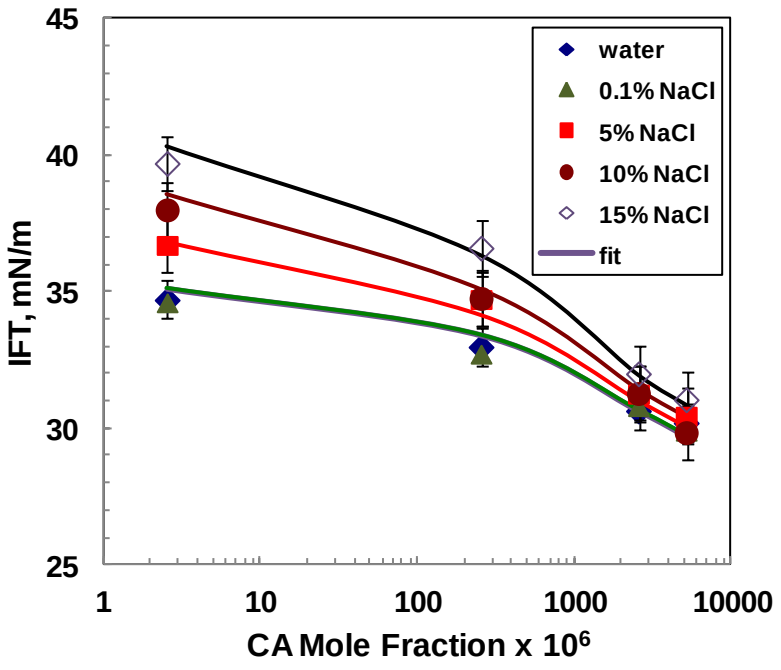

Figure 4.18 Measured (symbols) and modeled (lines) effect of Cholanic acid concentration on the interfacial tension of toluene versus NaCl brine.

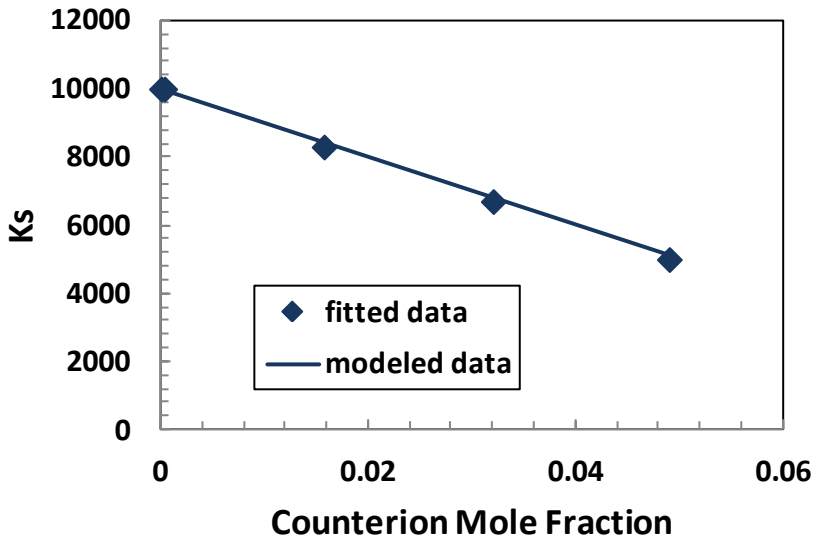

Figure 4.19 The effect of salt counterion concentration on K_S^{org} for toluene versus NaCl brine with cholanic acid. The data points (fitted data) are values fitted to IFT data and the line (modeled data) is Equation 4.13 fitted to the K_S^{org} values.

4.5.1 Interfacial Tension of Hydrocarbon versus Brine with Asphaltenes

The IFT of solutions of 0.5 g/L to 25 g/L WC_B1 asphaltenes in toluene was measured against NaCl brine with NaCl concentrations ranging from 0 to 15 wt%, Figures 4.20 and 4.21. The densities and molecular weights of the asphaltene solutions were required to calculate the IFT and the mole fraction of asphaltenes, and they are provided in Table 4.7. Note, since asphaltenes self-associate in toluene, the molecular weight depends on its concentration.

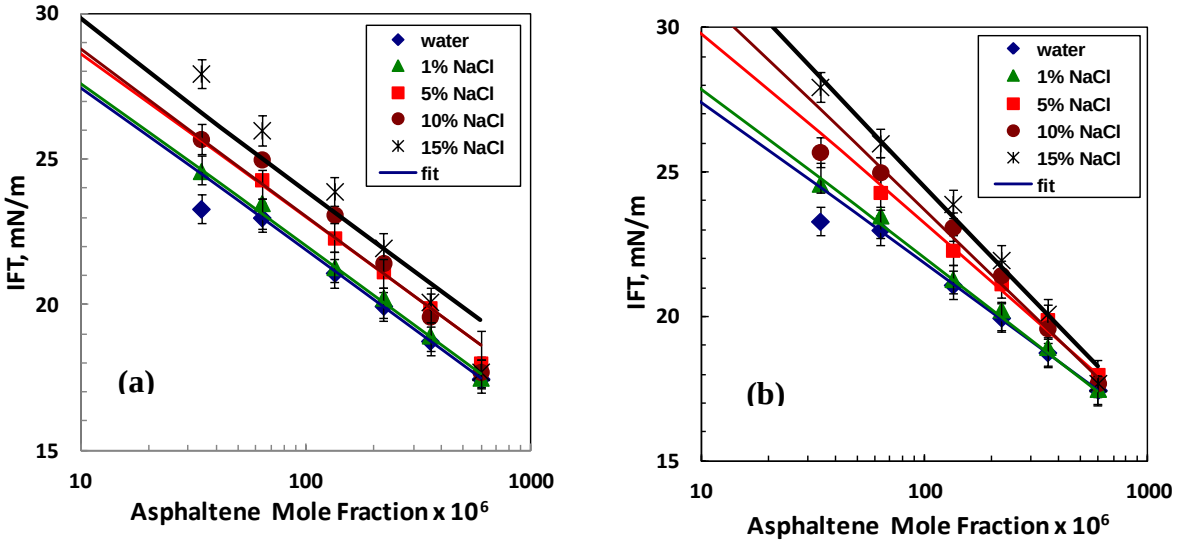

Figure 4.20 Measured (symbols) and modeled (lines) IFT of asphaltenes in toluene versus NaCl brine at 23°C: a) modeled with constant surface excess concentration; b) surface excess concentration varies with salt concentration.

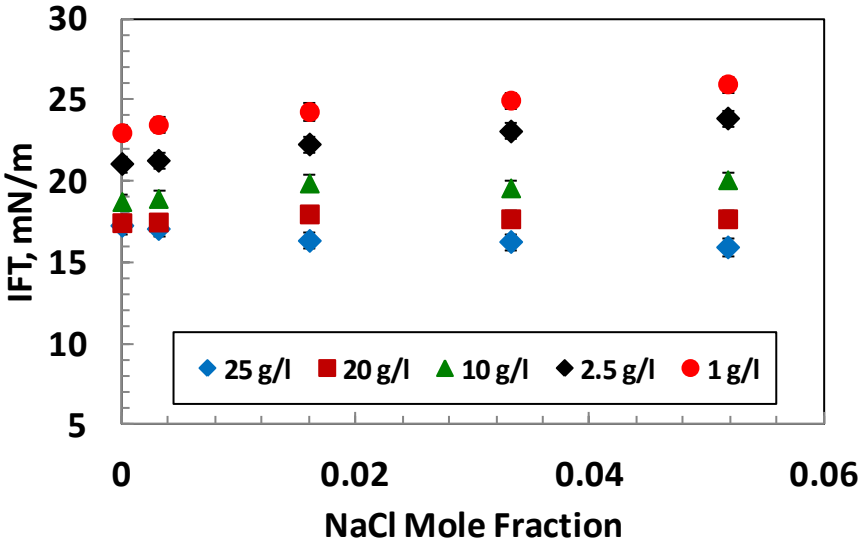

Figure 4.21 Interfacial tension of asphaltenes dissolved in toluene versus NaCl brine.

Table 4.7 Density and molecular weight of asphaltenes dissolved in toluene at 23°C.

Asphaltenes (g/L)	Density (g/cm^3)	Molecular Weight (g/mol)
0.5	0.8670	1560
1	0.8671	1670
2.5	0.8676	1980
5	0.8682	2410
10	0.8696	2990
20	0.8722	3560
25	0.8736	3690

Asphaltenes are oil soluble and the IFT was modeled based on their concentration in the organic phase. The IFT data for asphaltenes was first modeled using Equation 4.8, Figure 4.20(a). The monolayer surface excess concentration of the asphaltenes was $1.0 \cdot 10^{-6}$ mol/m². This value is in good agreement with the monolayer surface excess concentration of $1.07 \cdot 10^{-6}$ mol/m² previously reported for Athabasca asphaltenes (Sztukowski et al., 2003) and slightly less than the value of $1.4 \cdot 10^{-6}$ mol/m^2 reported by Varadaraj and Brons (2007) for asphaltenes derived from heavy oil. The adsorption constant decreased exponentially with increasing salt mole fraction, Figure 4.22, as opposed to a linear variation in case of 5β-cholanic acid, and was fitted with the following expression:

$$K_S^{org} = 2.16 \cdot 10^6 - 1.20 \cdot 10^6 (1 - \exp(-53.5 x_{counterion})) \qquad \textbf{Equation 4.15}$$

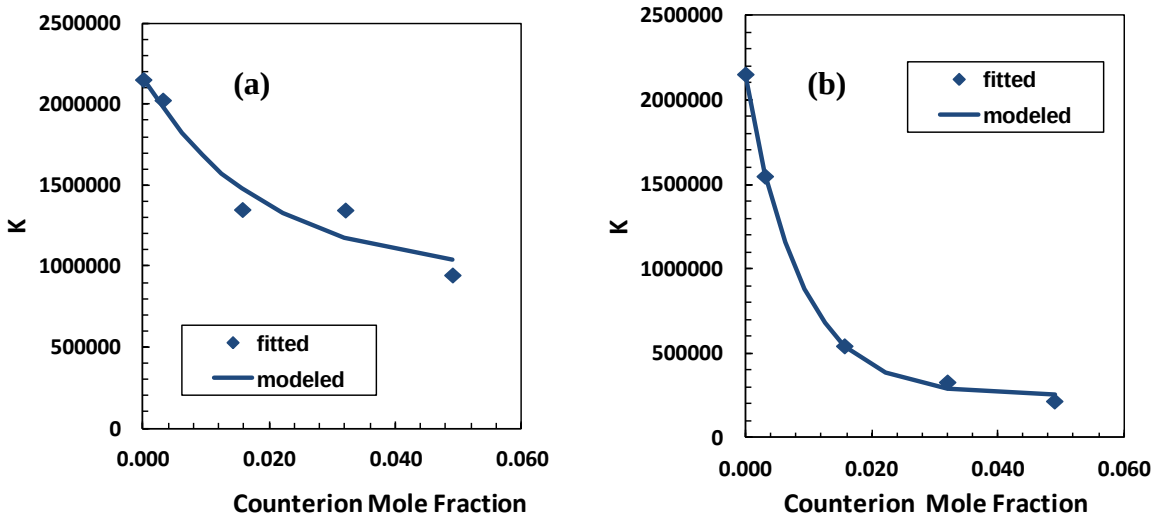

Figure 4.22 The effect of salt counterion concentration on the adsorption constant of asphaltenes in toluene versus NaCl brine at 23°C: a) constant surface excess concentration; b) surface excess concentration varies with salt concentration.

However, Figure 4.20(a) shows that the slope of IFT versus the log of the asphaltene mole fraction varies with salt concentration, which means that the monolayer surface excess concentration of the asphaltenes varies with salt concentration. Therefore, the data were remodelled by adjusting the surface excess concentration and adsorption constant, Figure 4.20(b), as follows:

$$\Gamma_s = 1.0 + 0.50(1 - \exp(-31.5x_{counterion})) \qquad \textbf{Equation 4.16}$$

$$K_S^{org} = 2.15 \cdot 10^6 - 1.90 \cdot 10^6(1 - exp(-120x_{counterion})) \qquad \textbf{Equation 4.17}$$

Note that the surface excess concentration did not change with salt concentration for any of the pure surfactants. This observation suggests that the change in surface excess concentration occurs because asphaltenes are a mixture of millions of components each of which can interact differently with salt ions. The increase in surface excess concentration with increased salt concentration suggests that more or smaller asphaltenes are adsorbing at the interface at higher salt concentrations. The adsorption constant

decreases at higher salt concentrations indicating that their relative attraction to the interface is reduced.

The values of the asphaltene adsorption constant are approximately 200 times higher than the values found for 5β-cholanic acid, but are approximately 200 times lower than the values found for CTAB and SDS. The asphaltenes also reduce interfacial tension more than the 5β-cholanic acid at a given concentration, but much less than the strong surfactants. Hence, the surface activity of the asphaltenes appears to be intermediate between the 5β-cholanic acid and the strong surfactants.

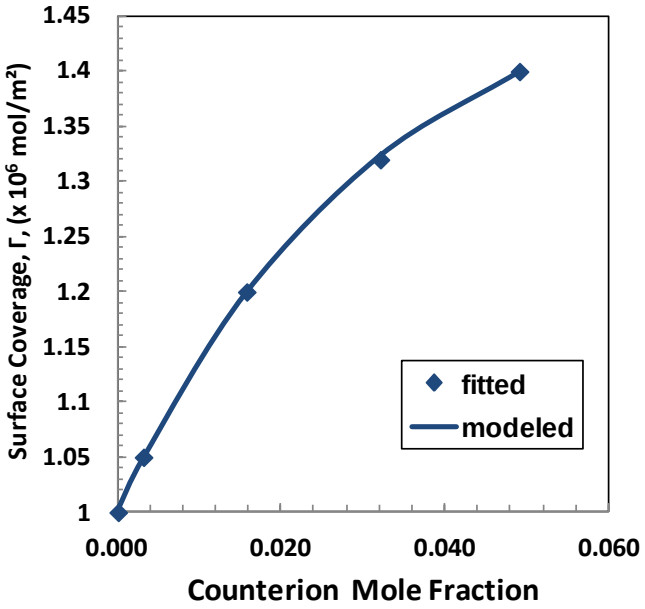

Figure 4.23 The effect of salt counterion concentration on the surface excess concentration of asphaltenes in toluene versus NaCl brine at 23°C.

The effect of salt on the asphaltene IFT, Figure 4.21, was similar to the effect on 5β-cholanic acid. Figure 4.24 compares the normalised IFT of the asphaltenes with 5β-cholanic acid at different concentrations. In both cases, the IFT increased with salt concentration up to about 20 g/L (2.2 wt%) asphaltenes (or 2 wt% 5β-cholanic acid) in toluene. At higher asphaltene concentrations, the IFT decreased with salt concentration

while at higher 5β-cholanic acid concentrations the IFT became invariant with salt concentration. Hence, on average, asphaltenes are similar to weak ionic surfactants.

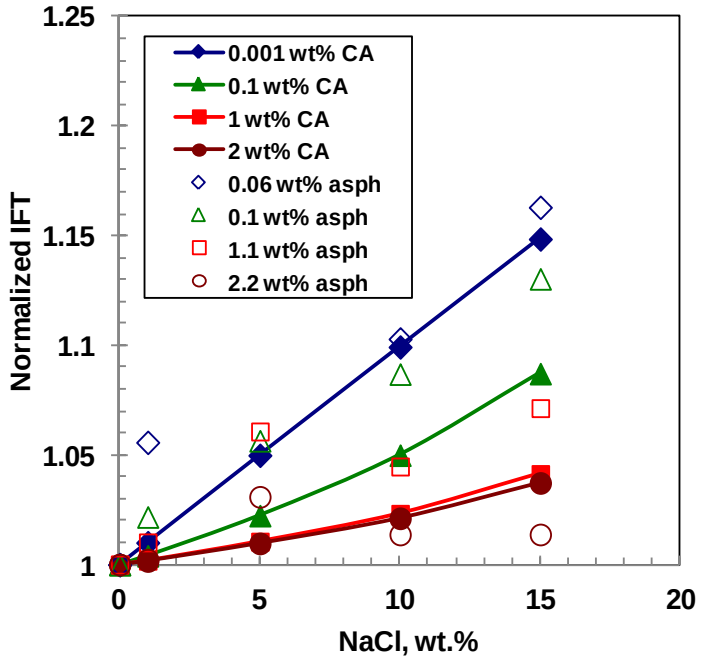

Figure 4.24 Comparison of normalized IFT versus NaCl brine concentration for 5β-cholanic acid (CA) and asphaltenes in toluene.

4.6 Summary of Interfacial Tension of Hydrocarbon versus Brine

The IFT of pure hydrocarbons versus brine increases with increasing salt concentration. However, a variety of trends are observed when a surfactant is introduced to these systems. Non-ionic surfactants can reduce IFT significantly but do not interact with the salt. Ionic surfactants also reduce IFT but interact with the salt in two ways: 1) the salt effect on IFT is eliminated at sufficiently high surfactant concentration; 2) the adsorption of the surfactant varies with counter ion concentration. All of the data could be fitted with the Gibbs-Langmuir model framework but the model is not predictive.

Some trends in the model parameters are noted in Table 4.8. For ionic surfactants, the adsorption constant appears to be exponentially related to the salt content. For lower values of K_s, a linear approximation is sufficient. The adsorption constant increases with increasing salt concentration for water soluble surfactants (SDS and CTAB) but decreases for oil soluble surface active components (cholanic acid and asphaltenes). In other words, salt makes water soluble surfactants adsorb more and oil soluble surfactants adsorb less. These trends can be explained in terms of the reduced ionization of the surfactant at higher salt concentrations. When a water soluble surfactant is less ionized, it becomes less water soluble and will adsorb more. When an oil soluble surfactant is less ionized it becomes more oil soluble and will adsorb less. With data on more surfactants, it may be possible to correlate the effect of salt concentration on the surfactant adsorption constant to the hydrophilic lipophilic balance of the surfactant molecules.

Table 4.8 Summary of adsorption constants for various systems

System	Solubility	K_S in HC/water	Trend with Salt Content
Nonionic			
NEO-10	Water	$4.2\ 10^9$	Constant
Triton X-100	Water	$2.5\ 10^9$	Constant
Ionic			
CTAB	Water	$1.0\ 10^7$	Exponential Increase
SDS	Water	$5.0\ 10^5$	Linear Increase
Cholanic Acid	Oil	$1.0\ 10^4$	Linear Decrease
Asphaltenes	Oil	$2.2\ 10^6$	Exponential Decrease

4.7 Crude Oil/Brine Systems

Four crude oils and a database were examined to assess the effect of salt concentration on IFT in crude oils. The observations from the hydrocarbon/brine systems were used to guide the interpretation. Three of the crude oil samples were provided by Chevron (Light Crude, Medium Crude, and Heavy Crude). Western Canadian bitumen, WC_B1, was

provided by Shell Canada. The densities and total acid number of each crude oil are provided in Tables 4.9 and 4.10, respectively. The interfacial tensions of the three crude oils were measured against water and brines with sodium chloride concentrations from 1 to 15 wt%.

Table 4.9 Density of Light, Medium, and Heavy Crude oils and *n*-decane diluted Heavy Crude at 23°C.

Fluid	Density (g/cm^3)
Light crude	0.8378
Medium crude	0.9049
Heavy Crude	0.9830
Diluted Heavy crude (25 wt% decane)	0.9043
Diluted Heavy crude (30 wt% decane)	0.8891
Diluted Heavy crude (35 wt% decane)	0.8765
Diluted WC_B1 (35 wt% decane)	0.8920
Diluted WC_B1 (40 wt% decane)	0.8769
Diluted WC_B1 (45 wt% decane)	0.8627

Table 4.10 Total acid number of Light, Medium, and Heavy Crude oils as measured by Metro Tech Systems Ltd.

Fluid	TAN (mg KOH/g oil)
Light crude	0.41
Medium crude	0.84
Heavy crude	5.02

Light Crude

The IFT of light crude versus water was low, 14.5 mN/m compared with values of 20 mN/m or more for most crude oils (see database later on). On addition of salt, the IFT decreased to values too small to measure with drop shape analysis (DSA). The significant decrease in IFT with the addition of salt suggests the presence of a strong ionic surfactant, possibly a contaminant.

Medium Crude

The IFT of the Medium Crude versus water of 18.7 mN/m was low compared with hydrocarbons but not unusually low for a crude oil. Its IFT increased linearly with NaCl concentration. The normalized (IFT in brine /IFT in water) is remarkably similar to that of 0.1 wt% cholanic acid in toluene, Figure 4.25, suggesting the presence of low concentrations of weak ionic surfactants.

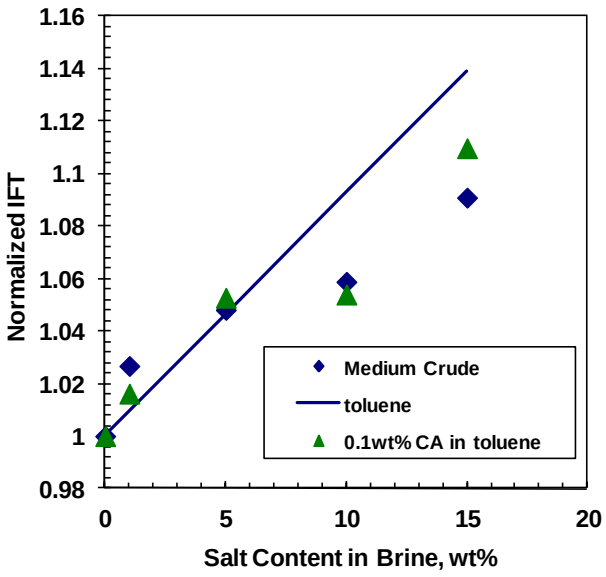

Figure 4.25 Comparison of normalised IFT versus NaCl brine of Medium Crude oil, toluene, and 0.1 wt% cholanic acid (CA) in toluene.

Heavy Crude

The density of the heavy crude oil was too close to that of water to use the drop shape analysis method; therefore, the oil was diluted with decane to obtain IFT measurements. The densities of the mixtures were required to calculate the IFT. The mixture of the heavy oil and decane formed nearly regular solutions, Figure 4.26, but were fitted more exactly with an excess volume based mixing rule of the form:

$$v_{mix} = w_H v_H + w_{C10} v_{C10} - 0.003 w_H w_{C10} (v_H + v_{C10}) \qquad \textbf{Equation 4.18}$$

where v is the specific volume, w is the mass fraction and subscripts H and $C10$ denotes Heavy Crude and *n*-decane, respectively.

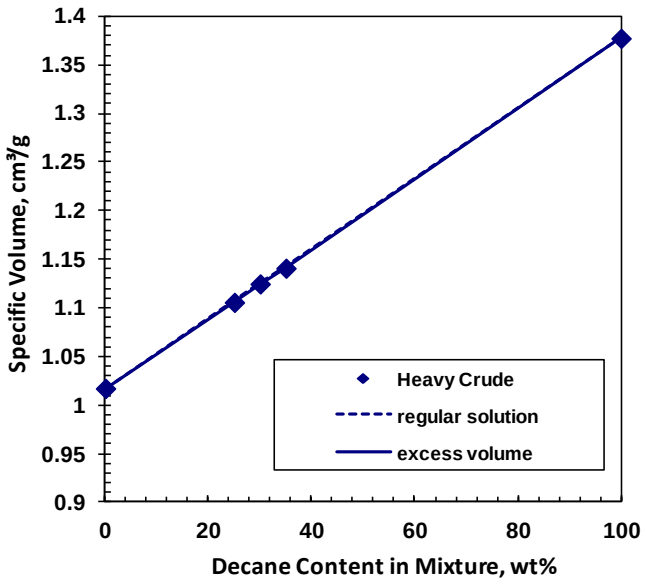

Figure 4.26 Density of solutions of *n*-decane and Heavy Crude at 23 °C.

The IFT of the diluted Heavy Crude sample versus water was between 17 and 18 mN/m, similar to that of the Medium Crude. However, unlike the Medium Crude, the IFT of all the diluted Heavy Crude samples decreased slightly with increasing salinity and stabilized at salt contents above 10 wt%, Figure 4.27. The behaviour is similar to that

observed for low concentrations of a strong ionic surfactant or, possibly, high concentrations of a weak ionic surfactant.

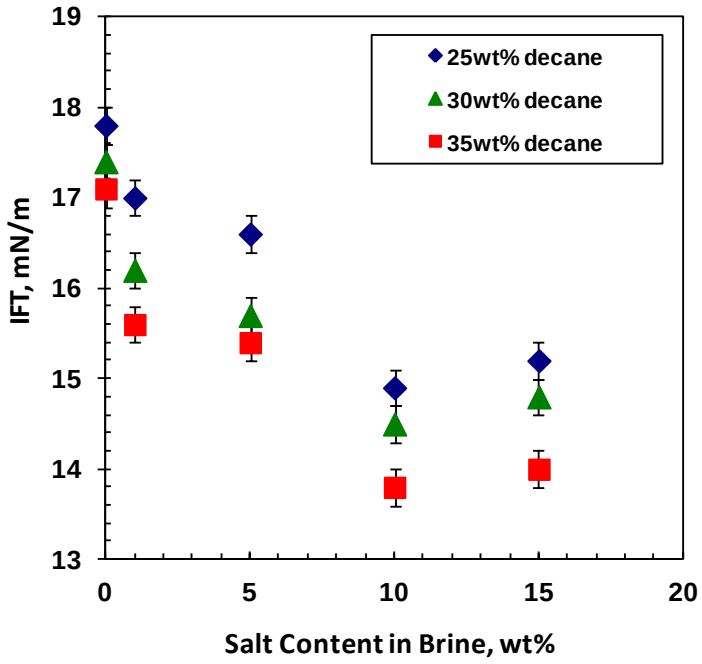

Figure 4.27 Effect of NaCl brine concentration on IFT of Heavy Crude oil versus brine.

Figure 4.28 shows the effect on *n*-decane dilution on the IFT of the Heavy Crude oil. The IFT of decane versus water is 50 mN/m, much higher than the IFT of the Heavy Crude versus water. And yet, IFT decreased with dilution with *n*-decane. A possible explanation is the surface active material is poorly soluble in decane; that is, it is asphaltenic. Asphaltenes will be more strongly bound to the interface when in a poor solvent medium and a decrease in IFT is to be expected. The solubility of asphaltenes in mixtures of n-decane and Heavy Crude oil was not tested but the onset of asphaltene precipitation from decane diluted heavy oil is expected to be at approximately 50 wt% *n*-decane.

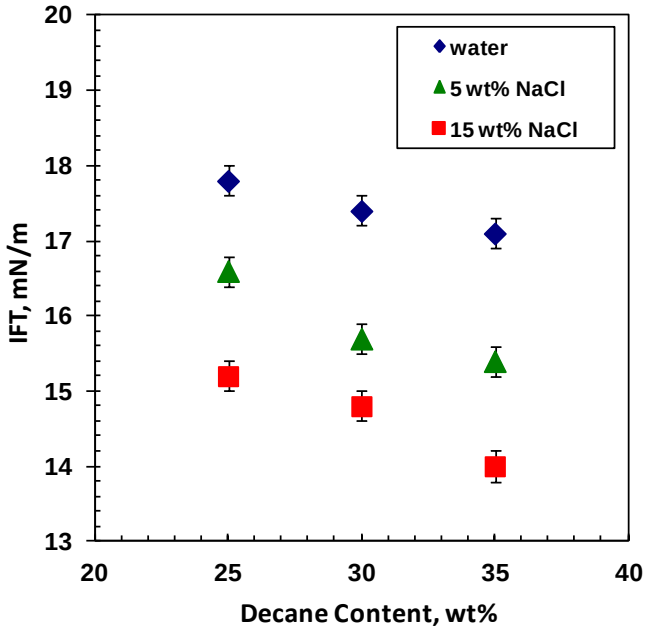

Figure 4.28 Effect of *n*-decane content on IFT of mixtures of *n*-decane and Heavy Crude oil versus brine.

WC_B1 Bitumen

Since dilution was required with the Heavy Crude, a Western Canadian bitumen was tested as well to confirm the observed trends. The densities of the mixture of bitumen and decane, Figure 4.29, could be fitted into Equation 4.18, using an excess volume of 0.01.

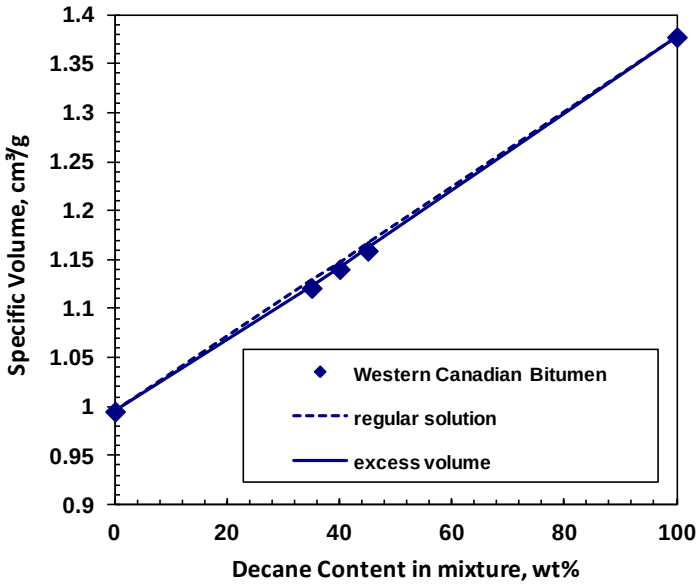

Figure 4.29 Density of solutions of *n*-decane and Western Canadian Bitumen at 23°C.

The IFT trends for the Western Canadian Bitumen were qualitatively similar to that of Heavy crude oil. The IFT changed less with decane dilution, Figure 4.31 and the effect of salt concentration was much more pronounced, Figure 4.30; suggesting the presence of low concentrations of strong ionic-surfactants or high concentrations of a weak ionic surfactant. The likeliest explanation is that a significant proportion of the asphaltenes are ionic surfactants given as high concentration of a weak surfactant. However, it is impossible to rule out a contaminant introduced when the sample was collected.

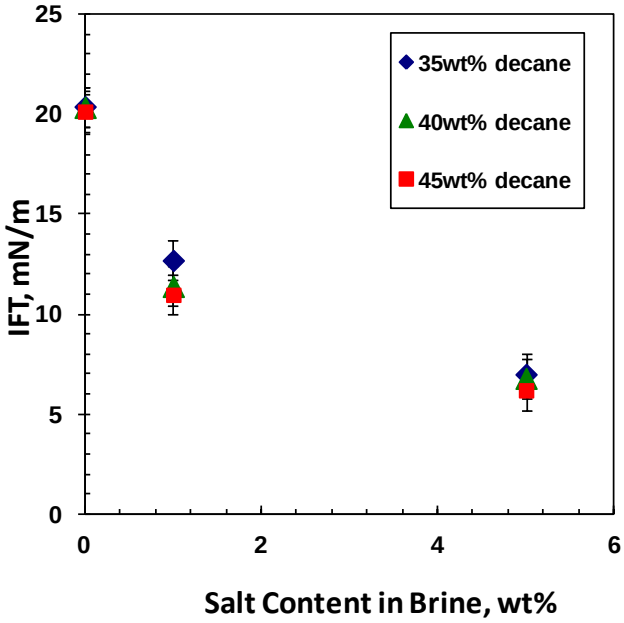

Figure 4.30 Effect of NaCl brine concentration on IFT of WC_B1 versus brine.

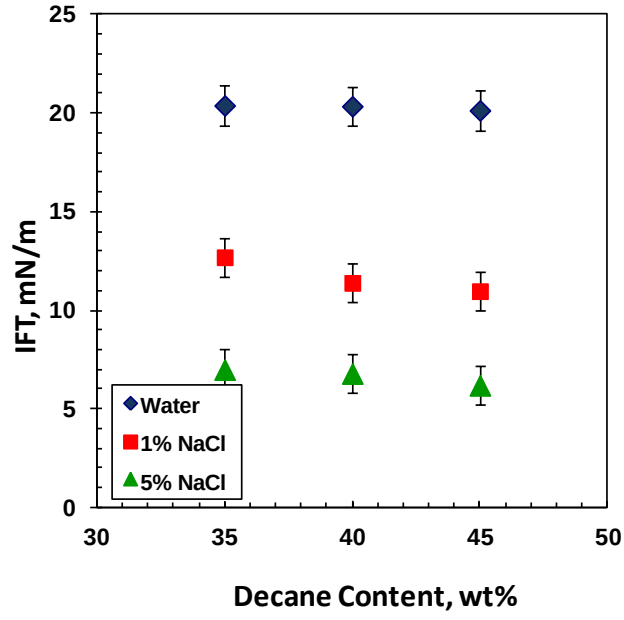

Figure 4.31 Effect of *n*-decane content on IFT of mixtures of *n*-decane and WC_B1 versus NaCl brine.

Crude Oil from Databases

A number of crude oil samples from Buckley and Fan (2007) and an undisclosed source were analysed for the effect of salinity on its IFT against water. Note, the type or composition of the salts was not specified, only the total salinity. Figure 4.32 shows that in general crude oil IFT exhibit a wide variety of trends with salinity. The IFT could not be related to any of the physical properties reported in the databases including density, acid number, base number, or their combinations.

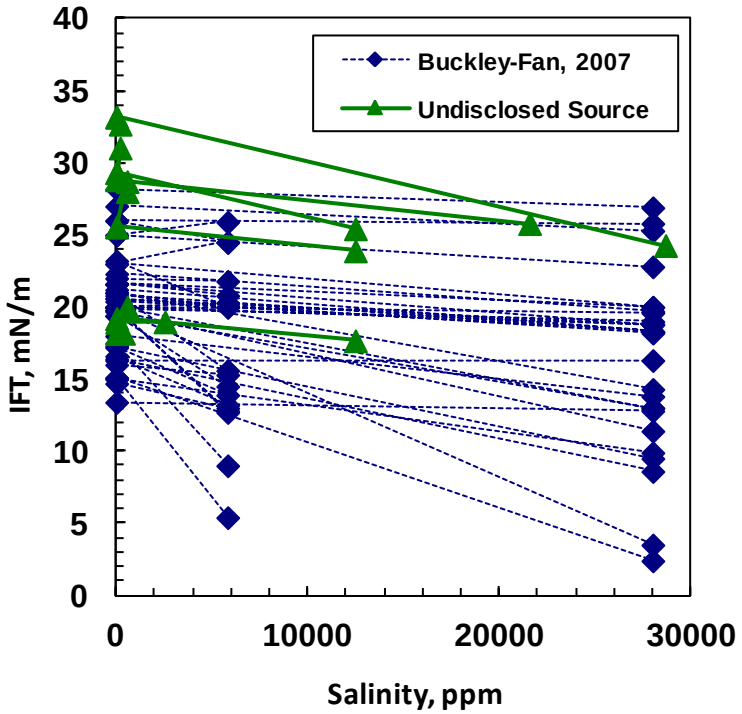

Figure 4.32 Effect of salinity on the interfacial tension of crude oils.

The data was screened to remove some of the samples suspected to be contaminated with a non-native surfactant which may have been introduced in the wellbore or during processing, sampling, and storage. All samples with a slope greater than 300 mN/m.ppm were screened out. The remaining data were then normalized by dividing the IFT in brine by the IFT in pure water. The normalised IFT data for the crude oils is compared with

that of SDS and asphaltenes in Figure 4.33. A small number of crude oils show an increase in IFT with salt content indicating that there is no surfactant or only very weak ionic surfactants in the oil. Most of the crude oils appear to contain weak ionic surfactants similar to asphaltenes or naphthenic acids. However, a significant number of oils appear to contain a strong ionic surfactant similar to SDS. Note, the presence of contaminants in these crude samples cannot be ruled out.

In general, the IFT of a crude oil and its response to salt content cannot be predicted *a priori* because small quantities of surfactant have a significant effect on the IFT. The amount and nature of this surface active material is not easily measured. Nonetheless, many oils exhibit a decrease in IFT with increasing salt content that is consistent with 2 to 5 wt% asphaltenes or naphthenic acids or less than 100 ppm of a surfactant like SDS.

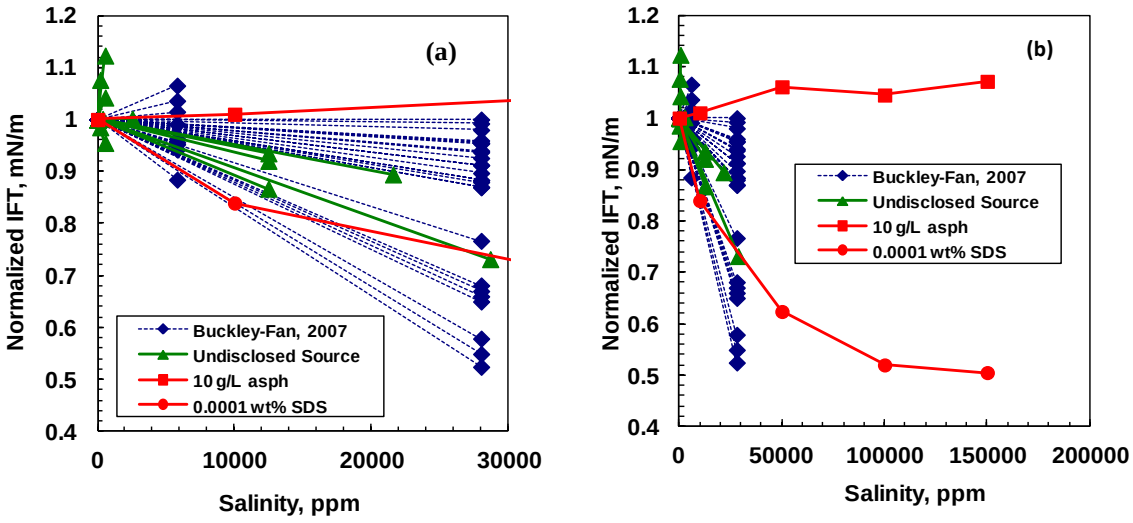

Figure 4.33 Comparison of IFT of crude oils with ionic surfactants (a) zoomed view (b) full scale view.

Chapter Five: Conclusions and Recommendations

The primary objective of this thesis was to study the effects of salinity on the interfacial tension of model hydrocarbon systems and relate its findings to the crude oil systems. This work was carried out in three major steps. First, the interfacial tension of pure hydrocarbons was measured against aqueous phase of varying salinity. A simple model was developed to model the effects of salt concentration on the interfacial tension of these hydrocarbons. In the second stage, surfactant was added to the system and the effects of both salts and surfactants on IFT were studied. The effect of various categories of surfactants was studied and simple models were developed. Finally, the IFT of crude oils were measured against aqueous phase of varying salinity. The results of crude oil systems were then interpreted in terms of the findings of the model systems. The conclusions of this work and some recommendations for future work in this area are presented below.

5.1 Conclusions

1. As expected from theoretical considerations, the interfacial tension of pure hydrocarbon versus brine systems increased with increasing salt concentration in the system.

2. The interfacial tension of hydrocarbons/brine/surfactant system depends on interaction between salts and surfactants.

    - Non-ionic surfactants do not have any charge and no interaction between the surfactant and salt was expected or observed. The interfacial tension of hydrocarbon/brine/non-ionic surfactant increased with increasing salt concentration at any given concentration of surfactant.
    - Ionic surfactant molecules contain charge and form a charged monolayer at the interface. There is an interaction between surfactant and salt and the IFT of the system depends on the relative concentration of salts and surfactants. At the

low concentrations of surfactants, when the interface is not fully saturated, the interfacial tension of hydrocarbon/brine/ionic surfactant increases with salt concentration. At higher concentrations of ionic surfactant in the system, when the interface becomes saturated with surfactant, the interfacial tension decreases with increasing salt concentration in the system.

3. The Gibbs-Langmuir model can be used to model the data for the interfacial tension of salts and surfactants.

    - For ionic surfactants the disappearance of salt depletion effect was related to the fractional surface coverage of the surfactant in the system.
    - The effect of salt concentration on the surfactant adsorption constant was fitted using experimental data. The adsorption constant was related to the mole fraction of counter ions in the solution. The adsorption constant could not be related to any measurable/known parameters.

4. Naphthenic acids act as weak ionic surfactants in terms of their IFT. The interfacial tension of 5-β cholanic acid increases with salt concentration up to about 2 wt% of acid in the solution.

5. The IFT of asphaltenes was qualitatively similar to naphthenic acids. Asphaltenes reduced IFT more at a given concentration but the response to salt was almost identical. On average, asphaltenes act like a weak to moderate ionic surfactant.

6. The interfacial tension of three crude oils provided by Chevron shows different trends with salt concentrations.

    - The IFT of the Light Crude was low and decreased dramatically with increasing salt concentration. This oil was likely contaminated with a strong ionic-surfactant possibly encountered during production and storage.

- The IFT of the Medium Crude increased with salt concentration as observed for naphthenic acid and asphaltenes.
- The Heavy Crude was diluted with n-decane in order to measure its IFT. Decane dilution decreased the IFT of heavy oil possibly because asphaltenes are less soluble in decane and therefore more likely to adsorb at the interface. The IFT of the diluted Heavy Crude decreased with salt concentration at any given concentration of decane. Similar behaviour was observed for Western Canadian bitumen. The bitumen appears to contain low concentrations of a strong ionic surfactant or, more likely, high concentrations of weak ionic surfactants such as asphaltenes and naphthenic acids.

7. A number of crude oils from unknown sources were analysed for the effect of salinity on their interfacial tension. The IFT showed a variety of trends with salinity including a slight increase, constant, and a significant decrease.

    - After screening the list for possible contaminated samples, the normalised IFT of these crudes was compared to the model systems. It was concluded that most crude oil contains an ionic surfactant the behaviour of which may vary between asphaltene-like and that of SDS at small concentrations.
    - The IFT of these crude oils could not be related to any known/measurable physical properties such as acid number, base number, density or any combination of these parameters.
    - Since there is no way of tracking the source of these crude oils, the possibility of contaminations being present in these systems cannot be ruled out. Trace contaminants can have a significant impact on IFT. Hence, any attempt to correlate IFT to oil properties or assays is unlikely to succeed.

8. Although it was not possible to relate the IFT of crude oils to any known/measurable parameters, this study developed a better understanding of the type and

concentration of surface active components to be expected in crude oils and their interactions with aqueous phase of varying salinity.

5.2 Recommendations for Future Work

This research improved the understanding of the effects of salt concentration on the interfacial tension of model hydrocarbons and crude oils in presence of various categories of surface active components. Some recommendations for future work are provided below.

1. All the interfacial tensions in this thesis were measured at ambient pressure and temperature. Some of these experiments can be repeated at the higher pressures and temperatures encountered at reservoir conditions to assess any changes in behaviour.

2. The surfactants considered in this thesis were highly soluble in one bulk phase and almost insoluble in the in the other bulk phase. Hence, surfactant partitioning between the bulk phases was considered negligible. The partitioning coefficients of these surfactants can be determined in future work for to validate and, if necessary, improve the modeling of the data.

3. The adsorption constant for salts and surfactants has been fitted using experimental data; it is not predictive at this stage. It is recommended to investigate the relationship between the adsorption constant and some known/measurable parameters to make the model more predictive. It is speculated that the magnitude of adsorption constant might depend on the strength of the surfactant. This can be verified by studying the effects of surfactants with varying effectiveness.

4. The effect of pH on the interfacial tension has not been considered in this thesis. This effect can be studied to broaden the findings and understanding developed from this research work.

5. Although a simple model was sufficient to fit the data for salts and surfactants, complex models which capture the physics of the process better could be developed for these systems. However, such an approach entails the measurement of surface potential and increases the experimental demands. It is not obvious if the potential improvement to the model would justify the additional complexity.

References

Acevedo, S., Escobar, G., Ranaudo, M.A., Khazen, J., Borges, B., Pereira, J.C., and Mendez, B., Isolation and Characterization of Low and High Molecular Weight Acidic Compounds from Cerro Negro Extra heavy Crude Oil. Role of These Acids in the Interfacial Properties of the Crude Oil Emulsions, *Energy Fuels*, **1999**, 13(2), 333-335.

Akstinat, M.H., Surfactants for Enhanced Oil Recovery Processes in High-Salinity Systems – Product Selection and Evaluation, Proceeding to the European Symposium on Enhanced Oil Recovery, Bournemouth, England, **1981.**

Alboudwarej, H., Akbarzadeh, K., Beck, I., Svrcek, W. Y., Yarranton, H.W., Regular Solution Model for Asphaltene Precipitation from Bitumens and Solvents, *AIChE Journal*, **2003**, 49(11), 2948-2956.

Alotaibi, M.B., and Nasr-El-Din, H.A., Effect of Brine Salinity on Reservoir Fluids Interfacial Tension, **2009**, SPE Paper Number 121569.

Al-Sahhaf, T., Elkamel, A., Ahmed S.A., and Khan, A.R., The Influence of Temperature, Pressure, Salinity and Surfactant Concentration on the Interfacial Tension of the n-Octane-Water System, *Chemical Engineering Communications*, **2005**, 192, 667-684.

Arps, J.J., Engineering Concepts Useful in Oil Finding, *AAPG Bulletin*, **1964**, 48, 157-165.

ASTM D664-04, Standard Test Method For Acid Number of Petroleum Products by Potentiometric Titration, **2004**.

Aveyard, R., and Saleem, S.M., Interfacial Tensions at Alkane-Aqueous Electrolyte Interfaces, *Journal of Chemical Society Faraday Transactions I*, **1976**, 72, 1609-1617.

Aveyard, R., and Haydon, D.A., Thermodynamic Properties of Aliphatic Hydrocarbon/Water Interfaces, *Transactions of Faraday Society*, **1965**, 61, 2255-2261.

Badakshan, A., and Bakes, P., The Influence of Temperature and Surfactant Concentration on Interfacial Tension of Saline Water and Hydrocarbon System in Relation to Enhanced Oil Recovery by Chemical Flooding, **1990**, SPE Paper Number 20290.

Bai, J., Fan, W., Nan, G., Li, S., and Yu, B., Influence of Interaction Between Heavy Oil Components and Petroleum Sulfonate on the Oil-Water Interfacial Tension, *Journal of Dispersion Science and Technology*, **2010**, 31, 551-556.

BenGhoulam, M., Moatadid, N., Graciaa, A. and Lachaise, J., Quantitative Effect of Nonionic Surfactant Partitioning on the Hydrophile-Lipophile Balance Temperature, *Langmuir*, **2004**, 20(7), 2584-2589.

Bennett, B., and Larter, S.R., Partition Behaviour of Alkylphenols in Crude oils-Brine Systems Under Subsurface Conditions, *Geochimica et Cosmochimica Acta*, **1997**, 61, 4393.

Berg, R.R., Capillary Pressure in Stratigraphic Traps, *AAPG Bulletin*, **1975**, 59, 939-956.

Bonfillion, A., Sicoli, F., and Langevin, D., Dynamic Surface Tension of Ionic Surfactant Solutions, *Journal of Colloid and Interface Science*, **1994**, 168(2), 497-504.

Borwankar, R.P., and Wasan, D.T., Equilibrium and Dynamics of Adsorption of Surfactants at Fluid-Fluid Interfaces, *Chemical Engineering Science*, **1988**, 43, 1323-1337.

Brient, J.A., Commercial Utility of Naphthenic Acids Recovered from Petroleum Distillates, *Preprints – American Chemical Society, Division of Petroleum Chemistry*, **1998**, 43(1), 131-133.

Brient, J.A., Wessner, P.J., Doyle, M.N., Naphthenic Acids, *Encyclopaedia of Chemical Technology*, Kirth-Othmer, Ed., John Wiley & Sons, New York, **1995**, 1017-1029**.**

Buckley, J.S., and Fan, T., Crude Oil/Brine Interfacial Tensions, *Petrophysics*, **2007**, 48(3), 175-185.

Buckley, J.S., Mechanism and Consequences of Wettability Alteration by Crude Oils, ph.D. Thesis, Department of Petroleum Engineering, Heriott-Watt University, Edinburg, United Kingdom, **1996**.

Cai, B., Yang, J. and Guo, T., Interfacial Tension of Hydrocarbon + Water/Brine Systems Under High Pressure, *Journal of Chemical and Engineering Data*, **1996**, 41(3), 493-496.

Calvo, E., Ramon, B., Amigo, A., and Gracia-Fadrique, J., Dynamic Surface Tension, Critical Micelle Concentration, and Activity Coefficients of Aqueous Solutions of Nonyl Phenol Ethoxylates, *Fluid Phase Equilibria*, **2009**, 282, 14-19.

Campanelli, J.R., and Wang, X., Comments on Modelling the Diffusion-Controlled Adsorption of Surfactants, *The Canadian Journal of Chemical Engineering*, **1998**, 76, 51-57.

Carale, T.R., Pham, Q.T., and Blankschtein, D., Salt Effects on Intramicellar Interactions and Micellization of Nonionic Surfactants in Aqueous Solutions, *Langmuir*, **1994**, 10(1), 109-121.

Chan, K.S., and Shah, D.O., The Molecular Mechanism for Achieving Ultra Low Interfacial Tension Minimum in a Petroleum Sulfonate/Oil/Brine System, *Journal of Dispersion Science and Technology*, **1980**, 1(1), 55-95.

Collins, A.G., Properties of Produced Waters, Petroleum Engineering Handbook, Ch. 24, **1992**.

Cratin, P.D., Mathematical Modeling of Some pH dependent Surface and Interfacial Properties of Stearic Acid , *Journal of Dispersion Science and Technology*, **1993**, 14, 559.

Dandekar, A.Y., Petroleum Reservoir Rocks and Fluids Properties, Taylor and Francis, **2006**.

Danielli, J.F., The Relation between Surface pH, Ion Concentration, and Interfacial Tensions, *Proceedings of Royal Society of London B*, **1937**, 122, 155.

Davies, J.T., Adsorption of Long-Chain Ions. I, *Proceedings of Royal Society of London A*, **1958**, 245, 417-428.

Defay, R., and Petre, G., Dynamic Surface Tension, Surface and Colloid Science, **1971**, Vol. 3, Wiley, New York.

Diamant, H., and Andelman, D., Kinetics of Surfactant Adsorption at Fluid/Fluid Interfaces: Non-ionic Surfactants, *Europhysics Letters*, **1996**, 34(8), 575-580.

Diamant, H., Ariel, G., and Andelman, D., Kinetics of Surfactant Adsorption: The Free Energy Approach, *Colloids and Surfaces A*, **2001**, 259, 183-185.

Diana, P.O., Effect of Surfactants on Asphaltene Interfacial Films and Stability of Water-in-Oil Emulsions, M.Sc. Thesis, **2009**.

Dickie, J.P. and Yen, T.F., Macrostructures of the Asphaltic Fractions by Various Instrumental Methods, *Analytical Chemistry*, **1967**, 39(14), 1847-1852.

Drelich, J. and Miller, J.D., Surface and Interfacial Tension of the Whiterocks Bitumen and Its Relationship to Bitumen Release from Tar Sands During Hot Water Processing, *Fuel*, **1994**, 73(9), 1504-1507.

Dukhin, S.S., Kretzschmar, G., and Miller, R., Dynamics of Adsorption at Liquid Interfaces: Theory, Experiment, Applications, *Elsevier*, **1995**.

Fan, T., and Buckley, J.S., Acid Numbers Measurements Revisited, *SPE Journal*, December, **2007**.

Fan, T., Wang, J., and Buckley, J. S. "Evaluating Crude Oils by SARA Analysis." Tulsa, OK, United States, **2002**, 883.

Firoozabadi, A. and Ramey, H.J., Surface Tension of Water-Hydrocarbon Systems at Reservoir Conditions, *Journal of Canadian Petroleum Technology*, **1988**, 27(3), 41-48.

Frumkin, A., *Z. Phys. Chem*., **1925**, 116, 466-483.

Germansheva, I., and Panaeve, S., *Kolloidn Zh*., **1981**, 44, 661.

Gibbs, J.W., The collected works of J.W. Gibbs, Thermodynamics 1, Yale University Press, New Haven, **1957**.

Gray, M. (ed.), Upgrading Petroleum Residues and Heavy Oils, Marcel Dekker, New York, **1994**.

Gurkov, T.D., Dimitrova, D.T., Marinova, K.G., Bilke-Crause, C., Gerber, C., and Ivanov, I.B., Ionic Surfactants on Fluid Interfaces: Determination of the Adsorption; Role of the Salt and the Type of the Hydrophobic Phase, *Colloids and Surfaces A*: *Physiochemical Engineering Aspects*, **2005**, 261, 29-38.

Hamouda, A.A., and Karoussi, O., Effect of Temperature, Wettability and Relative Permeability on Oil Recovery from Oil-Wet Chalk, *Energies*, **2008**, 1, 19-34.

Hartridge, H., and Peters, R.A., Interfacial Tension and Hydrogen-Ion Concentration, *Proceedings of Royal Society of London A*, **1922**, 101, 348.

Hassan, M.E., Nielson, R.F., and Calhoun, J.C., Effect of Pressure and Temperature on Oil-Water Interfacial Tensions for a Series of Hydrocarbons, *AIME Transactions*, **1953**, 198, 299-306.

Havre, T.E., Sjoblom, J. and Vindstad, J.E., Oil/Water Partitioning and Interfacial Behaviour of Naphthenic Acids, *Journal of Dispersion Science and Technology*, **2003**, 24, 789-801.

He, Y., Howes, T., and Litster, J.D., Dynamic Interfacial Tension of Aqueous Solutions of PVAAs and its Role in Liquid-Liquid Dispersion Stabilisation, **2002**, 9th APCChE.

Headley, J.V., Peru, K.M., McMartin, D.W., and Winkler, M., Determination of Dissolved Naphthenic Acids in Natural Waters by using Negative-Ion Electrospray Mass Spectrometry, *The Journal of AOAC International*, **2002**, 85(1), 182-187.

Henaut, I., Barre, I., Argillier, J., Brucy, F., and Bouchard, R., Rheological and Structural Properties of Heavy Crude Oils in Relation with their Asphaltenes Content, **2001**, SPE Paper Number 65020.

Hiemenz, P.C., and Rajagopalan, R., Principles of Colloid and Surface Chemistry, 3rd Edition, Marcel Dekker, New York, **1997**.

Hirasaki, G.J., Thermodynamics of Thin Films and Three-phase Contact Regions, in Morrow, N.R., ED, Interfacial phenomenon in petroleum Recovery, New York , Marcel Dekker, Inc., **1999**, 23-76.

Hjelmeland, O.S., and Larrondo, L.E., Experimental Investigation of the Effects of Temperature, Pressure and Crude Oil Composition on Interfacial Properties, *SPE Reservoir Engineering*, **1986**, 321-328.

Hoeiland, S., Barth, T., Blokhud, A.M., and Skauge, A., The Effect of Crude Oil Acid Fractions on Wettability as Studied by Interfacial Tension and Contact Angles, *Journal of Petroleum Science and Engineering*, **2001**, 30, 91-103.

Hough, E.W., Rzasa, M.S., and Wood, B.B., Interfacial Tension at Reservoir Pressures and Temperatures: Apparatus and the Water-Methane System, *AIME Transactions*, **1951**, 192, 57-60.

Hsu, C.S., Dechert, G.J., Robbins, W.K., and Fukuda, E.K., Naphthenic Acids in Crude Oils Characterized by Mass Spectrometry, *Energy Fuels*, **2000**, 14(1), 217-223.

Hughey, C.A., Rodgers, R.P., and Marshall, A.G., Resolution of 11,000 Compositionally Distinct Components in a Single Electrospray Ionization Fourier Transform Ion Cyclotron Resonance Mass Spectrum of Crude Oil, *Analytical Chemistry*, **2002**, 74(16), 4145-4149.

Ikeda, N., Aratono, M., and Motomura, K., Thermodynamic Study on the Adsorption of Sodium Chloride at the Water/Hexane Interface, *Journal of Colloid and Interface Science*, **1992**, 149(1), 208-215.

Isaacs, E.E., and Smolek, K.F., Interfacial Tension Behavior of Athabasca Bitumen/Aqueous Surfactant Systems, *The Canadian Journal of Chemical Engineering*, **1983**, 61, 233-240.

Jafvert, C.T., Westall, J.C., Grieder, E., and Schwarzenbach, R.P., *Environmental Science Technology*, **1990,** 24, 1795.

Jennings, H.Y., and Newman, G.H., The Effect of Temperature and Pressure on the Interfacial Tension of Water against Methane-Normal Decane Mixtures, *Society of Petroleum Engineers Journal*, **1971**, 251, 171-175.

Jennings, H.Y., The Effect of Temperature and Pressure on the Interfacial Tension of Benzene-Water and Normal Decane-Water, *Journal of Colloid and Interface Science*, **1967**, 24(3), 323-329.

Jeribi, M., Almir-Assad, B., and Langevin, D., Adsorption Kinetics of Asphaltenes at Liquid Interfaces, *Journal of Colloid and Interface Science*, **2002**, 256, 268-272.

Joos, P., Fang, J.P., and Serrien, G., Comments on Some Dynamic Surface Tension Measurements by the Dynamic Bubble Pressure Method, *Journal of Colloid and Interface Science*, **1992**, 151(1), 144-149.

Kalinin, V.V., and Radke, C.J., An Ion-Binding Model for Ionic Surfactant Adsorption at Aqueous-Fluid Interfaces, *Colloids and Surfaces A*, **1996**, 114, 337-350.

Kelesoglu, S., Meakin, P., and Sjoblom, J., Effect of Aqueous phase pH on the Dynamic Interfacial Tension of Acidic Crude Oils and Myristic Acid in Dodecane, *Journal of Dispersion Science and Technology*, **2011**, 32, 1682-1691.

Langmuir, I., The Constitution and Fundamental Properties of Solids and Liquids. II Liquids, *Journal of American Chemical Society*, **1917**, 39(9), 1848-1906.

Laughlin, R.G., The Aqueous Phase Behavior of Surfactants, Academic Press, London, **1996**.

Li, B., and Fu, J., Interfacial Tensions of Two-Liquid-Phase Ternary Systems, *Journal of Chemical Engineering Data*, **1992,** 37(2), 172-174.

Livingston, H.K., Surface and Interfacial Tension of Oil-Water Systems in Texas Oil Sands, American Institute of Mining Metallurgical and Petroleum Engineers, **1938**, Technical Paper 1001.

Lucassen, J., and Drew, M.G.B., The Crystal Structure of Sodium Diheptylsulphosuccinate Dihydrate and Comparison with Phospholipids, *Journal of Chemical Society Faraday Transactions 1*, **1987**, 83(10), 3093.

McCaffery, F.G., Measurements of Interfacial Tension and Contact Angles at High Temperature and Pressure, *Journal of Canadian Petroleum Technology*, **1972**, 11, 26-32.

Miller, R., and Kretzschmar, G., Adsorption Kinetics of Surfactants at Fluid Interfaces, *Advances in Colloids and Interface Science*, **1991**, 37, 97-112.

Miller, R., Journal of Colloid and Polymer Science, **1980**, 258, 179-185.

Mohamed, R.S., Ramos, A.C.S., and Loh, W., Aggregation Behaviour of Two Asphaltenic Fractions in Aromatic Solvents, *Energy Fuels*, **1999**, 13(2), 323-327.

Murgich, J., Abanero, J.A., and Strausz, O.P., Molecular Recognition in Aggregates Formed by Asphaltene and Resin Molecules from the Athabasca Oil Sand, *Energy and Fuels*, **1999**, 13(2), 278-286.

Myers, D., Surfaces, Interfaces and Colloids: Principles and Applications, Wiley-VCH, New York, **1999**, 501.

O'Connor, S.J., Hydrocarbon-Water Interfacial Tension Values at Reservoir Conditions: Inconsistencies in the Technical Literature and the Impact on Maximum Oil and Gas Column Height Calculations, *AAPG Bulletin*, **2000**, 84(10), 1537-1541.

Okasha, T.M., and Al-Shiwaish, A.A., Effect of Brine Salinity on Interfacial Tension in Arab-D Carbonate Reservoir, Saudi Arabia, **2009**, Paper presented at the SPE Middle East Oil & Gas show and conference, Kingdom of Bahrain, 15-18 March.

Payzant, J.D., Lown, E.M., and Strausz, O.P., Structural Units of Athabasca Asphaltene: the Aromatics with a Linear Carbon Framework, *Energy Fuels*, **1991**, 5(3), 441-444.

Peters, R.A., Interfacial Tension and Hydrogen-Ion Concentration, *Proceedings of Royal Society of London A*, **1931**, 133, 140-154.

Pollard, J.M., Shi, A.J., and Goklen, K.E., Solubility and Partitioning Behaviour of Surfactants and Additives Used in Bioprocesses, *Journal of Chemical and Engineering Data*, **2006**, 51, 230-236.

Poteau, S., Argillier, J.F., Influence of pH on Stability and Dynamic Properties of Asphaltenes and other Amphiphilic Molecules at the Oil-Water Interface, *Energy and Fuels*, **2005**, 19, 1337-1341.

Price, L.C., Aqueous Solubility of Petroleum as Applied to its Origin and Primary Migration, *AAPG Bulletin*, **1976**, 60, 213-244.

Prosser, A.J., and Franses, E.I., Adsorption and Surface Tension of Ionic Surfactants at the Air-Water Interface: Review and Evaluation of Equilibrium Models, *Colloids and Surfaces A*: *Physicochemical and Engineering Aspects*, **2001**, 178, 1-40.

Purcell, W.R., Capillary Pressure – Their Measurements using Mercury and the Calculation of Permeability There From, *AIME Petroleum Transactions*, **1949**, 186, 39-48.

Reinsel, M.A., Borkowski, J.J. and Sears, J.T., partition Coefficients for Acetic, Propionic, and Butyric Acids in a Crude Oil/Water System, *Journal of Chemical Engineering Data*, **1994**, 39, 513-516.

Reisberg, J., and Doscher, T.M., Interfacial Phenomenon in Crude-Oil-Water Systems, *Producers Monthly*, **1956**, November, 43-50.

Robbins, W.K., Challenges in the Characterization of Naphthenic Acids in Petroleum, *American Chemical Society*, **1998**, 43(1), 137-140.

Rosen, M.J., and Gao, T., Dynamic Surface Tension of Aqueous Surfactant Solutions, *Journal of Colloid and Interface Science*, **1995**, 173, 42-48.

Rudin, J., and Wasan, D.T., Mechanism of Lowering Interfacial Tension in Alkali/Acidic Oil Systems.1. Experimental Studies, *Colloids and Surfaces*, **1992**, 68, 67-79.

Schildberg Y, Sjoblom, J., Christy, A., Volle, J., and Rambeau, O., Characterization of Interfacially Active Fractions and Their Relations to Water-in-Oil Emulsion Stability, *Journal of Dispersion Science and Technology*, **1995**, 16(7), 575-605.

Schowalter, T.T., Mechanics of Secondary Hydrocarbon Migration and Entrapment, *AAPG Bulletin*, **1979**, 63, 723-760.

Serrano-Saldana, E., Dominguez-Ortiz, A., Perez-Aguilar, H., Komhauser-Strauss, I., and Rojas-Gonzalez, F., Wettability of Solid/Brine/n-dodecane Systems: Experimental Study of the Effects of Ionic Strength and Surfactant Concentration, *Colloids and Surfaces A: Physiochemical and Engineering Aspects*, **2004**, 241(1-3), 343-349.

Serrien, G., and Joos, P., Dynamic Surface Properties of Aqueous Sodium Dioctyl Sulfosuccinate Solutions, *Journal of Colloid and Interface Science*, **1990**, 139, 149-159.

Sjoblom, J., Johnsen, E.E., Westvik, A., Bergflodt, L., Auflem, I.H., Havre, T.E., and Kallevik, H., Colloid Chemistry in Sub Sea Petroleum and Gas Processing, The 2nd International Conference on Petroleum and Gas Phase Behaviour and Fouling, Copenhagen, Denmark, **2000**.

Skauge, A., Standal, S., Boe, S.O., Skauge, T., and Blokhus, A.M., Effects of Organic Acids and Bases, and Oil Composition on Wettability, SPE Paper Number 56673, **1999**.

Smith, D.A., Theoretical Considerations of Sealing and Non-sealing Faults, *AAPG Bulletin*, **1966**, 50, 363-374.

Standal, S.H., Blokhus, A.M., Haavik, J., Skauge, A., and Barth, T., Partition Coefficient and Interfacial Activity for Polar Components in Oil/Water Model Systems, *Journal of Colloid and Interface Science*, **1999**, 212, 33-41.

Strausz, O.P., Mojelsky, T.W., and Lown, E.M., The Molecular Structure of Asphaltene: An Unfolding Story, *Fuel*, **1992**, 71(12), 1355-1363.

Sutton, R.P., An Improved Model for Water-Hydrocarbon Surface Tension at Reservoir Conditions, **2009**, SPE Paper Number 124968.

Sztukowski, D.M., and Yarranton, H.W., Characterization and Interfacial Behavior of Oil Sands Solids Implicated in Emulsion Stability, *Journal of Dispersion Science and Technology*, **2004**, 25(3), 299-310.

Sztukowski, D.M., Jafari, M., Alboudwarej, H., Yarranton, H.W., Asphaltene Self-Association and Water-in-Hydrocarbon Emulsions, *Journal of Colloid and Interface Science*, **2003**, 265,179-186.

Szymczyk, K., and Janczuk, B., The Adsorption at Solution-air Interface and Volumetric Properties of Mixtures of Cationic and Anionic Surfactants, *Colloids and Surfaces A: Physicochemical and Engineering Aspects*, **2007**, 293, 39-50.

Szyszkowski, B., *Z. Phys. Chem*., **1908**, 64, 385-415.

Talal, M.A., Zhang, J., Chenevert, M.E., and Sharma, M.M., Estimating the Reservoir Hydrocarbon Capacity through Measurements of the Minimum Capillary Entry Pressure of Shale Cap-Rocks, **2009**, SPE Paper Number 121450.

Van Hunsel, J., ph.D. Thesis, Antwerpen, **1988**.

Van Voorst Vander, F., Adsorption of Detergents at the Liquid-Liquid Interface. Part 1, *Transactions of Faraday Society*, **1960**, 56, 1067.

Varadaraj, R., and Brons, C., Molecular Origins of Heavy Oil Interfacial Activity Part 1: Fundamental Interfacial Properties of Asphaltenes Derived from Heavy Crude Oils and Their Correlation to Chemical Composition, *Energy and Fuels*, **2007**, 21, 195-198.

Varadaraj, R., and Brons, C., Molecular Origins of Heavy Crude Oil Interfacial Activity Part 2: Fundamental Interfacial Properties of Model Naphthenic Acids and Naphthenic Acids Separated from Heavy Crude Oils, *Energy and Fuels*, **2007**, 21, 199-204.

Vavra, L., Kaldi, J., and Sneider,M., Geological Applications of Capillary Pressure: A Review, *American Association of petroleum Geologists*, **1992**, 76(6).

Vijapurapu, C.S., and Rao D.N, Compositional Effects of Fluid on Spreading, Adhesion and Wettability in Porous Media, *Colloids and Surfaces A: Physiochemical and Engineering Aspects*, **2004**, 241(1-3), 335-342.

Wang, W., and Gupta, A., Investigation of the Effect of Temperature and Pressure on Wettability Using Modified Pendant Drop Method, **1995**, SPE Paper Number 30544.

Ward A.F.H., and Tordai, L., Time-dependence of Boundary Tensions of Solutions. I. The Role of Diffusion in Time-effects, *Journal of Chemical Physics*, **1946**, 14, 453-461.

Watts, N.L., Theoretical Aspects of Cap-rock and Fault Seals for Single and Two-phase Hydrocarbon Columns, *Marine and Petroleum Geology*, **1987**, 4, 274-307.

Wiegand, G., and Franck, E.U., Interfacial Tension Between Water and Non-Polar Fluids up to 473 K and 2800 bar, *Ber. Bunsenges. Phys. Chem.*, **1994**, 98(6), 809-817.

Xu, W., Experimental Investigation of Dynamic Interfacial Interactions at Reservoir conditions, MSc. Thesis, Louisiana, USA, **2005**.

Yarranton, H.W., Alboudwarej, H., and Jakher, R., Investigation of Asphaltene Association with Vapor Pressure Osmometry and Interfacial Tension Measurements, *Industrial Engineering and Chemistry Research*, **2000**, 39(8), 2916-2924.

Yarranton, H.W., and Masliyah, J.H., Gibbs-Langmuir Model for Interfacial Tension of Nonideal Organic Mixtures over Water, *The Journal of Physical Chemistry*, **1996**, 100, 1786-1792.

Zeppieri, S., Rodriguez, J., and Ramos, A.L.L., Interfacial Tension of Alkane + Water Systems, *Journal of Chemical and Engineering Data*, **2001**, 46(5), 1086-1088.

Appendix A: Data Tables

Table A1: Experimental and modeled IFT values along with the error for toluene/salt systems.

NaCl	**Expt. IFT**	**Calc. IFT**	**AARD%**
0.1	34.64	34.4	0.59
5	36.36	36.1	0.70
10	37.15	37.8	1.74
15	39.4	39.5	0.16
CaCl2			
0.1	34.16	34.4	0.76
5	35.30	35.3	0.10
10	36.1	36.3	0.51
15	37.73	37.3	1.18
Na2SO4			
0.1	34.25	34.4	0.49
5	35.01	35.1	0.34
10	36.31	35.9	1.15
15	36.95	36.7	0.66

Table A2: Experimental and modeled data along with error percentages for heptane/salt.

NaCl	**Expt. IFT**	**Calc. IFT**	**AARD%**
0.1	49.25	49.7	0.96
5	50.95	50.8	0.23
10	51.77	52.0	0.44
15	53.35	53.2	0.35
CaCl2			
0.1	49.13	49.7	1.19
5	50.46	50.3	0.29
10	51.50	51.0	1.05
Na2SO4			
0.1	49.47	49.7	0.48
5	49.83	50.2	0.70
10	50.42	50.7	0.54
15	50.88	51.2	0.71

Table A3: Experimental and modeled data along with error percentage for cyclohexane/salt.

NaCl	**Expt. IFT**	**Calc. IFT**	**AARD %**
0.1	49.04	49.3	0.57
5	50.35	50.3	0.06
10	51.723	51.4	1.25
15	52.06	52.4	0.68
CaCl2			
0.1	48.66	49.3	1.35
5	49.57	49.8	0.55
10	50.20	50.4	0.44
15	53.03	51.0	3.75
Na2SO4			
0.1	48.08	49.3	2.56
5	48.62	49.7	2.29
10	49.56	50.2	1.25
15	50.94	50.7	0.50

Table A4: Experimental and modeled data along with error for Heptol/salt.

NaCl	**Expt. IFT**	**Calc. IFT**	**AARD %**
0.1	37.8	38.8	2.76
5	39.44	40.4	2.40
10	41.40	42.0	1.38
15	42.95	43.5	1.38
CaCl2			
0.1	38.25	38.8	1.48
5	39.85	39.7	0.49
10	41.13	40.6	1.40
15	42.47	41.5	2.30
Na2SO4			
0.1	38.9	38.8	0.24
5	40.53	39.5	2.60
10	40.53	40.2	0.83
15	41.4	40.9	1.08

Table A5: Experimental and modeled data along with error percentage for toluene at varying concentrations of SDS and NaCl. The Average deviation was calculated to be 4%.

SDS Conc.	Expt. IFT	Calc. IFT	AARD %
Water			
0.1	12.0	13.13	9.4
0.05	18.7	17.21	8.0
0.01	26.6	25.79	3.1
0.005	29.7	28.72	3.3
0.001	33.0	32.83	0.5
0.0001	33.7	34.31	1.9
1% NaCl			
0.005	11.2	9.57	14.6
0.002	16.7	15.06	9.8
0.001	20.34	19.08	6.2
0.0005	23.92	22.88	4.3
0.0001	28.26	29.99	6.1
0.00005	29.56	31.94	8.1
0.00001	32.1	34.12	6.3
0.000001	33.2	34.74	4.6
5% NaCl			
0.0001	21	22.34	6.4
0.00001	32.25	32.39	0.4
0.000001	34.7	35.59	2.6
0.0000001	35.3	36.02	2.0
10% NaCl			
0.0001	17.5	18.61	6.3
0.00005	25	22.64	9.5
0.00001	29.8	30.82	3.4
0.000001	35.5	36.54	2.9
15% NaCl			
0.0001	17	15.73	7.5
0.00005	21	19.91	5.2
0.00001	30	29.08	3.1
0.000001	37	37.21	0.6

Table A6: Experimental and modeled data along with error percentage for heptane at varying concentrations of SDS and NaCl. The Average deviation was calculated to be 4.7%.

SDS Conc.	Expt. IFT	Calc. IFT	AARD %
Water			
0.1	18.5	18.98	2.62
0.01	35.6	32.81	7.83
0.001	44.8	44.32	0.97
0.0001	48.3	49.21	1.93
1% NaCl			
0.005	17	16.07	5.5
0.002	23.9	21.67	9.3
0.001	28.8	25.88	10.1
0.0005	32.9	30.03	8.7
0.0001	37.62	39.08	3.9
0.00005	39.95	42.42	6.2
0.00001	44.6	47.72	7.0
0.000001	47.6	49.98	5.0
5% NaCl			
0.0001	28.35	28.56	0.7
0.00001	39.8	41.45	4.2
0.000001	50.25	49.12	2.3
0.0000001	50.6	50.85	0.5
10% NaCl			
0.0001	23.4	24.16	3.3
0.00005	26	28.37	9.1
0.00001	38.5	37.79	1.8
0.000001	48.5	48.13	0.8
15% NaCl			
0.0001	19	21.47	13.0
0.00005	24.5	25.70	4.9
0.00001	36	35.36	1.8
0.000001	47.6	47.17	0.9

Table A7: Experimental and modeled data along with error percentage for cyclohexane at varying concentrations of SDS and NaCl. The Average deviation was calculated to be 5.6%.

SDS Conc.	Expt. IFT	Calc. IFT	AARD %
Water			
0.1	14.3	17.07	19.4
0.01	34.4	30.95	10.0
0.001	42.9	42.81	0.1
0.0001	46.7	48.24	3.4
1% NaCl			
0.005	14.9	13.90	6.7
0.002	21.5	19.51	9.2
0.001	26.4	23.73	10.1
0.0005	30.5	27.90	8.5
0.0001	37.1	37.11	0.0
0.00005	38.5	40.60	5.4
0.00001	43.4	46.40	6.9
5% NaCl			
0.0001	25.6	25.73	0.5
0.00001	37.2	38.94	4.7
0.000001	49.1	47.59	3.1
0.0000001	49.15	49.84	1.4
10% NaCl			
0.0001	21	21.76	3.6
0.00005	28.6	25.98	9.2
0.00001	34.8	35.49	2.0
0.000001	49.5	46.37	6.3
15% NaCl			
0.0001	19	18.90	0.5
0.00005	26	23.14	11.0
0.00001	34	32.84	3.4
0.000001	43.5	45.03	3.5

Table A8: Experimental and modeled data along with error percentage for Heptol50 at varying concentrations of SDS and NaCl. The Average deviation was calculated to be 5.2%.

SDS Conc.	Expt. IFT	Calc. IFT	AARD %
Water			
0.1	13.1	13.26	1.2
0.01	28.3	26.62	5.9
0.001	36.1	35.82	0.8
0.0001	37.6	38.43	2.2
1% NaCl			
0.002	18.8	16.31	13.2
0.001	23	20.43	11.2
0.0005	26.54	24.40	8.1
0.0001	31.87	32.37	1.6
0.00005	32.88	34.85	6.0
0.00001	36.34	37.96	4.4
0.000001	36.64	38.94	6.3
5% NaCl			
0.0001	22.12	22.69	2.6
0.00001	32	34.26	7.1
0.000001	38.4	39.20	2.1
0.0000001	38.8	40.00	3.1
10% NaCl			
0.0001	19.3	19.23	0.3
0.00005	23.8	23.35	1.9
0.00001	28.9	32.15	11.2
0.000001	39.7	39.61	0.2
15% NaCl			
0.0001	17.5	16.54	5.5
0.00005	23	20.74	9.8
0.00001	34	30.13	11.4
0.000001	41	39.73	3.1

Table A9: Experimental and modeled data along with error percentage for Toluene at varying concentrations of 5-β cholanic acid (CA) and NaCl. The average deviation was calculated to be 1%.

CA Conc.	Expt. IFT	Calc. IFT	AARD %
Water			
2	30.2	29.7	1.6
1	30.64	30.6	0.0
0.1	32.98	33.4	1.2
0.001	34.7	35.1	1.1
0.1% NaCl			
2	29.9	29.7	0.6
1	30.8	30.7	0.5
0.1	32.72	33.4	2.1
0.001	34.6	35.1	1.4
5% NaCl			
2	30.45	30.0	1.4
1	31.26	31.0	0.9
0.1	34.72	34.1	1.7
0.001	36.7	36.8	0.3
10% NaCl			
2	29.85	30.4	1.7
1	31.28	31.4	0.3
0.1	34.76	35.0	0.8
0.001	38.0	38.5	1.4
15% NaCl			
2	31.05	30.8	0.7
1	32	31.9	0.3
0.1	36.6	36.3	0.8
0.001	39.7	40.3	1.5

Table A10: Experimental and modeled data along with error percentage for Toluene at varying concentrations of Nonylphenol Ethoxylate (NEO10) and NaCl. The average deviation was calculated to be 2.2%.

NEO Conc.	Expt. IFT	Calc. IFT	AARD %
Water			
0.01	21.42	21.28	0.6
0.001	24.56	24.68	0.5
0.0001	27.8	28.07	1.0
0.00001	32.25	31.36	2.8
0.000001	32.9	33.96	3.2
0.1% NaCl			
0.01	21.05	21.32	1.3
0.001	25.75	24.72	4.0
0.0001	27.5	28.10	2.2
0.00001	32.95	31.39	4.7
0.000001	32.9	34.00	3.3
5% NaCl			
0.01	23.5	23.01	2.1
0.001	27.3	26.41	3.3
0.0001	29.1	29.80	2.4
0.00001	33.6	33.09	1.5
0.000001	35.5	35.72	0.6
10% NaCl			
0.01	25	24.71	1.2
0.001	28.4	28.11	1.0
0.0001	30.2	31.50	4.3
0.00001	35.6	34.79	2.3
0.000001	35.7	37.44	4.9
15% NaCl			
0.01	26.2	26.38	0.7
0.001	29.9	29.78	0.4
0.0001	31.8	33.17	4.3
0.00001	36.6	36.47	0.4
0.000001	37.5	39.14	4.4

Table A11: Experimental and modeled data along with error percentage for Toluene at varying concentrations of Cetyltrimethylammonium bromide (CTAB) and NaCl. The average deviation was calculated to be 5.7%.

CTAB Conc.	Expt. IFT	Calc. IFT	AARD %
Water			
0.01	11.14	10.98	1.4
0.005	17.6	15.13	14.0
0.001	25.4	24.14	5.0
0.0001	31.5	32.63	3.6
0.00001	33.8	34.80	3.0
0.000001	34	35.07	3.1
0.1% NaCl			
0.001	10.1	10.98	8.7
0.0001	21	24.14	15.0
0.00005	24.7	27.45	11.1
0.00001	32.7	32.65	0.1
0.000001	33.84	34.84	2.9
1% NaCl			
0.0001	14	12.67	9.5
0.00005	17.8	16.78	5.7
0.00001	27	25.54	5.4
0.000001	33.6	33.15	1.3
5% NaCl			
0.00005	13.5	12.61	6.6
0.00001	21	22.01	4.8
0.000001	32	32.33	1.0

Table A12: Experimental and modeled data along with error percentage for Toluene at varying concentrations of Triton X-100 and NaCl. The average deviation was calculated to be 2.6%.

TX-100 Conc.	Expt. IFT	Calc. IFT	AARD %
Water			
0.1	13.2	13.07	1.0
0.01	17.88	17.61	1.5
0.001	22.5	22.14	1.6
0.0001	26	26.64	2.5
0.00001	30.8	30.95	0.5
0.000001	34.3	34.03	0.8
5% NaCl			
0.01	18.95	19.32	1.9
0.001	24.4	23.85	2.3
0.0001	28.2	28.36	0.6
0.00001	31.1	32.67	5.0
0.000001	34	35.78	5.2
10% NaCl			
0.01	19.3	21.00	8.8
0.001	25.7	25.53	0.7
0.0001	29.3	30.04	2.5
0.00001	-	34.36	-
0.000001	36	37.50	4.2
15% NaCl			
0.01	22.2	22.65	2.0
0.001	27.4	27.18	0.8
0.0001	31	31.69	2.2
0.00001	34.5	36.02	4.4
0.000001	37.5	39.20	4.5

Table A13: Experimental and modeled data along with error percentage for Toluene at varying concentrations of Asphaltenes and NaCl. The average deviation was calculated to be 1.06%.

Asph. Conc. (g/l)	Expt. IFT	Calc. IFT	AARD %
Water			
0.5	23.3	24.5	5.1
1	23	23.0	0.1
2.5	21.1	21.1	0.2
5	20.0	19.9	0.2
10	18.8	18.8	0.0
20	17.5	17.5	0.1
1% NaCl			
0.5	24.6	24.8	0.8
1	23.5	23.2	1.2
2.5	21.3	21.3	0.0
5	20.3	20.0	1.2
10	19.0	18.8	0.9
20	17.5	17.4	0.3
5% NaCl			
0.5	-	26.4	-
1	24.3	24.6	1.2
2.5	22.3	22.4	0.5
5	21.1	20.9	1.0
10	19.9	19.5	1.8
20	18.0	18.0	0.0
10% NaCl			
0.5	25.7	27.2	5.9
1	25	25.2	0.8
2.5	23.1	22.8	1.4
5	21.4	21.1	1.4
10	19.6	19.6	0.0
20	17.7	17.9	1.2
15% NaCl			
0.5	27.95	28.3	1.4
1	26	26.1	0.5
2.5	23.9	23.5	1.7
5	21.96	21.8	0.9
10	20.1	20.1	0.0
20	17.7	18.3	3.4

Table A14: Interfacial tension of Light, Medium, and Heavy Crude oils and *n*-decane diluted Heavy Crude versus water and brines at 21°C.

NaCl, wt.%	Light Crude	Medium Crude	Heavy Crude		
			Decane Dilution (%)		
			25	30	35
Water	14.5	18.7	17.8	17.4	17.1
1	TSTM *	19.2	17.0	16.2	15.6
5	TSTM	19.6	16.6	15.7	15.4
10	TSTM	19.8	14.9	14.5	13.8
15	TSTM	20.4	15.2	14.8	14

* Too small to measure

Table A15: Interfacial tension of Western Canadian Bitumen and *n*-decane diluted Heavy Crude versus water and brines at 21°C.

NaCl, wt.%	Western Canadian Bitumen		
	Decane Dilution (%)		
	35	40	45
Water	20.4	20.36	20.15
1	12.7	11.4	10.98
5	7	6.8	6.2

Appendix B: Error Analysis

The variability analysis of the data was performed by statistical *t*-distribution. The confidence interval of the data was calculated using mean, standard deviation, and 85% confidence interval for the *t*-distribution.

For a given dataset of interfacial tension values, the mean is calculated as follows;

$$\bar{y} = \frac{\sum_{i=1}^{n} y_i}{n} \qquad \textbf{Equation B.1}$$

where y_i is the measured value of interfacial tensions, n is the number of measurements of interfacial tension for a particular system, and $\bar{y}$ is the average value of the measured data.

The variability of scatter in the data is described by the sample standard deviation, *s*, defined by

$$s = \sqrt{\frac{\sum_{i=1}^{n}(y_i - \bar{y})^2}{n-1}} \qquad \textbf{Equation B.2}$$

In this work, the population mean μ, and the population standard deviation are unknown and the number of observations is small (n < 5). Hence *t*-distribution is employed to determine the confidence interval as follows:

$$\bar{y} - t_{\left(\frac{\alpha}{2},\nu\right)}\frac{s}{\sqrt{n}} \leq \mu \leq \bar{y} + t_{\left(\frac{\alpha}{2},\nu\right)}\frac{s}{\sqrt{n}} \qquad \textbf{Equation B.3}$$

where $\alpha = (1 - \%\ confidence\ interval/100)$, $\upsilon = n - 1$, is the degrees of freedom. In this study the confidence interval is chosen to be 85%, so α is 0.15.

B.1 Error Analysis for the IFT of various Systems

The variability analysis was calculated on systems with at least two experimental repeats. The error analysis for various systems is presented in the following section.

Table B1: Variability analysis for the IFT of hydrocarbon/brine systems.

Aqueous Phase	Data 1	Data 2	Data 3	Data 4	Mean	Standard Deviation
Toluene						
Water	34.7	34.3	35.0	34.4	34.6	0.275
10% NaCl	37.6	37.5	-	-	37.5	0.028
0.1% $CaCl_2$	34.6	34.2	33.5	-	33.9	0.408
5% $CaCl_2$	35.2	35.3	-	-	35.3	0.055
10% $CaCl_2$	36.7	36.3	-	-	36.5	0.333
15% $CaCl_2$	37.2	38.2	-	-	37.7	0.691
0.1% Na_2S0_4	33.9	34.4	-	-	34.1	0.307
15% Na_2S0_4	36.2	36.6	38.2	-	37.0	1.052
Heptane						
Water	49.7	49.8	50.1	-	49.9	0.216
5% NaCl	51.1	51.0	50.6	51.1	51.0	0.247
10% NaCl	51.7	51.3	52.3	-	51.8	0.510
15% NaCl	53.7	53.0	-	-	53.4	0.453
0.1% $CaCl_2$	49.1	49.1	-	-	49.1	0.019
5% $CaCl_2$	50.3	50.6	50.4	50.5	50.5	0.116
5% Na_2S0_4	49.2	50.0	-	-	49.6	0.561
10% Na_2S0_4	50.2	50.7	-	-	50.4	0.367
15% Na_2S0_4	50.8	51.3	50.7	50.8	50.9	0.260
Cyclohexane						
Water	49.1	49.5	-	-	49.3	0.226
5% NaCl	50.1	50.6	-	-	50.4	0.295
10% NaCl	51.4	51.4	-	-	51.4	0.005
5% $CaCl_2$	49.2	49.9	-	-	49.6	0.464

10% $CaCl_2$	50.2	49.8	-	-	50.0	0.261
15% $CaCl_2$	53.2	53.5	-	-	53.3	0.247
0.1% Na_2S0_4	48.0	48.1	-	-	48.1	0.079
10% Na_2S0_4	50.1	49.0	-	-	49.6	0.765
Heptol						
Water	38.9	38.7	-	-	38.8	0.191
0.1% NaCl	38.3	37.4	37.7	-	37.8	0.473
5% NaCl	39.5	39.4	-	-	39.4	0.056
0.1% $CaCl_2$	37.9	37.2	-	-	37.5	0.485
10% Na_2S0_4	40.3	40.2	40.5	-	40.3	0.166
					Average	**0.320**
					Error	**±0.087**

Table B2: Variability analysis for the IFT of hydrocarbon/brine/surfactant systems.

Aqueous Phase	**Data 1**	**Data 2**	**Mean**	**Standard Deviation**
Toluene				
Water + 0.01% SDS	25.6	27.7	26.6	1.450
Water + 0.0001% SDS	33.4	34.0	33.7	0.446
1% NaCl + 0.00001% SDS	32.1	31.9	32.0	0.141
5% NaCl + 0.00001% SDS	31.3	33.2	32.3	1.344
5% NaCl + 0.000001% SDS	34.7	33.6	34.2	0.778
15% NaCl + 0.0001% SDS	18.0	17.0	17.5	0.707
Water + 0.01% CTAB	11.0	11.4	11.2	0.304
Water + 0.005% CTAB	17.3	17.9	17.6	0.424
Water + 0.001% CTAB	25.4	25.5	25.5	0.071
0.1% NaCl + 0.001% CTAB	10.5	9.8	10.1	0.530
0.1% NaCl + 0.0001% CTAB	32.7	32.8	32.8	0.071
1% NaCl + 0.0001% CTAB	14.0	14.1	14.1	0.071
1% NaCl + 0.00005% CTAB	17.8	17.9	17.9	0.071
1% NaCl + 0.000001% CTAB	33.8	33.4	33.6	0.311
Water + 0.01% NEO	21.1	21.7	21.4	0.403
Water + 0.001% NEO	24.9	24.2	24.6	0.516
Water + 0.00001% NEO	31.5	33.0	32.3	1.061

Water + 0.000001% NEO	33.3	32.5	32.9	0.566
0.1% NaCl + 0.01% NEO	20.7	21.4	21.1	0.495
0.1% NaCl + 0.001% NEO	25.2	26.3	25.8	0.778
0.1% NaCl + 0.00001% NEO	32.9	33.0	33.0	0.071
5% NaCl + 0.01% NEO	23.5	23.6	23.6	0.071
5% NaCl + 0.001% NEO	27.2	27.4	27.3	0.141
10% NaCl + 0.001% NEO	28.9	27.9	28.4	0.707
10% NaCl + 0.00001% NEO	35.6	35.7	35.7	0.071
10% NaCl + 0.000001% NEO	35.6	35.8	35.7	0.141
15% NaCl + 0.01% NEO	28.8	26.2	27.5	1.839
15% NaCl + 0.001% NEO	29.3	30.5	29.9	0.849
15% NaCl + 0.000001% NEO	37.6	37.4	37.5	0.141
Heptane				
Water + 0.0001% SDS	48.0	48.6	48.3	0.460
1% NaCl + 0.000001% SDS	47.7	47.5	47.6	0.141
5% NaCl + 0.00001% SDS	38.5	38.6	38.6	0.071
10% NaCl + 0.00001% SDS	40.0	39.6	39.8	0.283
15% NaCl + 0.00001% SDS	35.0	37.0	36.0	1.414
Cyclohexane				
Water + 0.0001% SDS	46.6	46.7	46.7	0.071
5% NaCl + 0.00001% SDS	37.5	37.0	37.3	0.354
5% NaCl + 0.000001% SDS	48.4	49.4	48.9	0.707
5% NaCl + 0.0000001% SDS	48.4	49.9	49.2	1.061
10% NaCl + 0.00005% SDS	28.4	28.8	28.6	0.283
Heptol				
Water + 0.0001% SDS	37.5	37.7	37.6	0.141
5% NaCl + 0.000001% SDS	38.3	38.4	38.4	0.071
			Average	**0.479**
			Error	**±0.110**